Preliminary Hydrogeologic Assessment of Boreholes UE-25c #1, UE-25c #2, and UE-25c #3, Yucca Mountain, Nye County, Nevada

by Arthur L. Geldon

U.S. GEOLOGICAL SURVEY

Water-Resources Investigations Report 92-4016

Prepared in cooperation with the
NEVADA FIELD OFFICE,
U.S. DEPARTMENT OF ENERGY
(Interagency Agreement DE-AI08-92NV10874)

Denver, Colorado
1993

U.S. DEPARTMENT OF THE INTERIOR

BRUCE BABBITT, Secretary

U.S. GEOLOGICAL SURVEY

Robert M. Hirsch, Acting Director

For additional information
write to:

Chief, Hydrologic Investigations Program
Yucca Mountain Project Branch
U.S. Geological Survey
Box 25046, Mail Stop 421
Federal Center
Denver, CO 80225

Copies of this report can
be purchased from:

U.S. Geological Survey
Earth Science Information Center
Open-File Reports Section
Box 25286, MS 517
Federal Center
Denver, CO 80225

CONTENTS

FIGURES

TABLES

CONVERSION TABLE

Multiply metric unit	*By*	*To obtain inch-pound unit*
centimeter (cm)	0.3937	inch
cubic meter (m^3)	35.313	cubic foot
degree Celsius per kilometer (°C/km)	5.486×10^{-2}	degree Fahrenheit per 100 feet
gram per cubic centimeter (g/cm^3)	62.422	pound per cubic foot
kilobar (kb)	1.450×10^{4}	pound per square inch
kilometer (km)	0.6214	mile
liter per second (L/s)	15.85	gallon per minute
meter (m)	3.2808	foot
meter per cubic meter (m/m^3)	9.291×10^{-2}	foot per cubic foot
meter per day (m/d)	3.2808	foot per day
meter per kilometer (m/km)	5.2797	foot per mile
meter squared per day (m^2/d)	10.76	foot squared per day
meter squared per newton (m^2/N)	6.897×10^{3}	inch squared per pound
millidarcy (mD)	1.06×10^{-14}	square foot
milliequivalent per liter (meq/L)	1.0	equivalent per million
milligram per liter (mg/L)	1.0	part per million
millimeter (mm)	3.937×10^{-2}	inch
newton per cubic meter (N/m^3)	6.365×10^{-3}	pound per cubic foot
newton per square meter (N/m^2)	1.450×10^{-4}	pound per square inch
pascal (Pa)	1.450×10^{-4}	pound per square inch
reciprocal cubic meter (m^{-3})	2.832×10^{-2}	reciprocal cubic foot
reciprocal meter (m^{-1})	0.3048	reciprocal foot
square kilometer (km^2)	0.3861	square mile
square meter (m^2)	10.76	square foot

A common radioactivity unit that is used in this report, the millicurie per milliliter (mCi/mL), combines metric and inch-pound terms. In metric units, it is equivalent to 37.01 millibecquerels per milliliter.

Temperature in degrees Celsius (°C) can be converted to temperature in degrees Fahrenheit (°F) by the following equation:

$$°C=5/9(°F-32).$$

Sea Level: In this report, "sea level" refers to the National Geodetic Vertical Datum of 1929 (NGVD of 1929)--a geodetic datum derived from a general adjustment of the first-order level nets of both the United States and Canada, formerly called "Sea Level Datum of 1929."

PRELIMINARY HYDROGEOLOGIC ASSESSMENT OF BOREHOLES UE-25c #1, UE-25c #2, AND UE-25c #3, YUCCA MOUNTAIN, NYE COUNTY, NEVADA

By Arthur L. Geldon

ABSTRACT

Boreholes UE-25c #1, UE-25c #2, and UE-25c #3 (collectively called the C-holes) each were drilled to a depth of 914.4 meters at Yucca Mountain, on the Nevada Test Site, in 1983 and 1984 for the purpose of conducting aquifer and tracer tests. Each of the boreholes penetrated the Paintbrush Tuff and the tuffs and lavas of Calico Hills and bottomed in the Crater Flat Tuff. The geologic units penetrated consist of devitrified to vitrophyric, nonwelded to densely welded, ash-flow tuff, tuff breccia, ash-fall tuff, and bedded tuff. Below the water table, which is at an average depth of 401.6 meters below land surface, the rocks are argillic and zeolitic. The geologic units at the C-hole complex strike N. 2° W. and dip 15° to 21° NE. They are cut by several faults, including the Paintbrush Canyon Fault, a prominent normal fault oriented S. 9° W., 52.2° NW.

The rocks at the C-hole complex are fractured extensively, with most fractures oriented approximately perpendicular to the direction of regional least horizontal principal stress. In the Crater Flat Tuff and the tuffs and lavas of Calico Hills, fractures strike predominantly between S. 20° E. and S. 20° W. and secondarily between S. 20° E. and S. 60° E. In the Topopah Spring Member of the Paintbrush Tuff, however, southeasterly striking fractures predominate. Most fractures are steeply dipping, although shallowly dipping fractures occur in nonwelded and reworked tuff intervals of the Crater Flat Tuff. Mineral-filled fractures are common in the tuff breccia zone of the Tram Member of the Crater Flat Tuff, and, also, in the welded tuff zone of the Bullfrog Member of the Crater Flat Tuff. The fracture density of geologic units in the C-holes was estimated to range from 1.3 to 7.6 fractures per cubic meter. Most of these estimates appear to be the correct order of magnitude when compared to transect measurements and core data from other boreholes, but some estimates, particularly for intervals within the Paintbrush Tuff, probably are 0.3 to 1.3 orders of magnitude too low.

Geophysical data and laboratory analyses were used to determine matrix hydrologic properties of the tuffs and lavas of Calico Hills and the Crater Flat Tuff in the C-holes. The porosity ranged from 12 to 43 percent and, on the average, was larger in nonwelded to partially welded, ash-flow tuff, ash-fall tuff, and reworked tuff than in moderately to densely welded ash-flow tuff. The pore-scale horizontal permeability of nine samples ranged from 5.7×10^{-3} to 2.9 millidarcies, and the pore-scale vertical permeability of these samples ranged from 3.7×10^{-3} to 1.5 millidarcies. Ratios of pore-scale

horizontal to vertical permeability generally ranged from 0.7 to 2. Although the number of samples was small, values of pore-scale permeability determined were consistent with samples from other boreholes at Yucca Mountain. The specific storage of nonwelded to partially welded ash-flow tuff, ash-fall tuff, and reworked tuff was estimated from porosity and elasticity to be 2×10^{-6} per meter, twice the specific storage of moderately to densely welded ash-flow tuff and tuff breccia. The storativity of geologic units, based on their average thickness (corrected for bedding dip) and specific storage, was estimated to range from 1×10^{-5} to 2×10^{-4}.

Ground-water flow in the Tertiary rocks of the Yucca Mountain area is not confined by strata but appears to result from the random intersection of water-bearing fractures and faults. Even at the C-hole complex, an area of only 1,027 square meters, water-producing zones during pumping tests vary from borehole to borehole. In borehole UE-25c #1, water is produced mainly from the lower, nonwelded to welded zone of the Bullfrog Member of the Crater Flat Tuff and secondarily from the tuff-breccia zone of the Tram Member of the Crater Flat Tuff. In borehole UE-25c #3, water is produced in nearly equal proportions from these two intervals and the central, moderately to densely welded zone of the Bullfrog Member. In borehole UE-25c #2, almost all production comes from the moderately to densely welded zone of the Bullfrog Member. Intraborehole temperature surveys during pumping tests at the C-hole complex indicate that water apparently is transmitted from the faults that transect the site via interconnected south-southeasterly to south-southwesterly, southwesterly, and northeasterly trending fractures. There appears to be no relation between water production from boreholes and either fracture orientation, lithology, or the degree of welding of ash-flow tuff. In support of this interpretation, pumping tests in the C-holes produce curves of drawdown as a function of time that are characteristic of a fracture-dominated ground-water flow system. These curves also indicate that borehole storage commonly affects the drawdown in tested intervals during the first 1 to 15 minutes of pumping.

Hydraulic-head data for the Nevada Test Site and vicinity indicate that ground water in the area flows locally from block-faulted mountains to intermontane basins and regionally from basin to basin toward Death Valley and Alkali Flat. Hydraulic heads in the C-holes and in other boreholes indicate that an upward flux from the regional to the local flow system exists at Yucca Mountain. Hydrochemical data support this interpretation. These data include the predominance of sodium and bicarbonate ions in the water, small (pre-1952) tritium concentrations in the water, the "lightness" of the water in deuterium and oxygen-18 with respect to modern meteoric water, an apparent carbon-14 age of about 15,000 years before present for the water, and elevated ground-water temperatures.

INTRODUCTION

The U.S. Geological Survey is conducting investigations to determine the geologic and hydrologic suitability of Yucca Mountain, Nevada, as a potential site for a mined geologic repository for high-level nuclear wastes. These investigations are being conducted in cooperation with the U.S. Department of Energy, under Interagency Agreement DE-AI08-92NV10874, as part of the Yucca Mountain Site Characterization Project (formerly the Nevada Nuclear Waste Storage Investigations Project).

Purpose and Scope

The purpose of this report is to characterize the hydrogeology of saturated tuffaceous rocks penetrated by boreholes UE-25c #1, UE-25c #2, and UE-25c #3. These boreholes are referred to collectively in this report as the C-holes. The C-holes were drilled to perform multiwell aquifer tests and tracer tests; they comprise the only complex of closely spaced boreholes completed in the saturated zone at Yucca Mountain. Results of lithologic and geophysical logging, fracture analyses, water-level monitoring, temperature and tracejector surveys, aquifer tests, and hydrochemical sampling completed at the C-hole complex as of 1986 are assessed with respect to the regional geologic and hydrologic setting. A conceptual hydrogeological model of the Yucca Mountain area is presented to provide a context for quantitatively evaluating hydrologic tests performed at the C-hole complex as of 1985, for planning and interpreting additional hydrologic tests at the C-hole complex, and for possibly re-evaluating hydrologic tests in boreholes other than the C-holes.

Location of C-Hole Complex

The C-hole complex (fig. 1) is located in Nye County, Nevada, just east of the western boundary of the Nevada Test Site (NTS), approximately 145 km northwest of Las Vegas. Surface positions with respect to the Nevada State Central Zone Coordinate System, surface altitudes, and total depths of the C-holes are listed in table 1. The C-holes are located in an ephemeral, easterly draining valley that cuts across Bow Ridge, which is just east of Yucca Mountain and is separated from it by high-angle faults. Bow Ridge and Yucca Mountain are in the southern Basin and Range physiographic province (Frizzell and Shulters, 1990).

Table 1.--*Location data for boreholes UE-25c #1, UE-25c #2, and UE25c #3*

Borehole	Nevada State Central Zone Coordinates at the surface (meters)	Surface altitude above National Geodetic Vertical Datum of 1929 (meters)	Total depth (meters)
UE-25c #1	N 230,762.8 E 173,638.6	1,130.6	914.4
UE-25c #2	N 230,687.5 E 173,624.4	1,132.2	914.4
UE-25c #3	N 230,706.1 E 173,600.3	1,132.3	914.4

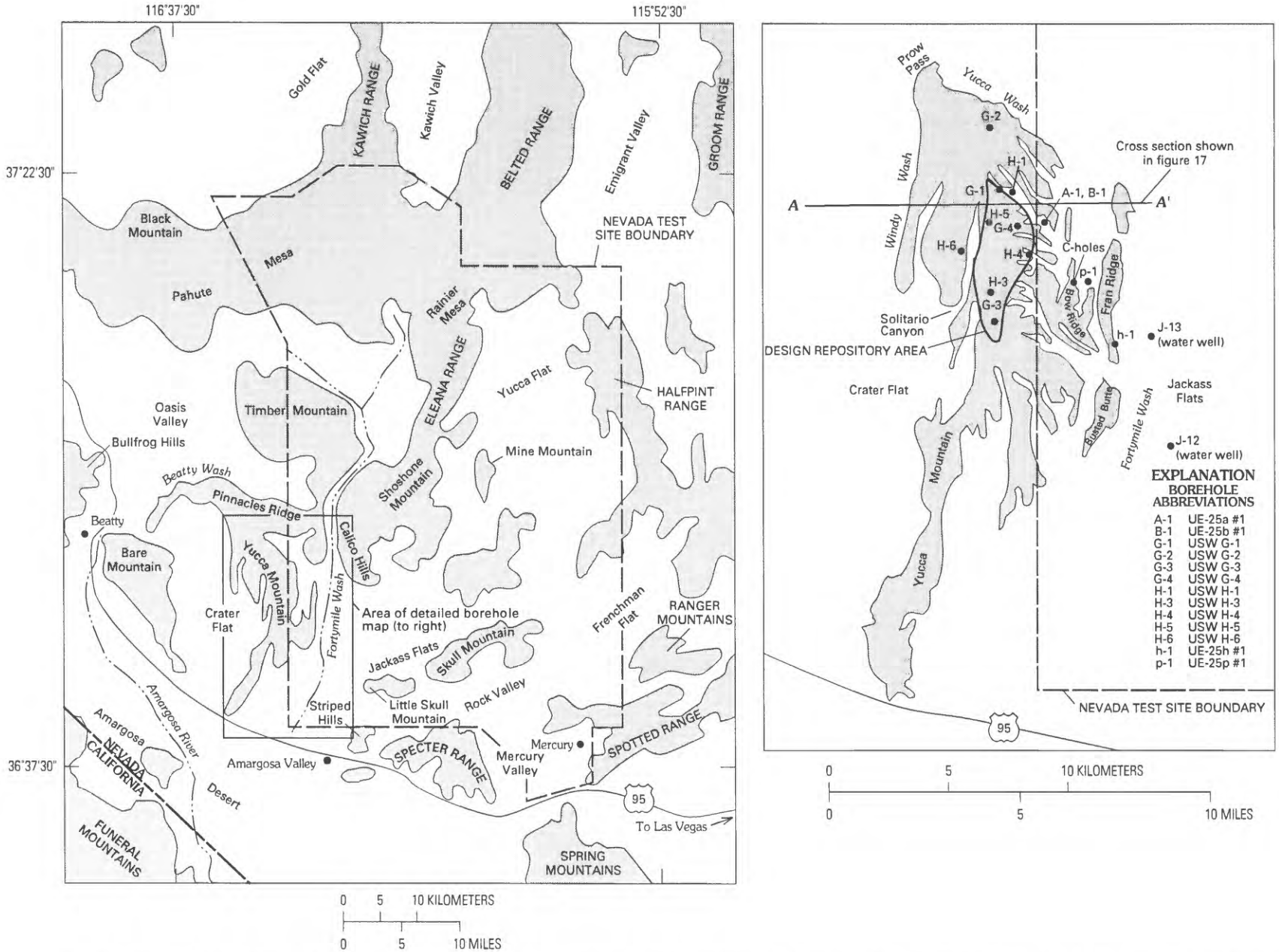

Figure 1.--Location of Nevada Test Site, Yucca Mountain, and boreholes completed in the saturated zone at Yucca Mountain, including the C-hole complex [modified from Frizzell and Shulters (1990); borehole locations from Scott and Bonk (1984) and Maldonado (1985); upland areas shaded].

Acknowledgments

The author would like to acknowledge the many people who preceded him on this project and without whose efforts this report would not have been possible. Many geologists from the U.S. Geological Survey and Fenix Scisson, Inc.[1], participated in logging the C-holes, monitoring water levels and conducting aquifer tests in these boreholes, and converting raw data collected at the C-hole complex into formats conducive to analysis and interpretation. Included among these people were B.A. Anderson, J.R. Erickson, D.L. Galloway, R.K. Waddell, and J.B. Warner. Lithologic logs and other geologic information were provided by R.W. Spengler, U.S. Geological Survey. Geophysical logs were provided by D.C. Muller, U.S. Geological Survey.

C-HOLE COMPLEX DEVELOPMENT AND INVESTIGATIONS

Boreholes UE-25c #1, UE-25c #2, and UE-25c #3 are 30.4 to 76.6 m apart at the land surface. Lines connecting the boreholes delineate a triangle with an area of 1,027 m^2 (fig. 2). Boreholes UE-25c #2 and UE-25c #3 were situated with respect to borehole UE-25c #1 on the basis of the assumed hydraulic-conductivity tensor at the complex site and the anticipated spread of the cone of depression during planned pumping tests (Devin L. Galloway, U.S. Geological Survey, written commun., 1989). Borehole UE-25c #2 was located with respect to borehole UE-25c #1 along the inferred major axis of hydraulic conductivity, and borehole UE-25c #3 was located along the inferred minimum axis, on the basis of the dominant structural trend in the vicinity of the C-hole complex.

Borehole Construction

Boreholes UE-25c #1, UE-25c #2, and UE-25c #3, each, were rotary drilled to a total depth of 914.4 m below land surface using air-foam, a mixture of compressed air, soap, and water. The drilling of borehole UE-25c #1 was started on August 13, 1983, and completed on September 18, 1983; the drilling of borehole UE-25c #2 was started on January 23, 1984, and completed on February 27, 1984; the drilling of borehole UE-25c #3 was started on March 27, 1984, and completed on April 26, 1984. Detailed histories of the drilling and testing of the C-holes are on file with the U.S. Geological Survey, Yucca Mountain Project Branch, Denver, Colo.

All three of the C-holes were telescoped downward. Boreholes UE-25c #1 and UE-25c #2 were drilled with a 91.4-cm-diameter bit from land surface to depths of 9.1 and 12.2 m, respectively; borehole UE-25c #3 was drilled with a 121.9-cm-diameter bit from land surface to a depth of 11.9 m (fig. 3). A 61.0-cm-diameter bit was used to extend borehole UE-25c #1 to a depth of 112.2 m, borehole UE-25c #2 to 97.5 m, and borehole UE-25c #3 to a depth of 96.0 m. A 37.5-cm-diameter bit then was used to extend borehole UE-25c #1 to a depth of 461.8 m and the other boreholes to a depth of 463.3 m. Borehole UE-25c #1 was extended to a depth of 911.4 m with a 25.1-cm-diameter bit and

---

[1]Use of firm names in this report is for identification purposes only and does not constitute endorsement by the U.S. Geological Survey.

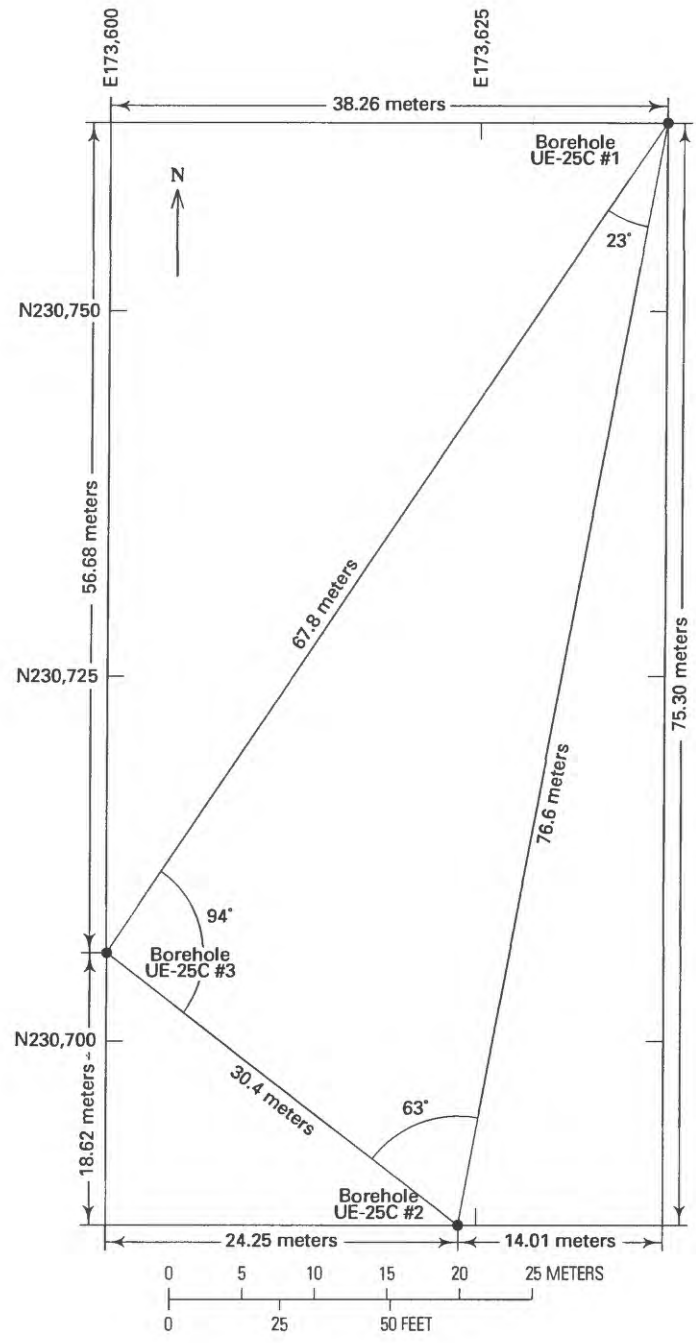

Figure 2.--Surface locations of boreholes UE-25c #1, UE-25c #2, and UE-25c #3. [Map is referenced to Nevada State Central Zone Coordinates.]

completed with a 22.2-cm-diameter bit; boreholes UE-25c #2 and UE-25c #3 were completed with a 25.1-cm-diameter bit. In the upper part of all three C-holes (above a depth of about 418 m in borehole UE-25c #1, about 416 m in borehole UE-25c #2, and about 417 m in borehole UE-25c #3), casing was set and grouted before changing to a smaller drill bit in order to prevent washing out of the borehole and to facilitate the circulation of drilling fluid and the return of cuttings. The lower part of each borehole was left uncased to make as much of the saturated zone as possible available for aquifer tests and to accommodate the 31.5-L/s submersible pump that was planned for use during these tests.

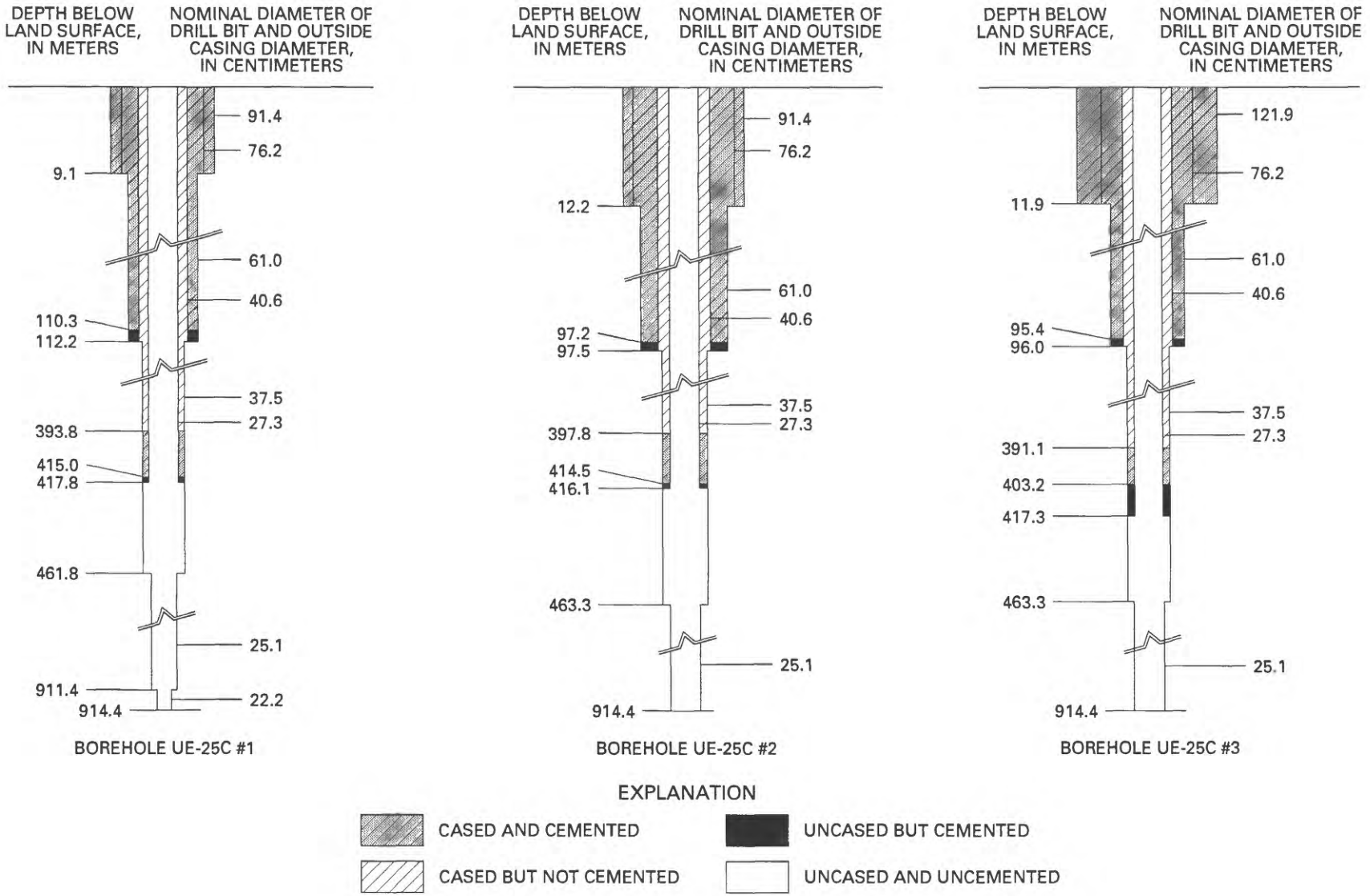

Figure 3.--Completion of boreholes UE-25c #1, UE-25c #2, and UE-25c #3.

Gyroscopic surveys made at 15-m intervals after the total depth was reached revealed that all three of the C-holes drifted substantially (fig. 4), most likely as a result of the drilling technique and equipment. Borehole UE-25c #1 drifted very little for the first 68.6 m, then drifted approximately north for the next 91.4 m, north-northeast for the next 106.7 m, northeast for the next 449.6 m, north-northwest for 83.8 m, and finally west-southwest for

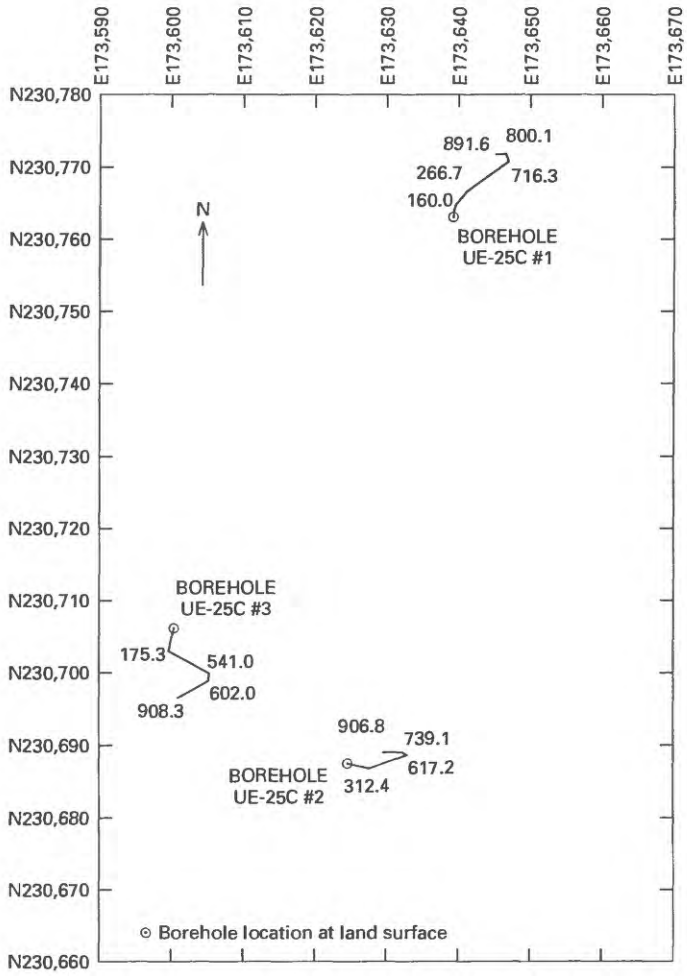

Figure 4.--Cumulative drift of boreholes UE-25c #1, UE-25c #2, and UE-25c #3.

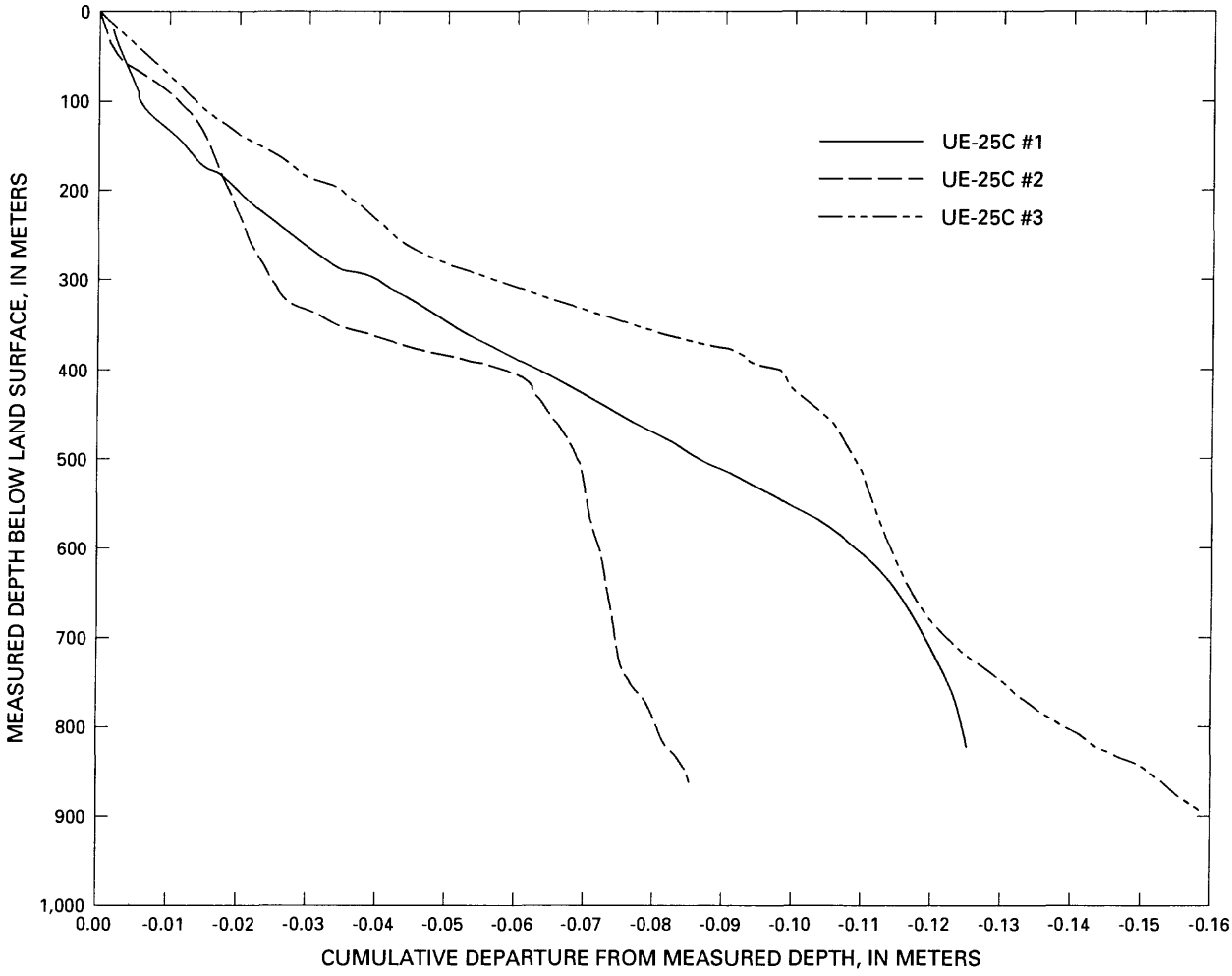

Figure 5.--Cumulative departure from measured depth in boreholes UE-25c #1, UE-25c #2, and UE-25c #3.

76.2 m and presumably to the bottom of the hole. The cumulative departure from the measured depth was about -0.12 m (fig. 5). Borehole UE-25c #2 drifted east-southeast for the first 312.4 m, east-northeast for the next 304.8 m, northwest for the next 68.5 m, and west-southwest for the bottom 228.7 m. The cumulative departure from the measured depth was about -0.085 m. Borehole UE-25c #3 drifted south-southwest for the first 175.3 m, southeast for the next 365.7 m, approximately south for the next 61.0 m, and southwest for the bottom 312.4 m. The cumulative departure from the measured depth was about -0.16 m. The principal effect of the borehole drift was in the determination of the orientation of stratigraphic and structural planes and the hydraulic gradient between the boreholes; measured depths on lithologic and geophysical logs and measured water levels were not affected appreciably by the drift.

Caliper logs indicate that all three of the C-holes contain thick intervals where the borehole diameter exceeded that of the drill bit and no intervals where the borehole diameter was less than that of the drill bit (fig. 6). About 70 percent of the upper 366 m in all three boreholes was enlarged 5 to 32 cm beyond the diameter of the drill bit. In borehole

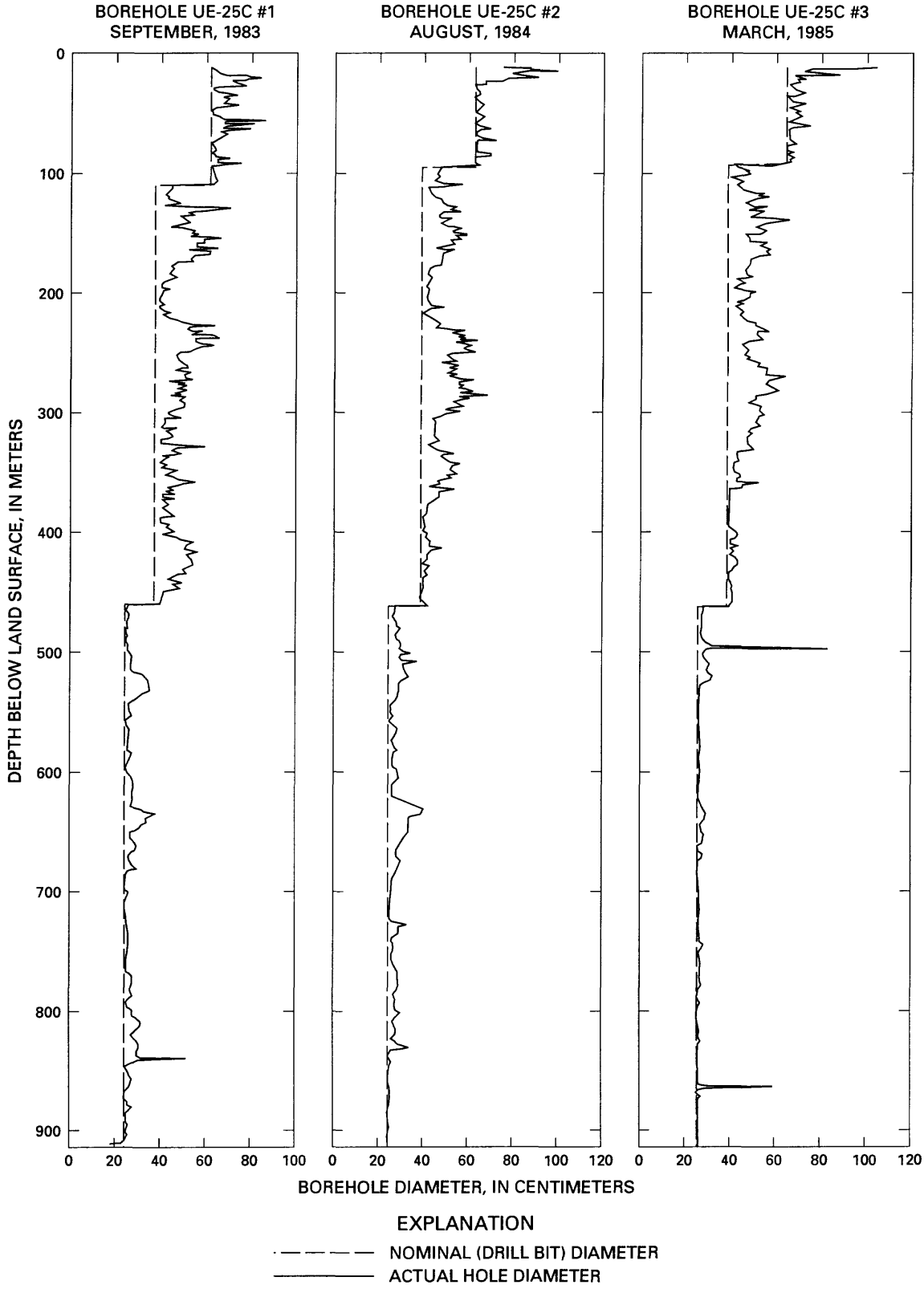

Figure 6.--Caliper logs of boreholes UE-25c #1, UE-25c #2, and UE-25c #3.

UE-25c #1, this enlargement continued to a depth of 460 m. Below a depth of 460 m, borehole diameters generally were close to those of the drill bit, except for three discrete zones between depths of 460 and 550 m, 625 and 675 m, and 725 and 865 m, where the boreholes were again enlarged. The consistent patterns of enlargement among the three C-holes are indicative of lithologic and structural controls. The enlarged intervals correspond to fractured, faulted, or nonwelded to partially welded intervals within the bedrock that were recorded on other geophysical logs and on lithologic logs.

Sample Collection

Samples of water were collected for chemical analyses of major, minor, and trace elements, stable isotopes (deuterium, oxygen-18, and carbon-13), and radioactive elements (tritium and carbon-14). The carbon-14 concentration was determined for calculation of the apparent age of the water. Measurements of the pH, specific conductance, bicarbonate concentration, and temperature were made in the field and compared against laboratory determinations of these properties. Samples were analyzed by the U.S. Geological Survey laboratory in Arvada, Colo., according to methods described by Skougstad and others (1979). All samples were collected from open boreholes after the final pumping tests were completed in each borehole.

As a check against contamination of the samples by drilling fluid, a lithium chloride tracer was added to the drilling fluid during the completion and testing of the C-holes. The lithium chloride tracer was selected because the background concentration of lithium in the water from well J-13, the well used to supply water during the drilling and testing of the C-holes, was known to be 0.040 mg/L (Benson and McKinley, 1985). Samples considered to be representative of uncontaminated ground water in the C-holes were not collected until lithium concentrations were equal to or almost the same as background concentrations.

Lithium concentrations in fluids added to and discharged from the C-holes during drilling, as determined by the drilling contractor, REECO, are shown in figure 7. These samples were collected every 9.1 m as the drilling progressed. Initial lithium concentrations ranged from 13 to 26 mg/L, but substantial decreases began occurring in boreholes UE-25c #1 and UE-25c #2 at the water table (a depth of about 400 m) and in borehole UE-25c #3 at about 129 m above the water table. In the first two boreholes, the initial substantial decrease in lithium easily can be attributed to dilution by ground water in the saturated zone. In borehole UE-25c #3, however, either a zone of perched water was encountered, or the borehole intercepted downward percolating water from the discharge pit for borehole UE-25c #2, which had been located at a site near where borehole UE-25c #3 was drilled.

Bit cuttings were collected continuously during the drilling of all three C-holes. The method used for collecting the cuttings consisted of installing a 5- by 5-cm piece of angle iron in the center of and about 0.3 m from the end of the discharge line. All cuttings hitting the angle iron were deflected downward into a bucket positioned under the discharge line. Every time the borehole was advanced 3 m, the bucket was dumped, and a representative sample of the cuttings in the bucket was collected for initial descriptions onsite. Additional samples were saved for later, more detailed analyses by U.S. Geological Survey personnel.

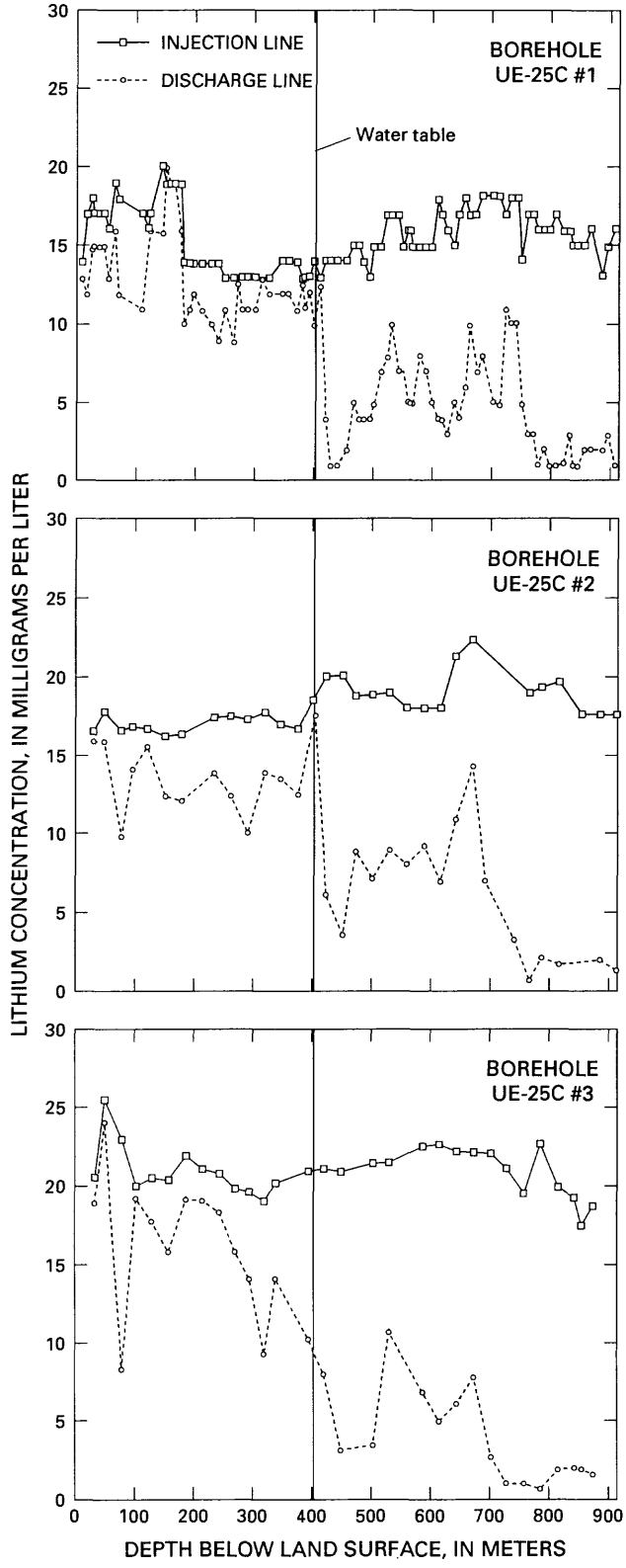

Figure 7.--Concentrations of lithium in fluids injected into and discharged from boreholes UE-25c #1, UE-25c #2, and UE-25c #3 during drilling.

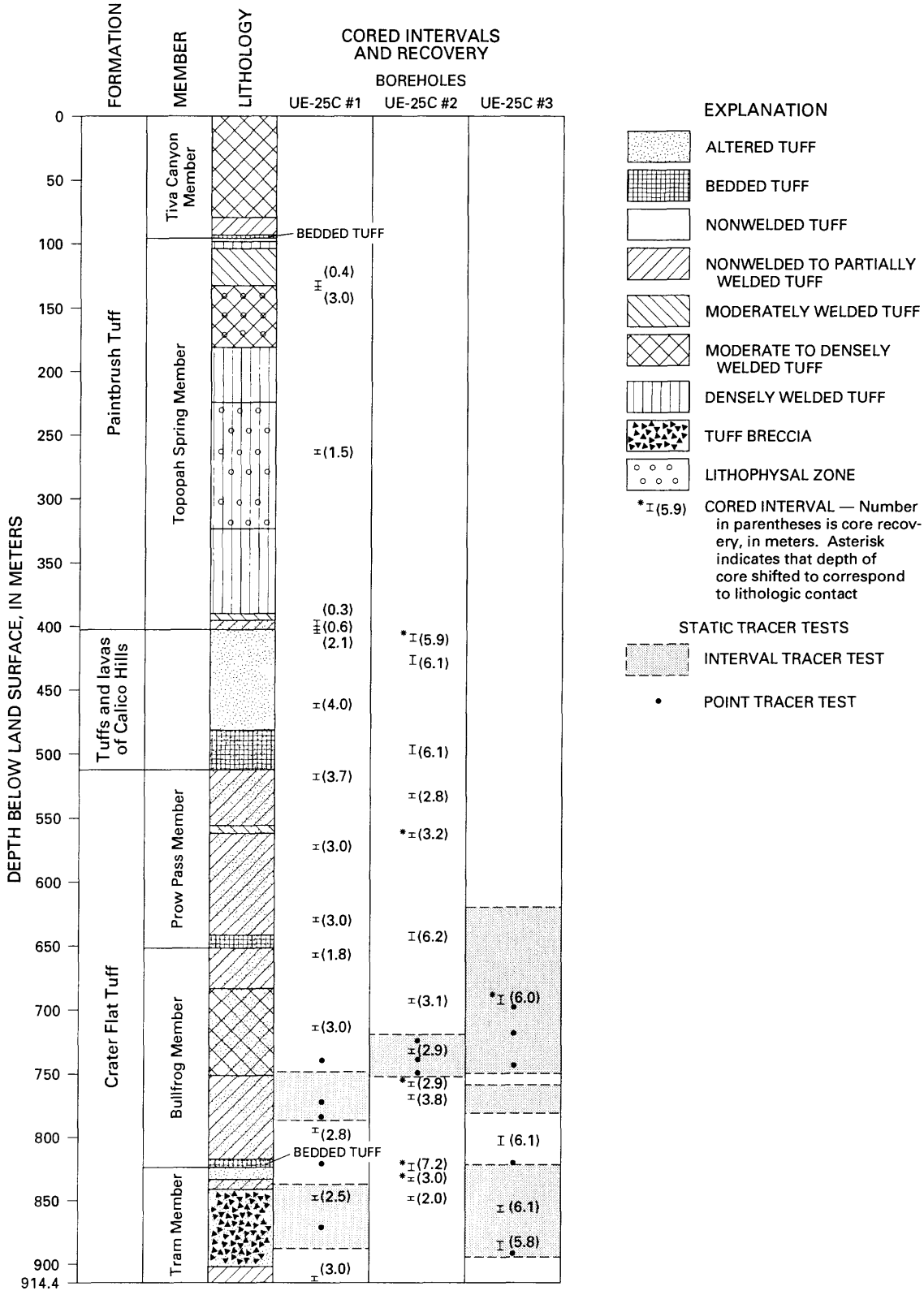

Figure 8.--Cored intervals and recovery in boreholes UE-25c #1, UE-25c #2, and UE-25c #3, and location of static tracer tests.

The drilling periodically was interrupted to collect samples of core that, when compiled, would be representative of all geologic intervals penetrated in the C-holes. The core was obtained using a 10.2-cm-diameter, diamond-tipped core bit and barrel. Cored intervals generally were 3 or 6 m long, but one 9-m-long interval was drilled. A total of 114.3 m of core was collected for geologic descriptions and hydrologic analyses (fig. 8). Selected pieces of core were preserved for later determination of the pore-water saturation and chemistry.

Lithologic and Geophysical Logs

Lithologic logs of the C-holes were prepared by Richard W. Spengler (U.S. Geological Survey, written commun., 1989). The logs were prepared from visual inspections of the drill cuttings and core, petrographic analyses of thin sections, and television-camera tapes.

Geophysical logs were run in the C-holes to: (1) Provide details about borehole construction; (2) refine lithologic contacts; (3) correlate geologic units among boreholes; (4) establish the depth of fracture and fault zones; (5) determine the strike and dip of fractures, faults, and bedding; (6) determine the physical properties of rocks; and (7) locate permeable or water-yielding intervals. All geophysical logs that were run are listed in table 2.

Only geophysical logging techniques that were used for geological or hydrological interpretation are described further. These include caliper, temperature, resistivity, borehole-compensated gamma-gamma, epithermal-neutron, borehole compensated acoustic, acoustic-televiewer, and television-camera logging. These logging techniques and most others listed in table 2 are described thoroughly by Keys (1988).

Caliper tools measure the diameter of boreholes. In holes larger than 10 cm in diameter, such as the C-holes, a six-arm tool is used at Yucca Mountain (Muller and Kibler, 1984). This tool measures three equiangular diameters and the average diameter. Data from the caliper log were used to calculate borehole volumes for cementing casing, to identify unstable zones where the borehole is washed out or caved, to identify fractured intervals, to indicate the roughness of the borehole walls, to interpret tracejector surveys, and to correct for borehole effects on data measured with other logging tools.

Temperature logs were obtained by lowering a thermistor down the borehole under pumping and nonpumping conditions. Temperature logs routinely are used to determine thermal gradients in boreholes. During pumping or static conditions, deflections in the temperature-versus-depth profile also can indicate where water is flowing into or out of a borehole and the direction the water is moving within the borehole (Erickson and Waddell, 1985). Thus, in this study, temperature logs were used, together with tracejector (borehole-flow) surveys, to identify water-producing zones in the C-holes.

Table 2.--*Geophysical logs run in boreholes UE-25c #1, UE-25c #2, and UE-25c #3*

Geophysical log	Primary uses of log	Depth interval (meters)[1]		
		Borehole UE-25c #1	Borehole UE-25c #2	Borehole UE-25c #3
	BOREHOLE CONSTRUCTION			
Gyroscopic	Deviation from vertical	0 to 914	0 to 914	0 to 914
Caliper	Borehole diameter, fracture zones	12 to 914	12 to 912	12 to 914
Nuclear annulus	Locating channels in cement	None	305 to 414	296 to 426
Nuclear cement top locator	Top of lowermost seal	366 to 415	None	332 to 402
3-D velocity	Interpreting nuclear annulus logs	302 to 419	304 to 413	331 to 401
	FORMATION CHARACTERISTICS			
Temperature	Thermal gradient and water inflow zones	0 to 911	2 to 914	2 to 914
Fluid density	Location of water table	379 to 420	321 to 408	387 to 411
Spontaneous potential	Lithology, shale content, water quality	399 to 909	417 to 912	417 to 913
Resistivity, induction	Effective porosity, water quality	10 to 909	13 to 913	13 to 913
Resistivity, focused	Effective porosity, water quality	405 to 909	417 to 911	407 to 913
Resistivity, dielectric	Effective porosity, water quality	112 to 913	98 to 913	95 to 914
Dielectric constant	Effective porosity, lithology	112 to 913	98 to 913	95 to 914
Gamma ray	Distinguishing sandstone from shale	9 to 908	12 to 913	12 to 912
Spectral gamma	Radionuclides	0 to 914	2 to 914	2 to 914
Gamma-gamma, borehole compensated	Bulk density, total porosity, storativity	112 to 907	98 to 914	97 to 914
Density, dual proximity	Total porosity in unsaturated zone	3 to 110	6 to 96	3 to 95
Epithermal neutron	Total porosity, moisture content	8 to 912	12 to 914	96 to 914

Table 2.--*Geophysical logs run in boreholes UE-25c #1, UE-25c #2, and UE-25c #3*--Continued

Geophysical log	Primary uses of log	Depth interval (meters)[1]		
		Borehole UE-25c #1	Borehole UE-25c #2	Borehole UE-25c #3
	FORMATION CHARACTERISTICS--Continued			
Acoustic, compressional, borehole compensated	Total porosity, lithology, storativity	418 to 914	417 to 910	501 to 914
Acoustic, shear	Elasticity	468 to 908	None	None
Seismic velocity (geophone)	Bulk density	0 to 908	0 to 910	0 to 911
Acoustic fraclog, borehole compensated	Location of fractures	400 to 910	416 to 910	None
Acoustic televiewer	Location and orientation of fractures	416 to 903	416 to 913	417 to 914
Television camera	Location and strike of fractures	399 to 903	401 to 852	None

[1]For many logs, the depth interval indicated is a composite of two to five segment runs.

Resistivity is a measure of the resistance of the rocks around a borehole to the transmission of an electric current through the rocks. Standard induction tools transmit an alternating current at a frequency of about 20 kilohertz, which induces an electromagnetic flux that is inversely proportional to the resistivity of the rocks. Focused resistivity is measured with a tool that directs a sheet-like current perpendicular to the borehole. This current results in a voltage decrease between two electrodes that is proportional to the resistivity. The induction-resistivity tool used at Yucca Mountain has a 152-cm radius of investigation; the focused-resistivity tool has an 81-cm radius of investigation. For rocks with large resistivity, a third resistivity measurement, dielectric resistivity, was made in the C-holes. Dielectric resistivity is measured concurrently with dielectric permittivity with a tool that induces an electric current into the rocks at a frequency of 47 megahertz (Muller and Kibler, 1984). The dielectric permittivity is used to calculate the dielectric constant. Because the minerals in most rocks present at Yucca Mountain are insulators, electric current there is transmitted mainly by fluids in the pores and fractures within the rock. Thus, the resistivity logs are particularly sensitive to permeable, water-yielding zones and primarily indicate changes in effective porosity. However, because borehole geometry, drilling fluids, the presence of zeolites, clays,

or metallic minerals in a rock, and changes in rock type also can affect resistivity, the resistivity logs were compared with the caliper, gamma-gamma, epithermal-neutron, and acoustic logs to interpret anomalies identified on the resistivity logs.

Three logs primarily used to determine porosity are the borehole-compensated gamma-gamma log, the epithermal-neutron log, and the borehole-compensated acoustic log. According to Keys (1988), the gamma-gamma and epithermal-neutron logs indicate total primary and secondary porosity, whereas the acoustic log indicates total primary porosity (it is not sensitive to fractures). Additionally, the gamma-gamma and acoustic logs can be used to calculate the bulk modulus of elasticity (Muller and Kibler, 1984), a property that can be used to calculate the storativity.

The borehole-compensated gamma-gamma log measures electron density, but it is calibrated to indicate bulk density. The density tool bombards the formation with gamma rays from a cesium-137 or cobalt-60 source and counts gamma rays backscattered from collisions with electrons at two detectors located at various distances from the source (Muller and Kibler, 1983; 1984). The gamma-gamma tool is a sidewall tool designed to minimize borehole effects. Changes in density primarily are due to changes in porosity and water content, but they also can be caused by rock alteration. Hence, the gamma-gamma logs were compared with the resistivity, epithermal-neutron, and acoustic logs to interpret anomalies. Porosity was calculated from the gamma-gamma log assuming the grain density to be that of sandstone. For each of the C-holes, porosity determined from the gamma-gamma log was plotted alongside porosity determined from the epithermal-neutron log to substantiate the determined porosity values.

Epithermal-neutron logs are produced by bombarding the formation with neutrons from a radioactive source, such as a mixture of plutonium-239 and beryllium-9 or a mixture of americium-241 and beryllium-9, and counting the backscattered, high-energy neutrons arriving at a detector some distance away from the source. The tool is attached to the sidewall to minimize borehole effects. The primary scattering mechanism is the collision of neutrons with hydrogen ions in the formation water. Thus, the tool responds primarily to porosity. Assuming that the siliceous volcanic rocks at Yucca Mountain have the same density as quartz sandstone (2.65 g/cm^3), it is possible to convert the epithermal-neutron log trace to show porosity values directly (Muller and Kibler, 1983).

Acoustic logs are obtained by measuring the time interval for sound waves to travel a known distance along the borehole wall parallel to the borehole axis. This distance is divided by the elapsed time to determine the velocity of the formation (Muller and Kibler, 1984). The logging tool has two traces: compressional waves and shear waves. The compressional wave is the fastest wave traveling through the rock and is detected automatically by the logging tool as the first signal to arrive at the receiver. The shear wave arrives later and is interpreted by examining displays of the full wave train. Borehole-compensated acoustic tools use two transmitters and two receivers. Travel times between each transmitter and receiver are averaged in calculating acoustic velocities. These velocities are sensitive to variations in the density of rock and, hence, can be used to detect changes in the degree of welding and the presence of lithophysal cavities. In this study, the acoustic logs were used only to calculate the bulk modulus of elasticity and storativity.

The acoustic televiewer and television camera are used to detect fractures. The acoustic televiewer scans the surface of the borehole by moving a horizontally rotating transducer along the borehole axis. The device is oriented to magnetic north, making it possible to determine the strike and dip of fractures intersected by the borehole. The amplitude of the reflected signal is displayed as a photograph, on which the fractures show up as sinusoidal curves (fig. 9). A Levenberg-Marquardt routine [International Mathematical and Statistical Libraries, Inc. (IMSL), 1982] was applied to a digitized televiewer trace of each fracture to determine its strike and dip.

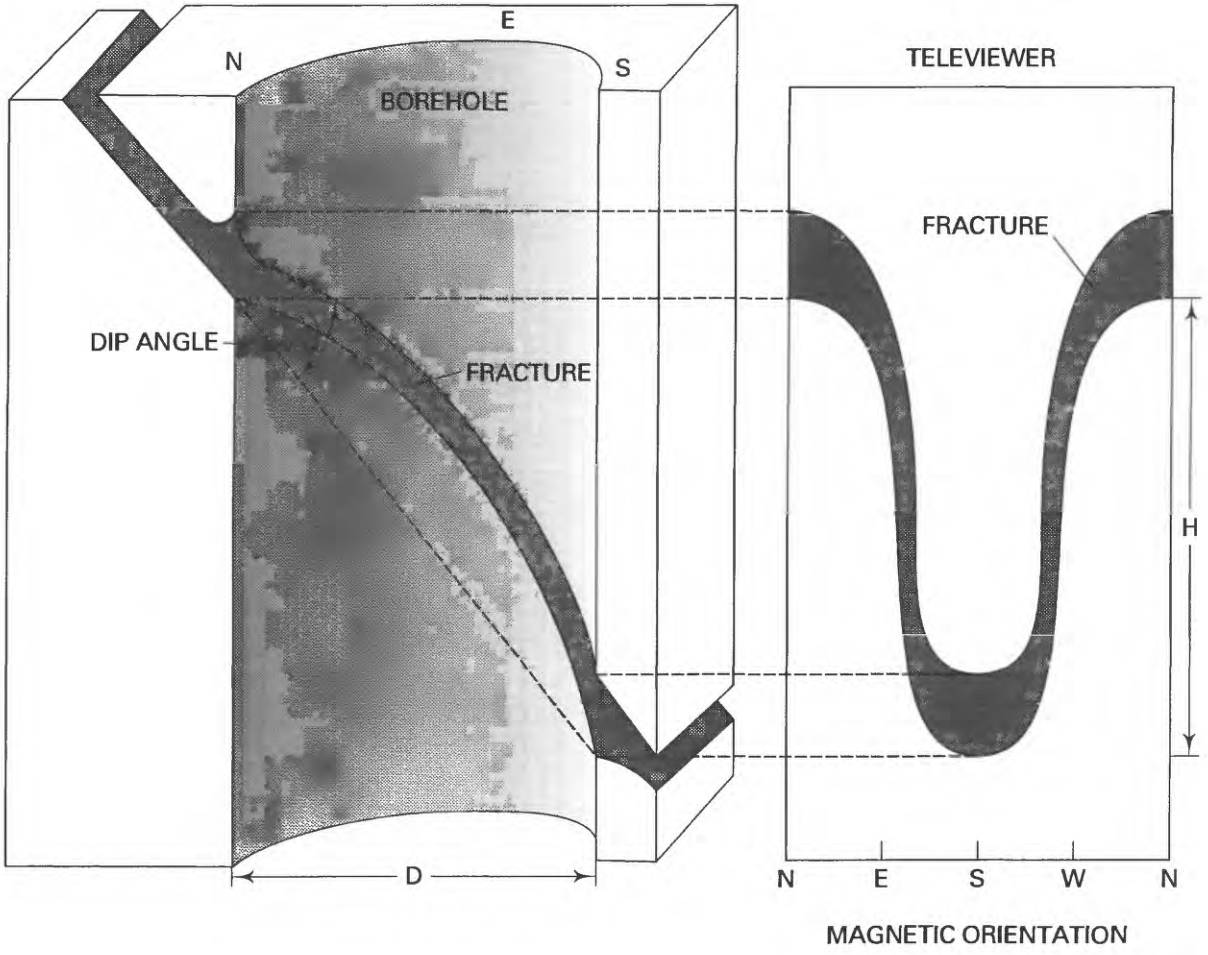

Figure 9.--Three-dimensional view of a fracture intersecting a borehole and appearance of the same fracture on an acoustic-televiewer log. D is the borehole diameter, and H is the length of the fracture intercept in the borehole (from Keys, 1988).

The television camera is an underwater video camera fitted with a compass for orientation and a light for illumination. A fish-eye lens provides a 360° view of the borehole walls. A videotape record is made as the camera is moved vertically along the borehole axis. The quality of the videotape depends on the turbidity of the fluid in the borehole, the intensity and contrast of the lighting, the smoothness of the borehole walls (abundant lithophysae or rough

texture, for example, can obscure fractures), and the straightness of the borehole (in a skewed borehole, the camera is forced to one side, which causes part of the borehole to be poorly illuminated or omitted from view). Strike and dip azimuths can be determined from the videotapes, but the dip angle cannot be determined quantitatively. In general, more fractures can be detected on television-camera tapes than on acoustic-televiewer logs.

Water-Level Measurements

Boreholes UE-25c #1, UE-25c #2, and UE-25c #3 were drilled to determine the hydraulic characteristics of the rocks within the saturated zone at Yucca Mountain and, as such, were not completed ideally as piezometers (Robison and others, 1988). For much of the time after they were drilled, these boreholes have had equipment or packers installed for testing that made monitoring of water levels unfeasible. However, it has been possible intermittently to monitor water levels in the C-holes, using either steel tapes, a single-conductor, armored cable (referred to as an "Iron Horse"), or a four-conductor, armored cable. The single-conductor cable is equipped with an electrical float switch to detect the water level; the four-conductor cable has been equipped with either a float switch or a pressure transducer to detect the water level. All of the water-level monitoring devices are calibrated routinely, and correction factors relating measured depths to water to actual depths are given by Robison and others (1988).

Prior to March 1985, the C-holes were open from the bottom of the casing or cement to the total depth, and measured water levels were a composite of the hydraulic heads throughout the open interval. In March and April 1985, dual-element, straddle packers were installed in borehole UE-25c #1 between depths of 796 and 799 m and in borehole UE-25c #3 between depths of 751 and 754 m, and a bridge plug was placed in borehole UE-25c #2 between depths of 756 and 758 m (Devin Galloway, U.S. Geological Survey, written commun., 1988). Measurements of hydraulic head in boreholes UE-25c #1 and UE-25c #3 have been made periodically since 1985 above and below the packers to determine if a vertical hydraulic-head gradient exists at the C-hole complex.

Tracejector Surveys

Tracejector surveys were made in the C-holes during pumping tests to determine which intervals in each borehole were producing water and the relative contributions of each interval. As described by Blankennagel (1967), a tracejector survey involves lowering a logging device below the pumping water level, injecting a slug of radioactive iodine-131 into the well and monitoring the movement of the centroid of the slug between the lower and upper detectors on the logging device. The velocity of flow for the interval between the lower and upper detectors is calculated by dividing the distance between the detectors by the time required for the centroid of the slug to travel from the lower to the upper detector. This velocity is then multiplied by the average cross-sectional area of the test interval, as recorded on the caliper log, to determine a flow rate for the interval. The logging device then is lowered down the borehole, and the test is repeated until the entire borehole below the pumping water level has been surveyed. The percentage of

flow contributed by each test interval is calculated by dividing the test interval flow rate by the sum of the flow rates for all of the test intervals in the well. Tracejector surveys were made in borehole UE-25c #1 between depths of 465 and 879 m, in borehole UE-25c #2 between depths of 457 and 767 m, and in borehole UE-25c #3 between depths of 469 and 874 m. Pumping rates during the three surveys, respectively, were 14.1, 16.9, and 26.5 L/s.

Static Tracer Tests

Although tracejector surveys during pumping tests yield information about the distribution of water production zones as an aquifer is being stressed, these tests cannot provide information on rates and directions of water movement in an undisturbed aquifer. Static (nonpumping) tests involving the injection of an iodine-131 tracer can provide information about water movement in an undisturbed aquifer (Erickson and Waddell, 1985).

Two types of static tracer tests were made in the C-holes, point tracer tests and interval tracer tests. In the point tracer tests, a small quantity (approximately 1 mCi/mL) of iodine-131 was ejected at a selected depth, and the position of the centroid of the slug in the borehole, as indicated by a gamma-ray detector, was recorded during repeated logging runs during the course of 1 to several hours. In the interval tracer tests, a continuous stream of iodine-131 was ejected into a selected interval as the logging tool was lowered through it. Repeated logging runs then were made through the test interval during a period of 0.5 to 3 days. Changes in the position and shape of the logs from these tests were used to indicate points of water egress or ingress, intraborehole-flow directions, and rates of water movement in the C-holes.

Static tracer tests were made in boreholes UE-25c #1 and UE-25c #3 above and below the packers. These tests were made in borehole UE-25c #2 only in the interval above the bridge plug. A total of 6 interval tracer tests and 13 point tracer tests were made in the C-holes, as indicated in figure 8. The results of these tests and the nonpumping temperature surveys indicate a complex pattern of undisturbed ground-water movement at the C-hole complex. These tests are not discussed further in this report.

Core Analyses

Laboratory analyses were made on nine core samples from the tuffs and lavas of Calico Hills and the Prow Pass, Bullfrog, and Tram Members of the Crater Flat Tuff in borehole UE-25c #1. The analyses were done by Holmes and Narver, Inc., a contractor for the U.S. Department of Energy. Plugs of core sent for testing were analyzed for bulk density, moisture content, porosity, grain density, saturated horizontal and vertical permeability, moisture tension, and saturation. The analyzed bulk density and moisture content were used to calculate dry bulk density. Porosity was calculated from the grain density and dry bulk density and also was determined by helium injection. Unsaturated vertical hydraulic conductivity was determined from the saturated vertical permeability, moisture tension, and saturation.

The laboratory analyses followed standard procedures of the American Society for Testing and Materials (ASTM) and the American Petroleum Institute (API). Bulk density was determined according to ASTM procedures D1188-71 and D2216-71 (American Society for Testing and Materials, 1971). Moisture content was determined according to ASTM procedure D2216-71. Grain density and helium porosity were determined according to API procedure RP40 (American Petroleum Institute, 1960).

Values of saturated permeability were calculated from helium-injection and water-injection tests. The helium-injection test consisted of injecting helium into the sample in pressure increments of 6.896×10^4 Pa, starting at 6.896×10^4 Pa, and increasing to 6.896×10^5 Pa, and measuring the helium-flow rate through the sample. Permeability at each injection pressure was calculated from the pressure gradient across the sample, the helium-flow rate, and the dimensions of the sample. A linear-regression analysis then was made using permeability as the dependent variable and the inverse of the injection pressure as the independent variable. The y-intercept of the regression plot was taken to be the permeability of the sample. Anomalous values believed to be caused by a switch in the meter used to measure the helium-flow rate were omitted from the regression analyses. For six samples, measurement errors prevented determination of a single value of permeability, and a range in possible values (determined by dividing the data into two sets and performing separate regressions on each set) was obtained.

Saturated water-injection tests were done on the same core samples used for the helium-injection tests. The analytical procedure for the water-injection tests was identical to the procedure for the helium-injection tests, with the exception that water was substituted for helium. For the water-injection tests, the values of permeability determined at the different injection pressures were averaged, even though linear trends in permeability with pressure were obtained for three of the samples and could indicate a problem with the analytical technique.

In general, permeability values determined by the water-injection tests consistently were smaller than those determined by the helium-injection tests. One possible explanation for this phenomenon is the presence of swelling clays in the sample that would tend to decrease permeability in the presence of water. If this is true, then the water-injection tests provided more accurate results than the helium-injection tests under conditions that would be present in the saturated zone.

Permeability is a scale-dependent hydrologic property and can differ by orders of magnitude depending on whether it is determined by laboratory tests, field tests, or numerical modeling (Dagan, 1986). The reason for these differences is interpreted to be the volume of rock tested by each analytical method. Because values of permeability given in this report either are laboratory-determined or correlate with laboratory-determined values, they are what Dagan (1986) termed pore-scale permeability. According to Dagan (1986) pore-scale permeability values are relevant only at distances of less than a meter from the boreholes (or outcrops) from which analyzed samples were obtained. In contrast, permeability values obtained by field tests (local-scale permeability) are applicable on the scale of formation thicknesses (typically 10 to 100 m), and permeability values obtained by numerical modeling are applicable on a regional scale.

Unsaturated hydraulic conductivity was determined by mercury-injection (porosimetry) tests. The mercury-injection tests involved placing a sample in a porosimeter chamber, evacuating the air from the chamber, and injecting mercury into the sample at fixed pressure increments. Using equations given by Weeks and Wilson (1984), the moisture tension and saturation of the sample were calculated and plotted against each other. For three of the samples, these plots were insufficient to determine unsaturated hydraulic conductivity. For the remaining six samples, relative unsaturated hydraulic conductivity was calculated by a method described by Brooks and Corey (1964, 1966) and modified by Mualem (1976). Plots of the relation between effective unsaturated vertical hydraulic conductivity and moisture tension in the Crater Flat Tuff, based on the values of relative unsaturated hydraulic conductivity determined for the samples from borehole UE-25c #1, are shown in figure 10. This information is presented without further elaboration because this report deals mainly with the saturated zone.

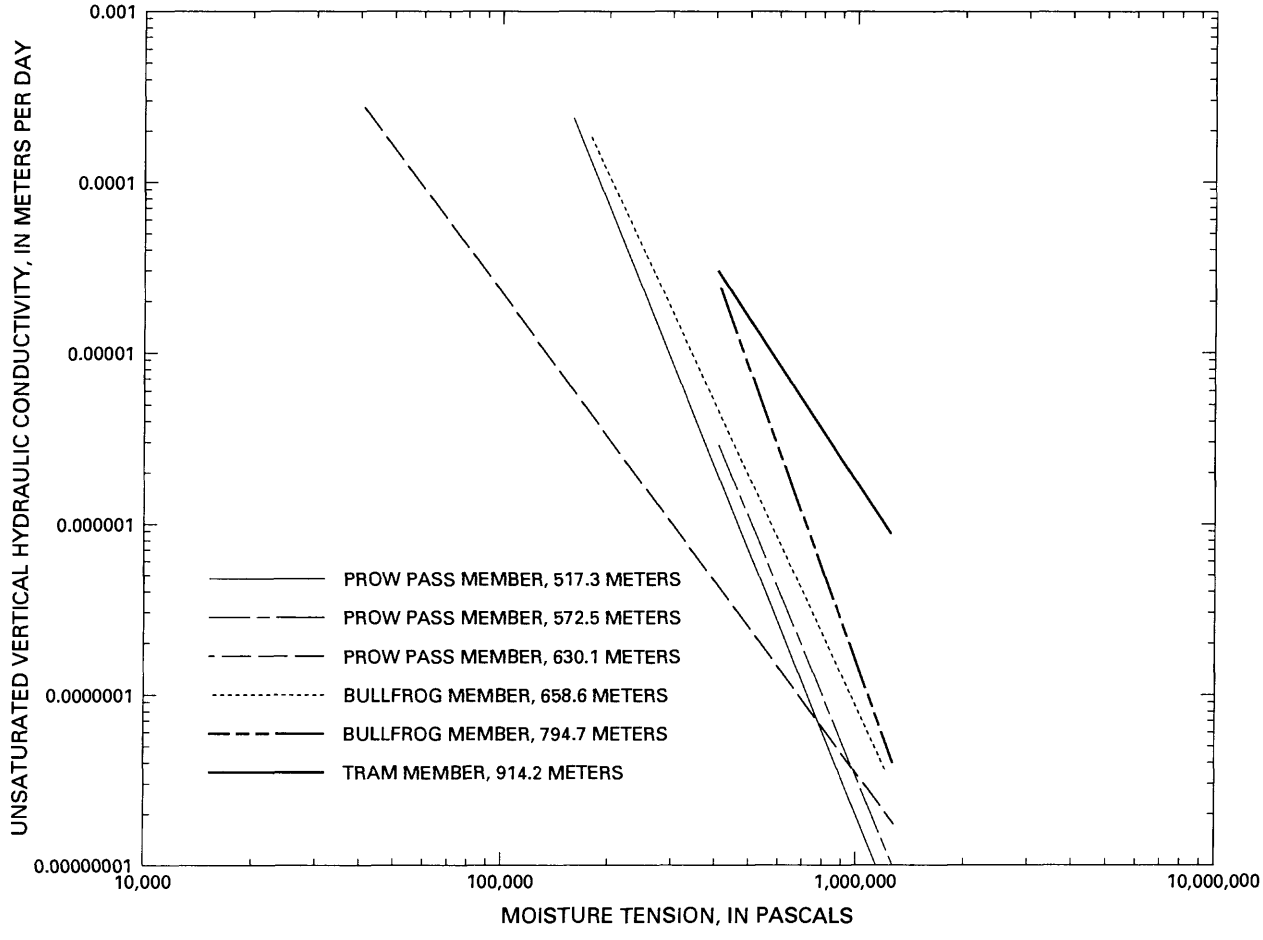

Figure 10.--Relation of unsaturated vertical hydraulic conductivity to moisture tension in core samples from the Crater Flat Tuff in borehole UE-25c #1.

Aquifer Tests

Pumping tests and packer-injection tests were conducted in the C-holes to develop them as wells, identify productive zones, and determine hydrologic properties of the geologic units that were penetrated. These tests had not been analyzed completely by the time this report was written (1989). Summary information for these tests, however, is given in this report, and the drawdown curves are used qualitatively to support the conceptual model of the ground-water flow system presented herein.

A pumping test was conducted in each of the C-holes immediately after drilling of the borehole was completed. In September 1983, borehole UE-25c #1 was pumped at 15.5 L/s for about 10 min, which lowered the water level in the borehole to near that of the pump intake, after which the pumping rate was decreased to 10.7 L/s, and the borehole was pumped for about 1.25 days with little additional drawdown. A plot of drawdown as a function of time during the pumping test is shown in figure 11. The interval tested, 418 to 914 m, included all geologic units from the tuffs and lavas of Calico Hills down to the Tram Member of the Crater Flat Tuff (geologic units present at the C-hole complex are summarized in figure 8 and discussed later in this report).

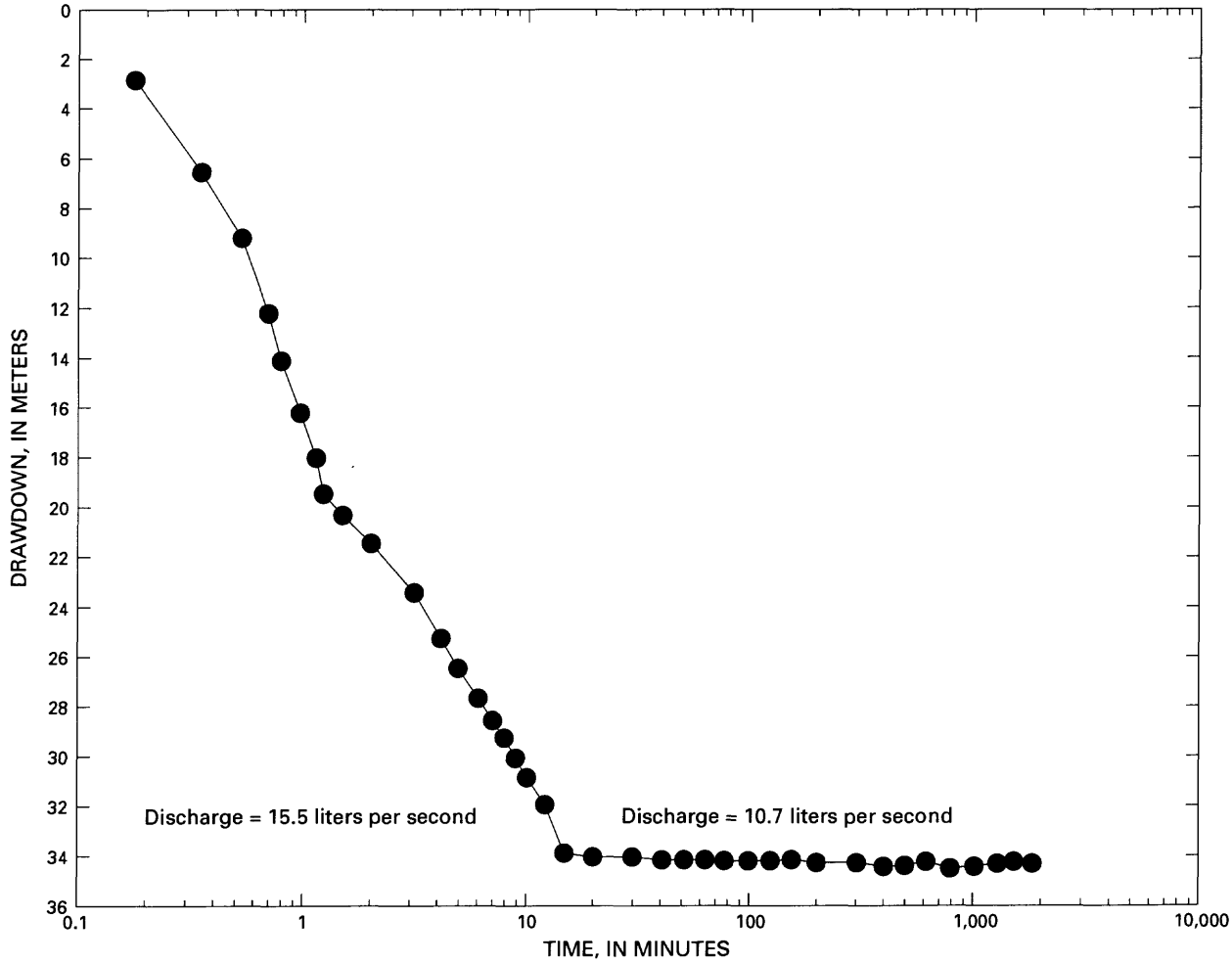

Figure 11.--Drawdown as a function of time in borehole UE-25c #1, September 1983.

A pumping test in borehole UE-25c #2 was conducted in March 1984, using borehole UE-25c #1 as an observation well. A dual-element straddle packer was placed in borehole UE-25c #1 between depths of 769 and 791 m (in the Bullfrog Member), and the borehole was monitored above, between, and below the packers. The pumped well, borehole UE-25c #2, was open from 416 to 914 m; the open interval extended from the tuffs and lavas of Calico Hills down to the Tram Member of the Crater Flat Tuff. The pumping rate during the test was 15.5 L/s, and the pumping period was about 7 days. Drawdown as a function of time in the pumped and observation wells during the test is shown in figure 12.

A pumping test in borehole UE-25c #3 was conducted in November 1984, using boreholes UE-25c #1 and UE-25c #2 as observation wells. For this test, the packers placed in borehole UE-25c #1 during the March 1984 pumping test were left in place, and water levels in borehole UE-25c #1 were monitored above, between, and below the packers. A dual-element straddle packer was placed in borehole UE-25c #2 between depths of 720 and 754 m (in the Bullfrog Member), and water levels in borehole UE-25c #2 were monitored above and

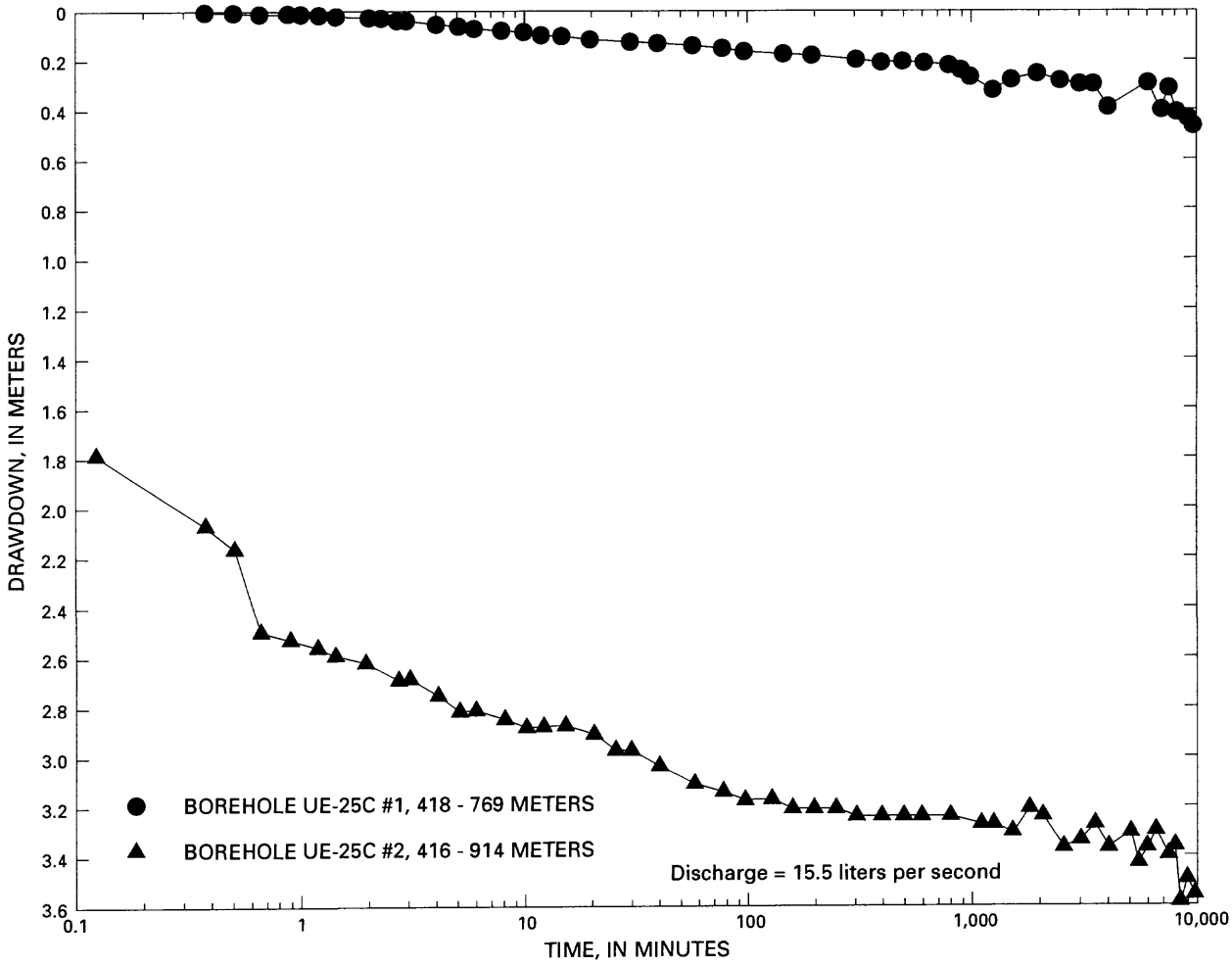

Figure 12.--Drawdown as a function of time in boreholes UE-25c #1 and UE-25c #2, pumping test in borehole UE-25c #2, March 1984.

between the packers (a malfunctioning transducer prevented water-level monitoring below the packers). The pumped well, borehole UE-25c #3, was open from 417 to 914 m, from the tuffs and lavas of Calico Hills to the Tram Member of the Crater Flat Tuff. The pumping rate during the test was 26.5 L/s, and the pumping continued for about 2 weeks. Drawdown as a function of time in the pumped and observation wells during the test is shown in figures 13 and 14.

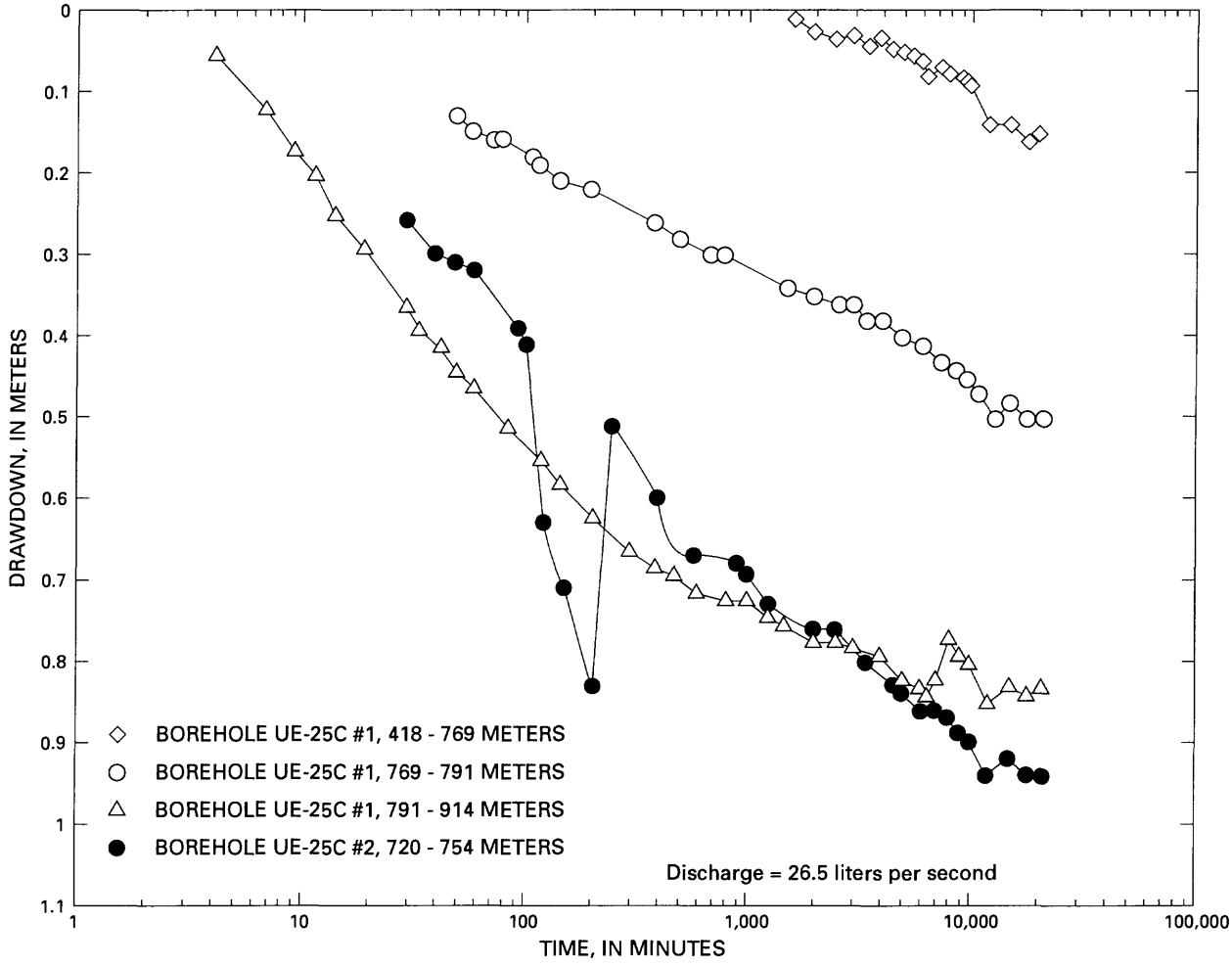

Figure 13.--Drawdown as a function of time in boreholes UE-25c #1 and UE-25c #2, pumping test in borehole UE-25c #3, November 1984.

Eighteen falling-head injection tests were done in borehole UE-25c #1 in October 1983. Hydraulic heads were monitored with a transducer suspended in the riser pipe. The injection tests were made with an induced head that was 213.4 m above the static water level. This induced head might have opened fractures during the tests and allowed the recorded hydraulic head to decline faster than it would have declined if the fractures had not been disturbed.

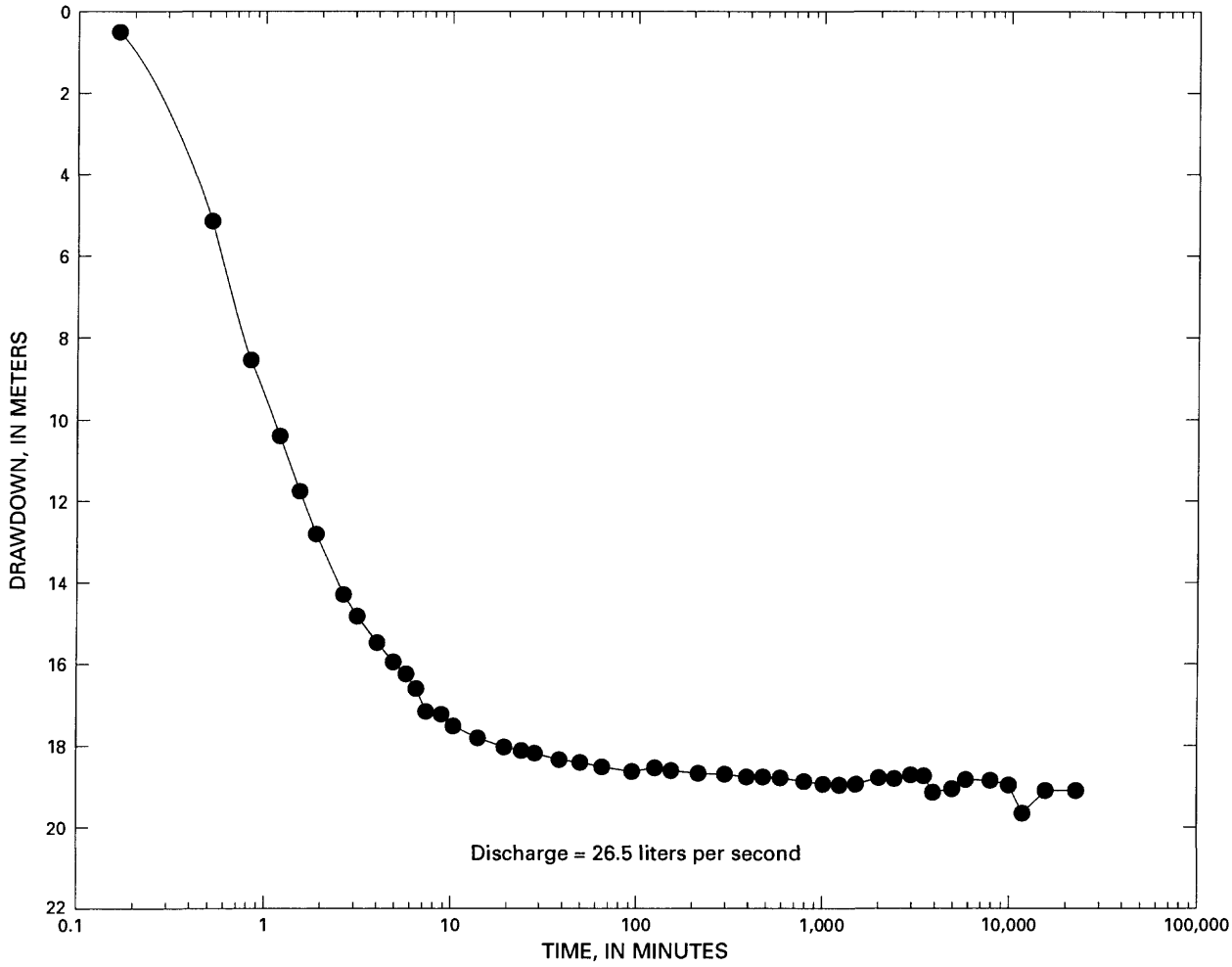

Figure 14.--Drawdown as a function of time in borehole UE-25c #3, pumping test in borehole UE-25c #3, November 1984.

Measuring error also might have been caused by locating the pressure transducer in the riser pipe. Between 35 and 40 percent of the hydraulic-head loss recorded by the transducer might have been caused by pipe friction. Modeling indicates that frictional hydraulic-head losses probably occurred primarily during the initial period of each test (Devin L. Galloway, U.S. Geological Survey, written commun., 1989). Recovery curves for 17 of the 18 falling-head tests are shown in figure 15.

A constant-head injection test was conducted in October 1984 in borehole UE-25c #2 in the interval between the packers placed in borehole UE-25c #2 for the November 1984 pumping test in borehole UE-25c #3. Hydraulic head was monitored above and between the packers in borehole UE-25c #2; above, between, and below the packers in borehole UE-25c #1; and in borehole UE-25c #3 below the casing. An average pressure head of 237.2 m was maintained between the packers in borehole UE-25c #2 for 87 minutes with an injection flow rate of 10.5 L/s. Plots of hydraulic head as a function of time are shown in figure 16 for all monitored intervals in boreholes UE-25c #1 and UE-25c #3. Monitored intervals in borehole UE-25c #2 are not shown in figure 16 because they provided no interpretable information.

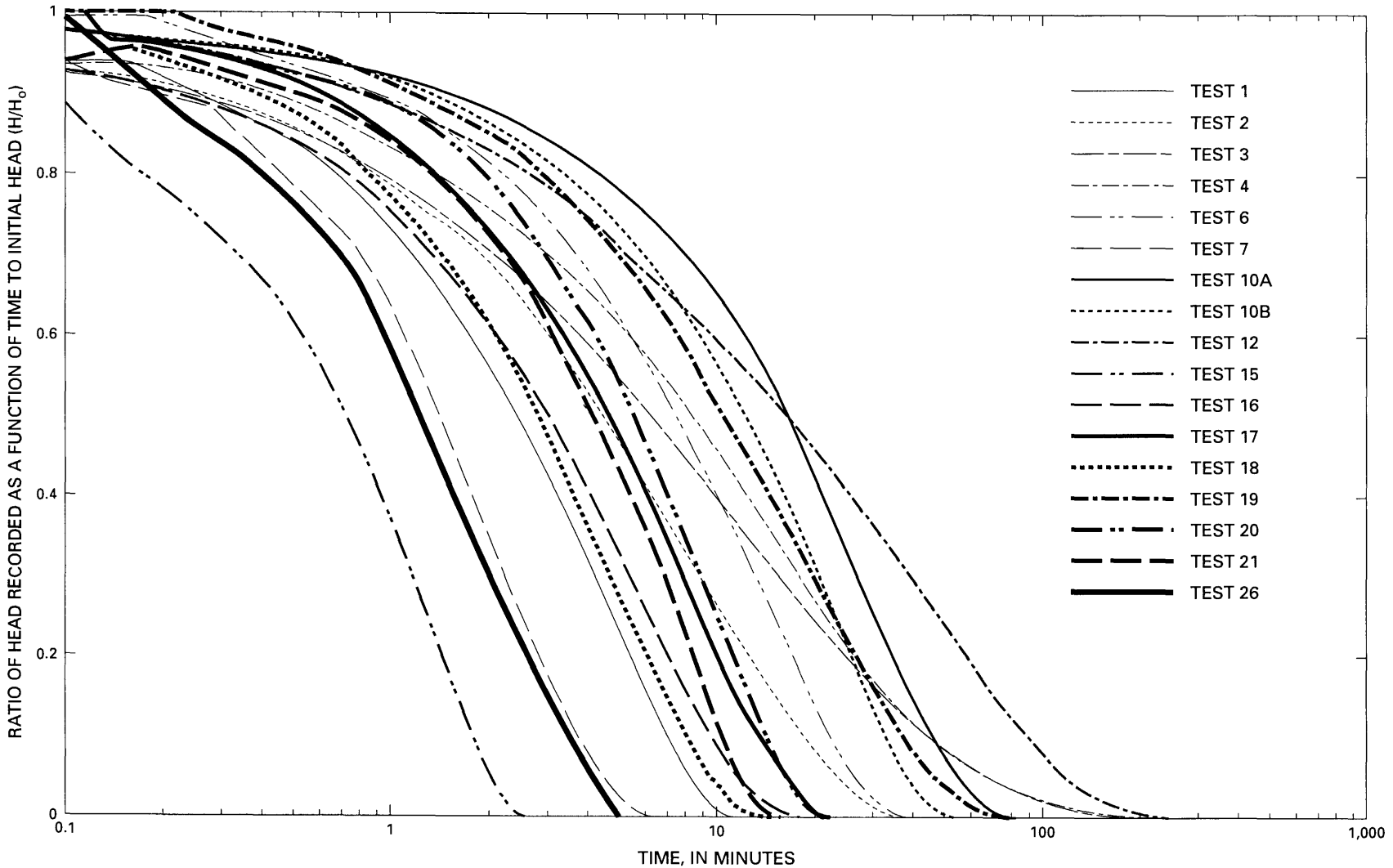

Figure 15.--Recovery curves for falling-head injection tests in borehole UE-25c #1, October 1983.

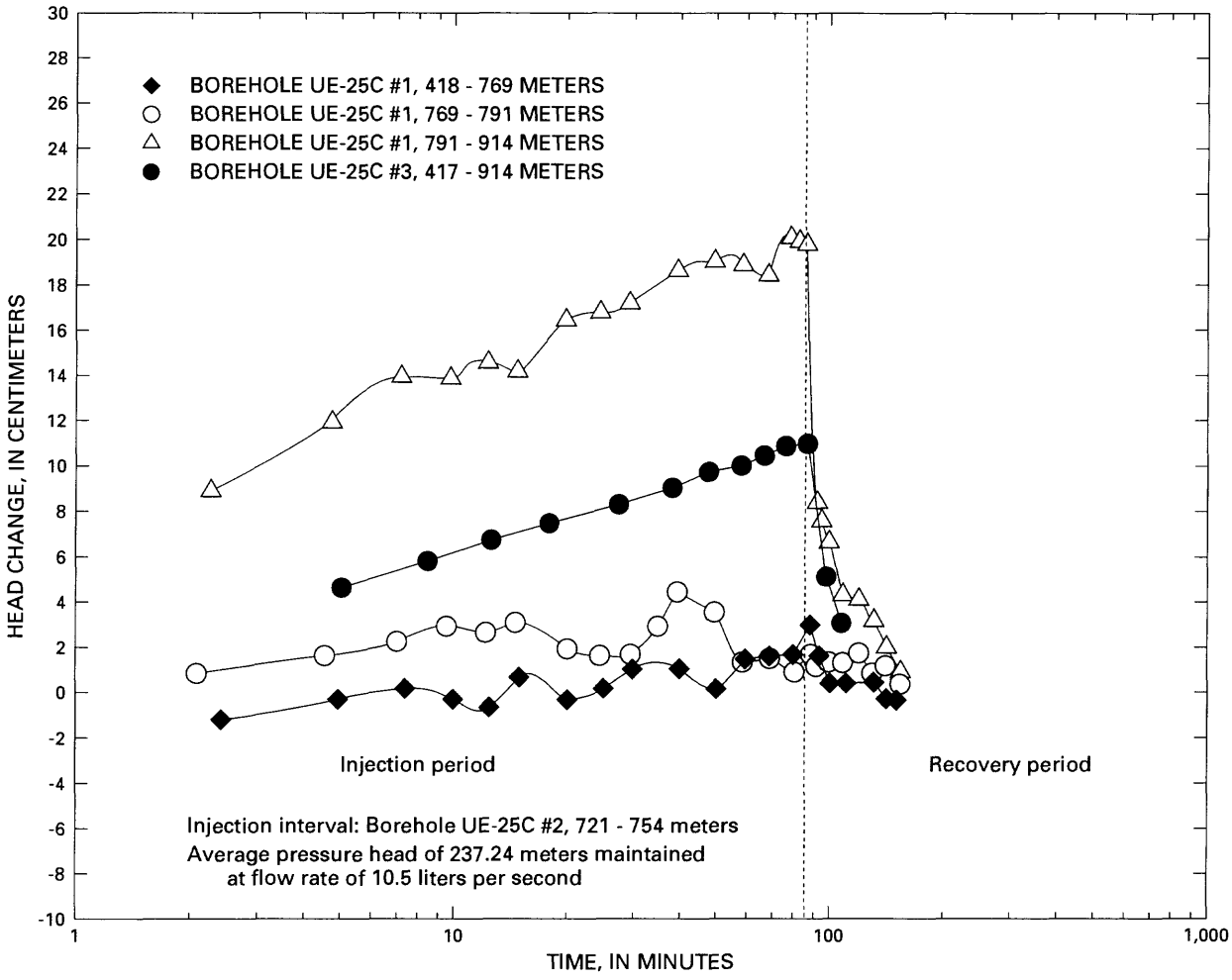

Figure 16.--Hydraulic-head data in observation wells, constant-head injection test in borehole UE-25c #2, October 1984.

GEOLOGY

Rocks of Proterozoic to Pleistocene (?) age blanketed by Tertiary and Quaternary alluvium are known to be present in the vicinity of Yucca Mountain and the C-hole complex (Cornwall and Kleinhampl, 1961; Christiansen and Lipman, 1965; Lipman and McKay, 1965; Scott and Bonk, 1984; Maldonado, 1985; Frizzell and Shulters, 1990). Proterozoic gneiss, schist, and granite probably underlie the oldest exposed rocks (Frizzell and Shulters, 1990).

The oldest known rocks at the Nevada Test Site are quartzite, sandstone, and siltstone of the Proterozoic to Lower Cambrian Johnnie Formation, Stirling Quartzite, Wood Canyon Formation, Zabriskie Quartzite, and Carrara Formation (lower part). According to Frizzell and Shulters (1990), these rocks are about 2,800 m thick. They are overlain by a sequence of predominantly carbonate rocks belonging to the Middle Cambrian to Mississippian Carrara Formation (upper part), Bonanza King Formation, Nopah Formation, Pogonip Group, Eureka Quartzite, Ely Springs Dolomite, Devils Gate Limestone, and unnamed units, that is about 5,200 m thick (Frizzell and Shulters, 1990).

Devonian and Mississippian carbonate rocks from northern Yucca Mountain and the Calico Hills grade northward and westward into the Eleana Formation, a 2,350-m-thick sequence of argillite, siltstone, and sparse quartzite and conglomerate (U.S. Geological Survey, 1984, p. 21-22). The Eleana Formation was formed by erosion of highlands that rose west of the area during the Antler orogeny (Frizzell and Shulters, 1990). North and east of Yucca Mountain, Mississippian rocks are overlain by the Pennsylvanian and Permian Tippipah Limestone, which is about 1,060 m thick (Frizzell and Shulters, 1990).

The Proterozoic and Paleozoic rocks were rearranged extensively into a chaotic assemblage of fault blocks during the late Mesozoic Sevier orogeny and subsequent tectonic events (Frizzell and Shulters, 1990). During the Tertiary Period, the Proterozoic and Paleozoic rocks in northern and western parts of the Nevada Test Site were covered by voluminous eruptions of silicic ash-flow and ash-fall tuffs (table 3) from several caldera complexes of the southwestern Nevada volcanic field (Frizzell and Shulters, 1990). Faulting continued during and after eruption of the tuffs that underlie Yucca Mountain (fig. 17).

The youngest volcanic features in the area are Pliocene and possibly Pleistocene in age. A cinder cone 10 km northwest of Amargosa Valley may be as young as 15,000 years, according to Frizzell and Shulters (1990). Intermontane valleys within and near the Nevada Test Site, such as Oasis Valley, Yucca Flat, Frenchman Flat, Jackass Flats, and Crater Flat, may contain as much as 600 m of Miocene to Holocene alluvium (Frizzell and Shulters, 1990).

The principal structures affecting the Yucca Mountain area are a series of high-angle, south-southeasterly to south-southwesterly trending faults [by convention, as in Barton and others (1989), the strike azimuth is calculated by subtracting 90° from the dip azimuth], including from east to west, the Fran Ridge, Paintbrush Canyon, Bow Ridge, Ghost Dance, Solitario Canyon, Fatigue Wash, and Windy Wash Faults (Scott and Bonk, 1984). These faults can have as much as several hundred meters of displacement, which typically decreases northward (Carr, 1988). Most fractures encountered in traverses of outcrops are aligned with the predominant fault set (fig. 18). The principal faults that transect Yucca Mountain have been interpreted by Scott and Whitney (1987) as listric-normal faults that merge into a detachment fault. Alternatively, Snyder and Carr (1984) interpreted the principal faults transecting Yucca Mountain as step faults bounding a caldera centered in Crater Flat.

Less prominent than the south-southeasterly to south-southwesterly trending faults, but also prevalent in the vicinity of Yucca Mountain, is a set of southeasterly trending faults and shear zones. The most prominent of these structures are the Las Vegas Valley Shear Zone and the Furnace Creek-Southern Death Valley Fault Zone, which locally demarcate the boundaries of the regionally extensive Walker Lane Belt (fig. 19). Southeasterly trending faults mapped by Scott and Bonk (1984) in Yucca, Sever, and Drill Hole Washes (fig. 18) at Yucca Mountain are believed to be part of the Walker Lane Belt. Associated with the southeasterly trending faults, but of secondary importance in the Walker Lane Belt, are conjugate southwesterly trending faults, such as those shown in figure 19. Faults within the Walker Lane Belt have predominantly right-lateral, strike-slip motion. Although displacements on individual faults can be only a few to several tens of meters, total right-lateral displacement on the Walker Lane Belt can be 130 to 190 km (U.S. Geological Survey, 1984).

Table 3.--*Generalized Cenozoic stratigraphy for Yucca Mountain and adjacent areas*

[Based on Cornwall and Kleinhampl (1961); McKay and Williams (1964); Christiansen and Lipman (1965); Lipman and McKay (1965); Lipman and others (1966); McKay and Sargent (1970); Orkild and O'Connor (1970); Sargent and others (1970); Byers and others (1976); Spengler and others (1979; 1981); Caporuscio and others (1982); Bentley and others (1983); Byers and Warren (1983); Craig and others (1983); Lobmeyer and others (1983); Bentley (1984); Rush and others (1984); Scott and Bonk (1984); Scott and Castellanos (1984); Thordarson and others (1984); Whitfield and others (1984); Carr and Parrish (1985); Maldonado (1985); Carr and others (1986a; 1986b); Thordarson and Howells (1987); and Carr (1988)]

Age		Area north of Yucca Mountain (Pinnacles Ridge and Calico Hills)		Area west of Yucca Mountain (Bare Mountain and Crater Flat)		Yucca Mountain-Busted Butte area		Area east of Yucca Mountain (Jackass Flats-Skull Mountain-Striped Hills)	
Millions of years	Time-stratigraphic unit	Unit	Thickness (meters)	Unit	Thickness (meters)	Unit	Thickness (meters)	Unit	Thickness (meters)
	Holocene to Pleistocene	Alluvium and colluvium	0 - 60+	Alluvium and colluvium	0 - 360	Alluvium and colluvium	0 - 160	Alluvium and colluvium	0 - 320
0.015(?)-3.8	Pleistocene to Pliocene			Basalt flows and cinder cones	0 - 300				
7.5-9.3	Miocene	Thirsty Canyon Tuff	0 - 30					Basalts of Kiwi Mesa and Jackass Flats, rhyolites of Shoshone Mountain	0 - 300
10.2-10.5				Older basalt flow	0 - 30+	Basalt dikes	0 - 1	Basalt of Skull Mountain	0 - 90
		Tuffaceous sandstone and gravel	0 - 150						
		Rhyolites of Fortymile Canyon	0 - 335						
11.1		Timber Mountain Tuff: Ammonia Tanks Member	0 - 40	Timber Mountain Tuff: Ammonia Tanks Member	0 - 60	Timber Mountain Tuff:		Timber Mountain Tuff: Ammonia Tanks Member	0 - 60
		Timber Mountain Tuff: Rainier Mesa Member	0 - 145	Timber Mountain Tuff: Rainier Mesa Member	0 - 90	Timber Mountain Tuff: Rainier Mesa Member	0 - 75	Timber Mountain Tuff: Rainier Mesa Member	0 - 90
11.3		Rhyolite of Windy Wash	0 - 110			Rhyolite of Windy Wash	0 - 110		
		Paintbrush Tuff and related lavas: Tuff of Pinyon Pass	0 - 150						
12.5		Paintbrush Tuff and related lavas: Tuff breccia: Tuff of Chocolate Mountain	0 - 170						
		Paintbrush Tuff and related lavas	0 - 670+						
12.6		Paintbrush Tuff and related lavas: Tiva Canyon Member	0 - 300+	Paintbrush Tuff: Tiva Canyon Member	0 - 180	Paintbrush Tuff: Tiva Canyon Member	25 - 150	Paintbrush Tuff: Tiva Canyon Member	0 - 65
		Paintbrush Tuff and related lavas: Yucca Mountain Member	0 - 335	Paintbrush Tuff: Yucca Mountain Member	0 - 75	Paintbrush Tuff: Yucca Mountain Member	0 - 75	Paintbrush Tuff:	
		Paintbrush Tuff and related lavas: Rhyolite lavas	0 - 200						
		Paintbrush Tuff and related lavas: Pah Canyon Member	0 - 300			Paintbrush Tuff: Pah Canyon Member	0 - 90	Paintbrush Tuff: Pah Canyon Member	0 - 45
		Paintbrush Tuff and related lavas: Rhyolite lavas	0 - 175						
13.2		Paintbrush Tuff and related lavas: Topopah Spring Member	0 - 370	Paintbrush Tuff: Topopah Spring Member	0 - 365	Paintbrush Tuff: Topopah Spring Member	45 - 370	Paintbrush Tuff: Topopah Spring Member	0 - 245
13.3		Tuffs and lavas of Calico Hills	0 - 460			Tuffs and lavas of Calico Hills	25 - 300	Wahmonie Formation	0 - 490
								Salyer Formation	0 - 460
13.4				Crater Flat Tuff: Prow Pass Member	0 - 100	Crater Flat Tuff: Prow Pass Member	45 - 200	Crater Flat Tuff: Prow Pass Member	0 - 85
13.5		Crater Flat Tuff: Bullfrog Member	0 - 100						
13.6		Crater Flat Tuff: Tram Member	0 - 400	Crater Flat Tuff: Bullfrog Member	0 - 400	Crater Flat Tuff: Bullfrog Member	90 - 200	Crater Flat Tuff: Bullfrog Member	0 - 140
				Crater Flat Tuff: Tram Member	0 - 400	Crater Flat Tuff: Tram Member	0 - 400	Crater Flat Tuff: Tram Member	0 - 265
13.7		Dacite lava plugs	Unknown	Dacite lava	Unknown	Dacite lava	0 - 250		
13.8		Lithic Ridge Tuff	0 - 250	Lithic Ridge Tuff	0 - 300	Lithic Ridge Tuff	0 - 305	Lithic Ridge Tuff: Sedimentary rocks and tuffs of Pavits Spring	0 - 150
13.9		Quartz latite and rhyolite	Unknown	Quartz latite flows and dikes	Unknown	Quartz latite and rhyolite	0 - 305		
				Older tuffs and sedimentary rocks (indicated by a negative gravity anomaly)	≤2,100	Older tuffs and conglomerate	0 - 330		0 - 280+
15(?)		Tuff of Yucca Flat	0 - 60+			Tuff of Yucca Flat (?)	0 - 40		
	Oligocene			(?)					
29								Horse Spring Formation	0 - 30

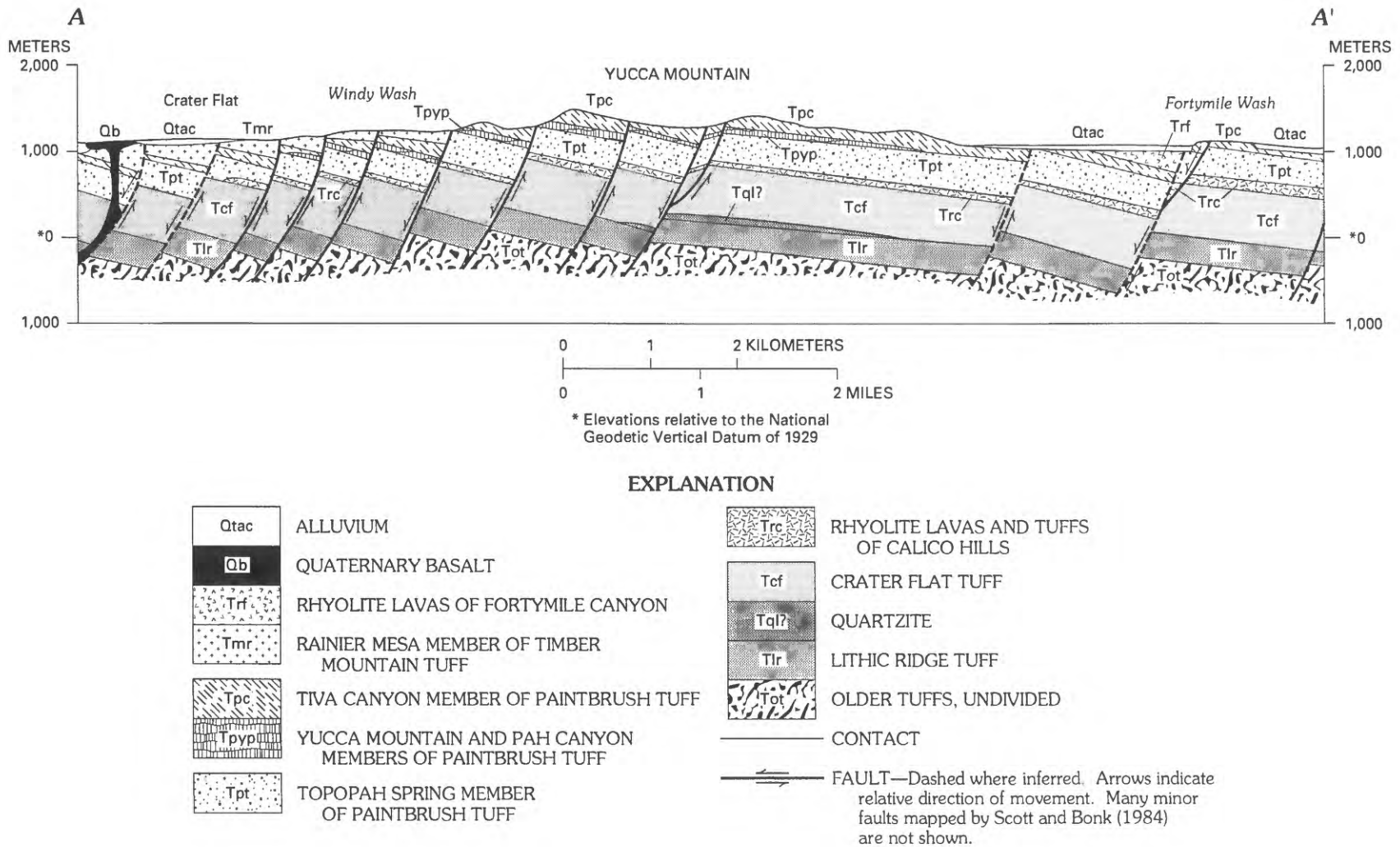

Figure 17.--Geologic section across Yucca Mountain from Crater Flat to Fortymile Wash (from Frizzell and Shulters, 1990; location shown in figure 1).

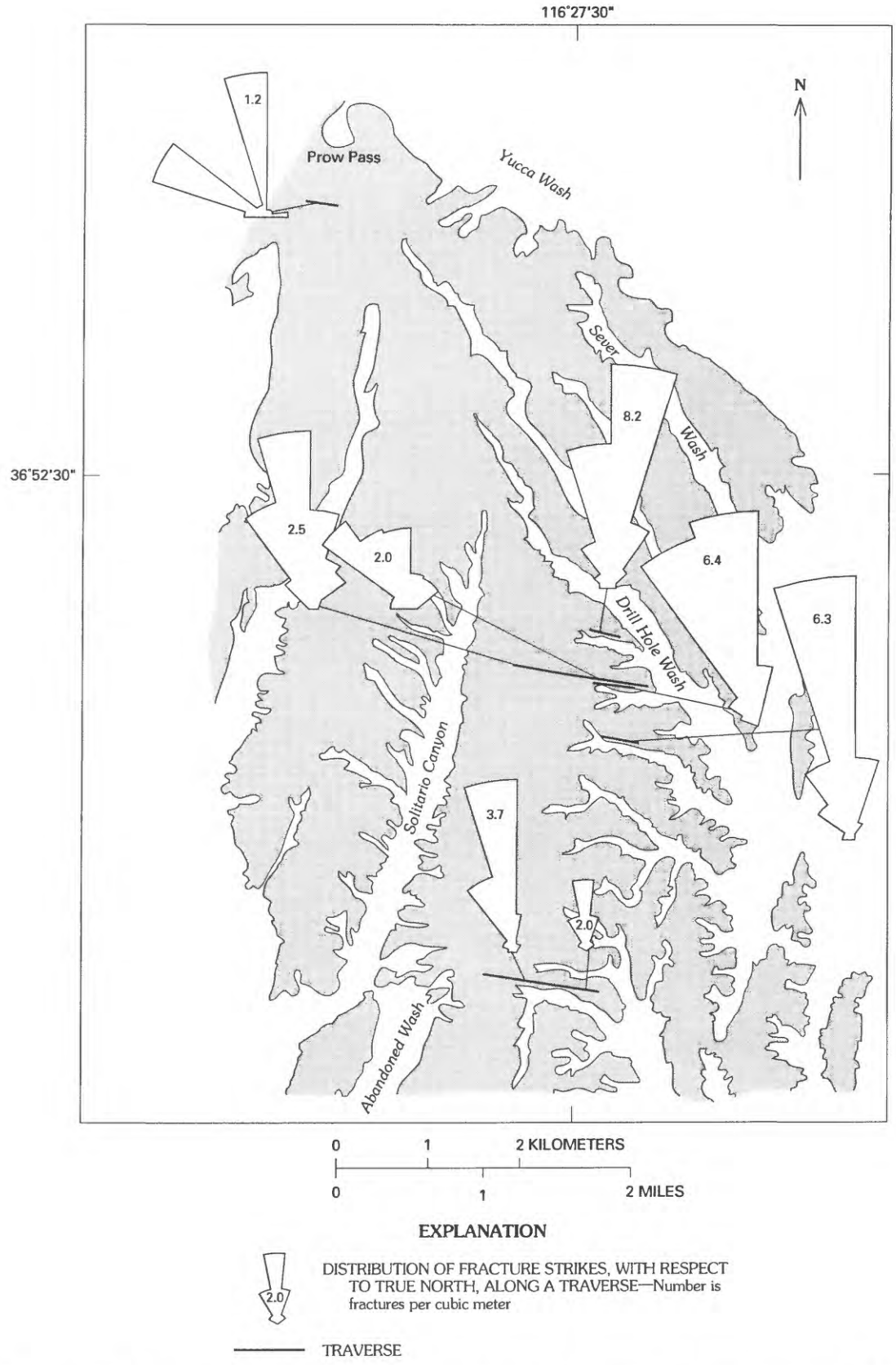

Figure 18.--Rose diagrams of the strikes of fractures encountered along traverses of outcrops at Yucca Mountain (modified from U.S. Geological Survey, 1984).

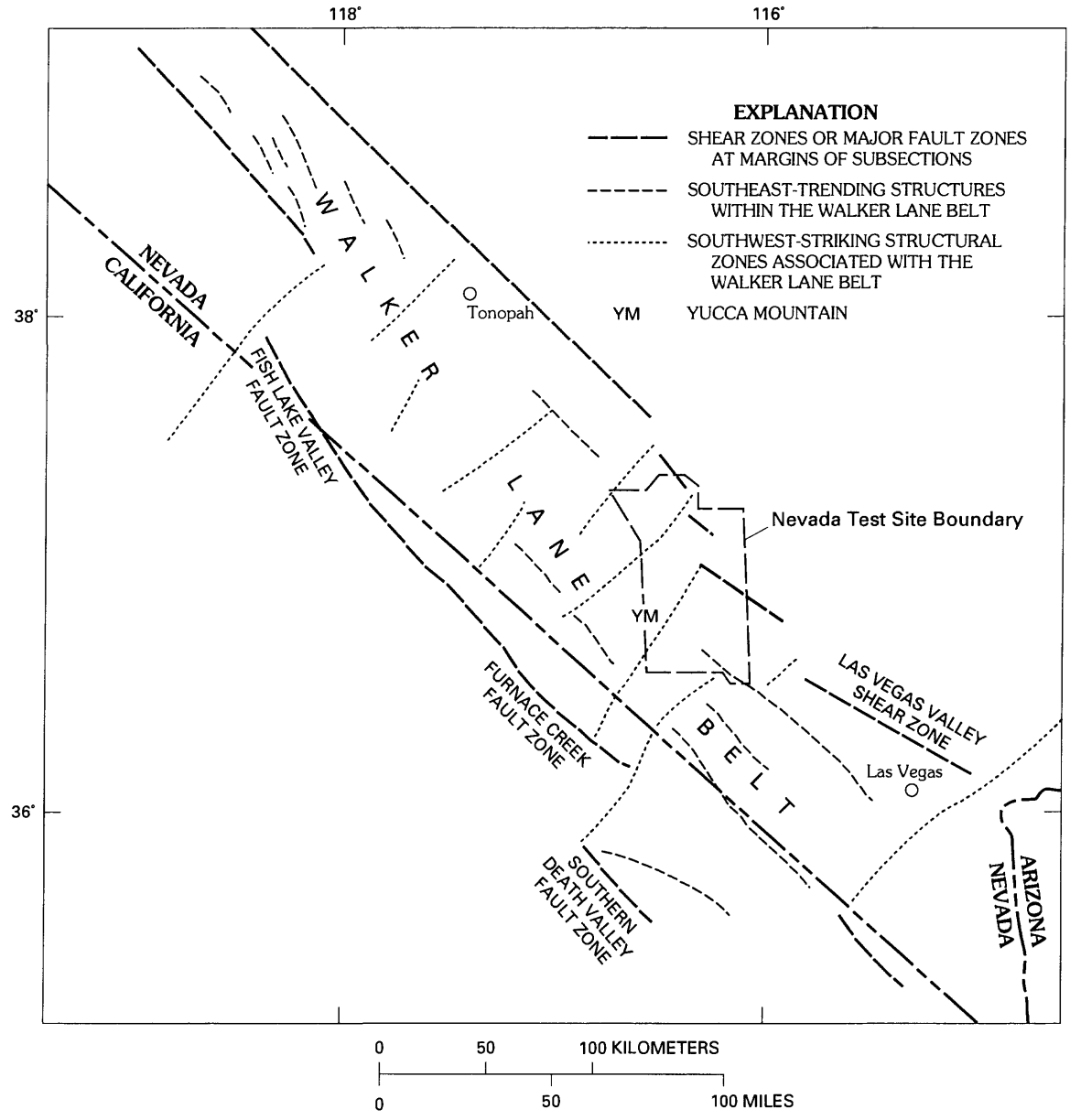

Figure 19.--The Walker Lane Belt (modified from Carr, 1988).

The principal effect of the various faults mapped at Yucca Mountain is to divide the mountain into seven blocks characterized by distinct variations in the dip of strata and the intensity and orientation of faults and fractures (U.S. Geological Survey, 1984). For example, in the block potentially designated to contain the high-level nuclear-waste repository, the central block, beds dip uniformly 5 to 10 degrees eastward, and faults are scarce. In contrast, in the block where the C-hole complex is located, the eastern block, beds dip 15 to 50 degrees eastward, and several prominent south-southeasterly to south-southwesterly striking faults are present.

C-hole Complex Stratigraphy and Structure

Each of the C-holes penetrated the Paintbrush Tuff, the tuffs and lavas of Calico Hills, and the Prow Pass and Bullfrog Members of the Crater Flat Tuff and bottomed in the Tram Member of the Crater Flat Tuff (table 4). The tuffaceous rocks below the vitrophyre zone near the bottom of the Topopah Spring Member of the Paintbrush Tuff are partly altered to clay and zeolite minerals. The top of the zone of alteration corresponds approximately to the water table, which occurs at an average depth of 401.6 m (730.1 m above the NGVD of 1929) in the C-holes.

The geologic units penetrated in the C-holes have been affected substantially by depositional thickening and thinning, erosion, and faulting. In the Crater Flat Tuff, the lower (lithic tuff) zone of the Tram Member is missing from borehole UE-25c #3, possibly because of fault truncation, and the upper part of the Tram Member has been brecciated where it is intersected by faults. A fault between depths of 820.5 and 821.9 m in borehole UE-25c #2 juxtaposes ash-fall tuff against reworked tuff in the bedded zone of the Bullfrog Member of the Crater Flat Tuff and probably has increased the drilled thickness of this zone by 7 to 8 m in borehole UE-25c #2. Most zones within the Bullfrog Member have similar thicknesses among the C-holes, but a prominent parting between the Prow Pass and Bullfrog Members (visible on videotapes of boreholes UE-25c #1 and UE-25c #2) indicates that some erosion of the Bullfrog Member might have preceded deposition of the Prow Pass Member. In the Prow Pass Member, zones thicken and thin at the expense of each other, and the entire member thickens southwestward, from a drilled thickness of 140.6 m in borehole UE-25c #1 and 142.1 m in borehole UE-25c #2 to 146.3 m in borehole UE-25c #3. Combined with a thinning of the tuffs and lavas of Calico Hills from 109.7 m in borehole UE-25c #1 and 108.5 m in borehole UE-25c #2 to 100.6 m in borehole UE-25c #3 and the existence of a prominent parting at the contact between the tuffs and lavas of Calico Hills and the Prow Pass Member (visible on videotapes of boreholes UE-25c #1 and UE-25c #2), it would appear that the top of the Prow Pass Member was eroded after its eruption, and that the tuffs and lavas of Calico Hills were deposited over irregularities on the surface of the older unit. In the Paintbrush Tuff, all zones except for the interval from the bottom of the lower lithophysal zone to the top of the upper lithophysal zone of the Topopah Spring Member thicken and thin at the expense of each other. The uppermost member of the Paintbrush Tuff at Yucca Mountain, the Tiva Canyon Member, was eroded and covered by alluvium.

True thicknesses of most of the formal geologic units (formations and members) and informal geologic units (zones) penetrated in the C-holes can be calculated by correcting for the strike and dip, as determined from the orientations of stratigraphic horizons interpreted to be relatively unaffected by depositional thickening or thinning, erosion, or faulting. As shown in figure 20, three-point solutions using the tops of uniformly thick intervals in the Crater Flat and Paintbrush Tuffs indicate that geologic units present at the C-hole complex strike between north and N. 4° W. (averaging N. 2° W.). The dip of these geologic units apparently increases downward in the section from about 15° to about 21° NE at a gradient of 0.0066° per meter. True thicknesses of all geologic units in the C-holes that are stratified (the tuff breccia is not) and penetrated fully are listed in table 5.

Table 4.--*Geologic units penetrated by boreholes UE-25c #1, UE-25c #2, and UE-25c #3*

[Bedded tuffs are grouped with overlying ash-flow tuffs for correlation, because they are assumed to represent reworking of the previous deposits and the initial phase of the next eruptive event]

Lithologic description	Borehole UE-25c #1		Borehole UE-25c #2		Borehole UE-25c #3		Average drilled thickness of interval (meters)
	Depth of interval (meters)	Drilled thickness of interval (meters)	Depth of interval (meters)	Drilled thickness of interval (meters)	Depth of interval (meters)	Drilled thickness of interval (meters)	
			Alluvium				
Angular fragments of caliche-coated tuff of Tiva Canyon Member.	Absent	0	0-21.3	21.3	0-24.4	24.4	15.2
			PAINTBRUSH TUFF				
			Tiva Canyon Member				
Welded zone.--Grayish-red, gray, and brown, devitrified, moderately to densely welded, ash-flow tuff with 1 to 2 percent sanidine and biotite phenocrysts.	0-79.2	79.2	21.3-76.2	54.9	24.4-68.6	44.2	59.4
Columnar zone.--Grayish-orange to light brown, vitric, partially welded, ash-flow tuff with pumice, abundant black glass shards, and 1 percent sanidine phenocrysts.	79.2-93.0	13.8	76.2-86.9	10.7	68.6-77.7	9.1	11.2
Bedded zone.--White, yellowish-gray, and orange, poorly consolidated, vitric, ash-fall (?) tuff, dominantly composed of rounded pumice clasts.	93.0-96.0	3.0	86.9-88.4	1.5	77.7-88.4	10.7	5.1
			Topopah Spring Member				
Nonwelded zone.--Pink and gray, vitric, nonwelded, ash-flow tuff with 1 percent sanidine and biotite phenocrysts, and pumice.	96.0-98.4	2.4	88.4-96.6	8.2	88.4-89.9	1.5	4.0
Upper vitrophyre.--Reddish brown and black, glassy, ash-flow tuff with 8 to 10 percent sanidine and biotite phenocrysts.	Absent	0	Absent	0	89.9-93.0	3.1	1.0
Caprock.--Grayish-red and grayish-brown, devitrified, densely welded, ash-flow tuff with pumice and 10 to 15 percent sanidine, plagioclase, and bronze-biotite phenocrysts.	98.4-103.6	5.2	96.8-108.8	12.2	93.0-97.5	4.5	7.3
Upper welded zone.--Grayish-red and brown, moderately welded, ash-flow tuff with pumice and 7 to 10 percent sanidine, plagioclase, and bronze-biotite phenocrysts.	103.6-131.1	27.5	108.8-129.2	20.4	97.5-121.9	24.4	24.1
Upper lithophysal zone.--Mottled gray, red, and brown, devitrified, moderately to densely welded ash-flow tuff with pumice and less than 1 to 2 percent sanidine and black-biotite phenocrysts.	131.1-181.4	50.3	129.2-188.1	58.9	121.9-170.7	48.8	52.7
Middle welded zone.--Brown, devitrified, densely welded, ash-flow tuff with pumice and 1 to 3 percent sanidine and biotite phenocrysts.	181.4-224.3	42.9	188.1-221.3	33.2	107.7-216.4	45.7	40.6
Lower lithophysal zone.--Mottled red, gray, and brown, devitrified, densely welded, ash-flow tuff with pumice and 1 percent sanidine phenocrysts.	224.3-325.2	100.9	221.3-322.2	100.9	216.4-313.9	97.5	99.8
Lower welded zone.--Orange, yellowish-brown, and grayish-red, devitrified, slightly zeolitized and argillized, densely welded, ash-flow tuff with pumice and 1 to 2 percent sanidine and biotite phenocrysts.	325.2-372.5	47.3	322.2-367.6	45.4	313.9-365.8	51.8	48.2
Lower vitrophyre.--Black, glassy, densely welded ash-flow tuff with perlitic cracks and 1 to 2 percent sanidine phenocrysts.	372.5-392.3	19.8	367.6-384.0	16.4	365.8-381.0	15.2	17.1

Table 4.--*Geologic units penetrated by boreholes UE-25c #1, UE-25c #2, and UE-25c #3*--Continued

Lithologic description	Borehole UE-25c #1		Borehole UE-25c #2		Borehole UE-25c #3		Average drilled thickness of interval (meters)
	Depth of interval (meters)	Drilled thickness of interval (meters)	Depth of interval (meters)	Drilled thickness of interval (meters)	Depth of interval (meters)	Drilled thickness of interval (meters)	
PAINTBRUSH TUFF--Continued							
Topopah Spring Member--Continued							
Vitric zone.--Dark gray and brown, vitric, zeolitized (?), moderately welded, ash-flow tuff with abundant black glass shards.	392.3-398.7	6.4	384.0-392.9	8.9	381.0-387.1	6.1	7.1
Basal zone.--Yellow-orange and brown, vitric, zeolitic, partially welded to nonwelded ash-flow tuff with pumice, 1 to 2 percent sanidine and biotite phenocrysts, and abundant rhyolitic xenoliths.	398.7-406.0	7.3	392.9-401.1	8.2	387.1-396.2	9.1	8.2
Tuffs and lavas of Calico Hills							
Nonwelded zone.--Salmon and yellowish-brown, nonwelded, ash-flow tuff with pumice, 1 percent sanidine phenocrysts, and abundant rhyolitic xenoliths.	406.0-485.6	79.6	401.1-478.5	77.4	396.2-475.5	79.3	78.8
Bedded zone.--Reddish-brown, pink, grayish-yellow, and white, zeolitic, bedded, reworked, ash-fall tuff and tuffaceous sandstone with pumice and rhyolite fragments.	485.6-515.7	30.1	478.5-509.6	31.1	475.5-496.8	21.3	27.5
CRATER FLAT TUFF							
Prow Pass Member							
Upper flow zone.--Light-gray and brown, devitrified, slightly argillic, nonwelded to partially welded, ash-flow tuff with pumice, 5 to 10 percent sanidine, quartz, biotite, snd pyroxene pseudomorph (?) phenocrysts, and sparse to abundant mudstone xenoliths.	515.7-560.2	44.5	509.6-551.7	42.1	496.8-542.5	45.7	44.1
Central flow zone.--Brown and gray, devitrified, moderately welded, ash-flow tuff with pumice, 8 to 12 percent sanidine, quartz, biotite, and pyroxene pseudomorph (?) phenocrysts, and sparse to common mudstone xenoliths.	560.2-566.9	6.7	551.7-560.8	9.1	542.5-557.8	15.3	10.4
Lower flow zone.--Gray, olive, yellow, brown and salmon, devitrified, argillic to zeolitic, nonwelded to partially welded, ash-flow tuff with pumice, 5 to 10 percent quartz, sanidine, biotite, and pyroxene pseudomorph (?) phenocrysts, and sparse to abundant mudstone xenoliths.	566.9-645.9	79.0	560.8-643.0	82.2	557.8-635.5	77.7	79.6
Bedded zone.--Salmon, red, and reddish-brown, zeolitic and argillic, bedded, reworked tuff and tuffaceous sandstone with pumice and mudstone fragments.	645.9-656.2	10.4	643.0-651.7	8.7	635.5-643.1	7.6	8.9
Bullfrog Member							
Upper flow zone.--Light-olive-gray to brownish-gray, devitrified, slightly argillic to zeolitic (?), nonwelded to partially welded, ash-flow tuff with pumice, 8 to 10 percent quartz, sanidine, biotite, plagioclase, and hornblende pseudomorph phenocrysts, and rhyolite xenoliths.	656.2-688.8	32.6	651.7-682.8	31.1	643.1-673.6	30.5	31.4
Central flow zone.--Brown, gray, and red, devitrified, slightly argillic, moderately to densely welded, ash-flow tuff with pumice, 10 to 17 percent plagioclase, sanidine, quartz, bronze-biotite, and hornblende pseudomorph phenocrysts, and rare to abundant volcanic xenoliths.	688.8-755.9	67.1	682.8-749.8	67.0	673.6-740.7	67.1	67.1

Table 4.--*Geologic units penetrated by boreholes UE-25c #1, UE-25c #2, and UE-25c #3*--Continued

Lithologic description	Borehole UE-25c #1		Borehole UE-25c #2		Borehole UE-25c #3		Average drilled thickness of interval (meters)
	Depth of interval (meters)	Drilled thickness of interval (meters)	Depth of interval (meters)	Drilled thickness of interval (meters)	Depth of interval (meters)	Drilled thickness of interval (meters)	
CRATER FLAT TUFF--Continued							
Bullfrog Member--Continued							
Lower flow zone.--Gray, olive-gray, brown, and orange, devitrified, argillic to zeolitic (?), partially welded to nonwelded, ash-flow tuff with pumice, 8 to 12 percent quartz, sanidine, plagioclase, biotite, and hornblende phenocrysts, and sparse volcanic xenoliths.	755.9-821.4	65.5	749.8-815.3	65.5	740.7-807.7	67.0	66.0
Bedded zone.--Salmon, grayish-red, and reddish-brown, zeolitic (?), poorly sorted, poorly bedded, reworked tuff with abundant pumice and volcanic fragments. A fault intersects borehole UE-25c #2 from 820.5 to 821.9 meters; apparent dip is 75 to 90 degrees.	821.4-827.8	6.4	815.3-831.8	16.5	807.7-813.8	6.1	[1]6.7
Tram Member							
Upper zone.--Reddish-brown, yellowish-brown and orange, zeolitic (?), nonwelded, ash-flow tuff with pumice, and 10 to 12 percent quartz, sanidine, plagioclase, and black biotite phenocrysts.	827.8-838.2	10.4	Absent	0	813.8-841.2	27.4	12.6
Salmon, brownish-gray, and gray, devitrified, partially welded, ash-flow tuff with pumice, 10 to 12 percent quartz, sanidine, biotite, plagioclase, and hornblende (?) phenocrysts, and rare to sparse volcanic xenoliths.	838.2-845.8	7.6	831.8-845.8	14.0	841.2-853.4	12.2	11.3
Tuff breccia zone.--Brown, red, and gray, moderately to very indurated tuff breccia composed of angular to subrounded clasts of Tram Member tuff in matrix of fine-grained tuffaceous sediment. Fault zones noted in borehole UE-25c #1 at depths from 849.5 to 850.1 meters, dipping 70 degrees; in borehole UE-25c #2 at a depth of 851.3 meters, dipping 56 degrees; and in borehole UE-25c #3 at depths from 855.3 to 861.4 meters. Fault zone in borehole UE-25c #3 contains 1- to 15-millimeter-thick bands of breccia, inclined 34 to 57 degrees.	845.8-906.8	61.0	845.8-894.6	48.8	853.4-914.4	61.0	56.9
Lower zone.--Gray, olive-gray, and red, devitrified, slightly zeolitic and argillic, partially welded, ash-flow tuff with pumice, 10 to 15 percent quartz, sanidine, and biotite phenocrysts, and sparse to abundant volcanic and tuffaceous xenoliths.	906.8-914.4	7.6	894.6-914.4	19.8	Absent	0	9.1

[1]Average based on interpreted prefaulting thickness of 7.6 meters in borehole UE-25c #2.

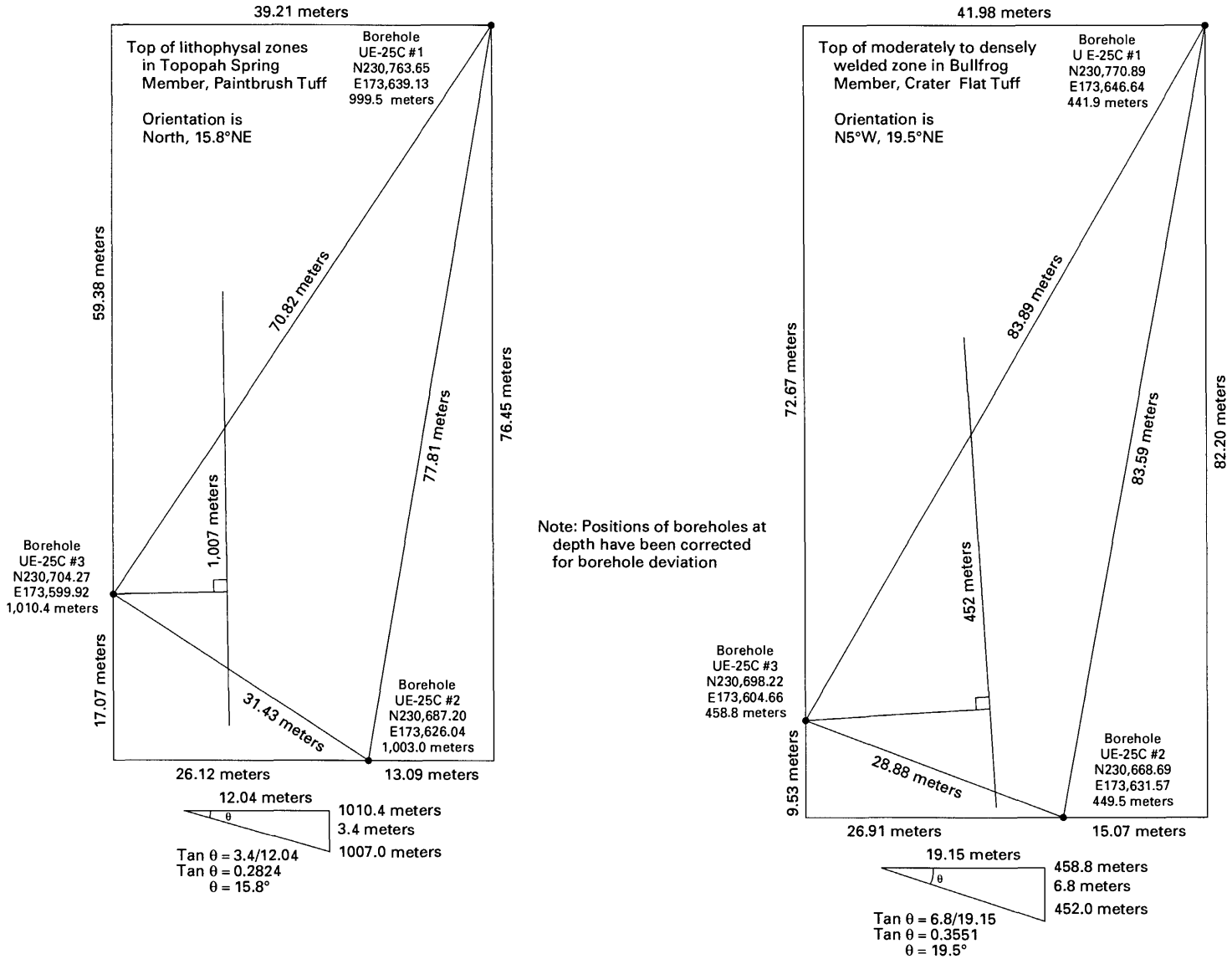

Figure 20.--Orientation of geologic units at the C-hole complex determined by three-point solutions.

Table 5.--*Thicknesses corrected for dip of stratified geologic units penetrated fully by the C-holes*

Geologic unit	Dip angle (degrees)[1]	Corrected thickness (meters)			
		Borehole UE-25c #1	Borehole UE-25c #2	Borehole UE-25c #3	Average
Paintbrush Tuff		390.5	365.0	359.5	371.6
Tiva Canyon Member		92.7	64.7	61.8	73.1
Welded zone	15.0	76.5	53.0	42.7	57.4
Columnar zone	15.5	13.3	10.3	8.8	10.8
Bedded zone	15.6	2.9	1.4	10.3	4.9
Topopah Spring Member		297.8	303.3	297.7	298.5
Nonwelded zone	15.6	2.3	7.9	1.4	3.9
Upper vitrophyre and caprock	15.6	5.0	11.8	7.3	8.0
Upper welded zone	15.6	26.5	19.6	23.5	23.2
Lithophysal zone[2]	15.8	186.8	185.7	184.7	185.7
Lower welded zone	17.1	45.2	43.4	49.5	46.0
Lower vitrophyre	17.4	18.9	15.6	16.8	17.1
Vitric zone	17.5	6.1	8.5	5.8	6.8
Basal zone	17.6	7.0	7.8	8.7	7.8
Tuffs and lavas of Calico Hills		104.5	103.4	95.8	101.2
Nonwelded zone	17.6	75.9	73.8	75.6	75.1
Bedded zone	18.1	28.6	29.6	20.2	26.1
Crater Flat Tuff		>311.7	>309.1	>336.5	>319.2
Prow Pass Member		133.2	134.7	138.7	135.5
Upper flow zone	18.3	42.2	40.0	43.4	41.9
Central flow zone	18.6	6.4	8.6	14.5	9.8
Lower flow zone	18.7	74.8	77.9	73.6	75.4
Bedded zone	19.2	9.8	8.2	7.2	8.4
Bullfrog Member		161.6	161.3	160.7	161.3
Upper flow zone	19.3	30.8	29.4	28.8	29.7
Central flow zone	19.5	63.2	63.2	63.2	63.2
Lower flow zone	19.9	61.6	61.6	63.0	62.1
Bedded zone	20.4	6.0	[3]7.1	5.7	6.3
Tram Member		>16.9	>13.1	>37.1	>22.4
Upper zone	20.4	16.9	13.1	37.1	22.4

[1]Based on a difference in dip of 3.7 degrees in the 557.4 meters between the top of the upper lithophysal zone in the Topopah Spring Member and the top of the central flow zone in the Bullfrog Member, a gradient of 0.0066 degree per meter.

[2]Includes upper lithophysal zone, middle welded zone, and lower lithophysal zone.

[3]Corrected for faulting in borehole.

As interpreted in figure 21, the fault cutting the Tram Member in borehole UE-25c #1 between depths of 849.5 and 850.1 m is the Paintbrush Canyon Fault mapped by Scott and Bonk (1984). Another fault mapped by Scott and Bonk (1984) between the C-holes and the Paintbrush Canyon Fault is interpreted in figure 21 to be a splay of the Paintbrush Canyon Fault. The apparent dip of

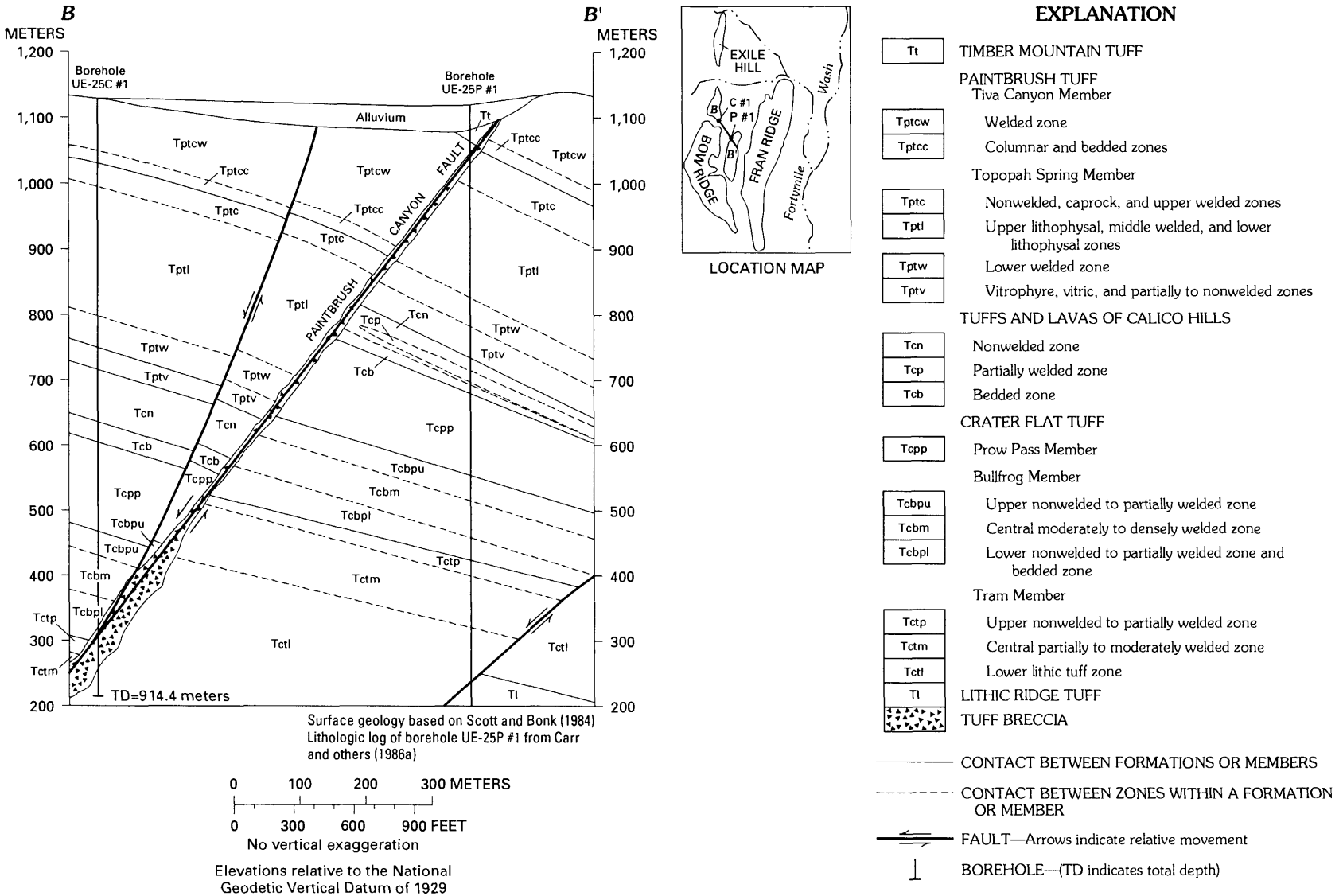

Figure 21.--Geologic section showing structure between boreholes UE-25c #1 and UE-25p #1 at Yucca Mountain.

the Paintbrush Canyon Fault, determined by connecting the fault zone penetrated in borehole UE-25c #1 to a fault penetrated in borehole UE-25p #1 that cuts out the columnar and bedded zones of the Tiva Canyon Member and the nonwelded, upper vitrophyre, and caprock zones of the Topopah Spring Member (Carr and others, 1986a), is 52° NW. Based on an angle of about 70° between the geologic section shown in figure 21 and the surface trace of the Paintbrush Canyon Fault, the true dip of this fault would be about 54°. This is consistent with a three-point solution using boreholes UE-25c #1, UE-25c #2, and UE-25p #1 as the plotted points (fig. 22), that indicates the orientation of the Paintbrush Canyon Fault to be S. 9° W., 52.2° NW. If figures 21 and 22 are correct interpretations of the structure at and near the C-hole complex, then the surface trace of the Paintbrush Canyon Fault beneath the alluvium is about 26 m east of where Scott and Bonk (1984) mapped it. Considering the uncertainties in the graphical solutions and in predicting the location of a concealed fault, the difference between the location of the surface trace of the Paintbrush Canyon Fault shown by Scott and Bonk (1984) and that shown in figure 21 is considered trivial. The graphical solutions discussed in this

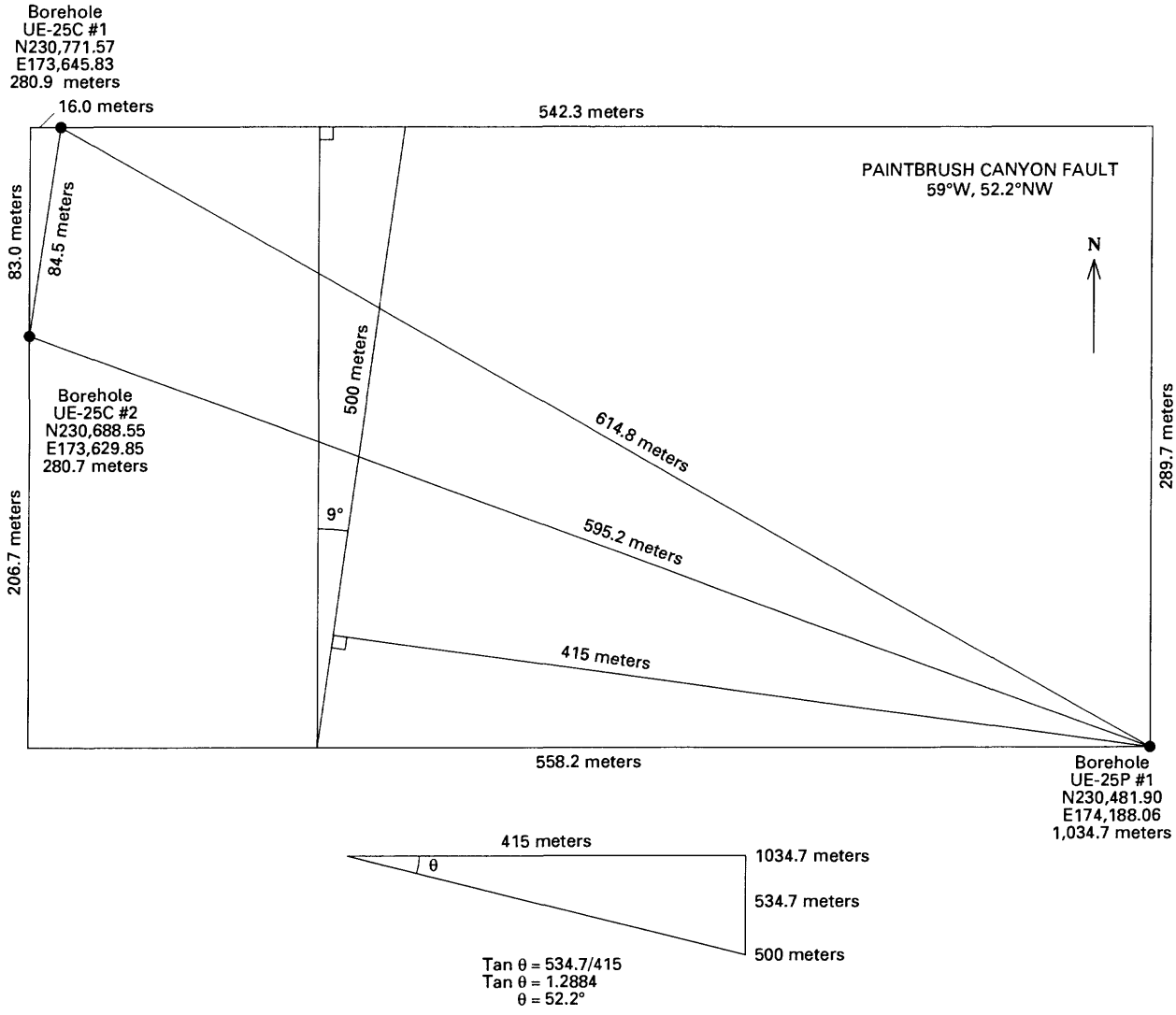

Figure 22.--Three-point solution of Paintbrush Canyon Fault orientation.

section overwhelmingly support the interpretation that the Paintbrush Canyon Fault intersects boreholes UE-25c #1 and UE-25c #2. As indicated in figure 21, vertical displacement on the Paintbrush Canyon Fault at the C-hole complex ranges from 160 to 225 m and increases with depth along the fault. The fault cuts out the central (partially to moderately welded) zone and most of the lower (lithic tuff) zone of the Tram Member at the location of borehole UE-25c #1.

The fault penetrated by borehole UE-25c #3 (table 4) either is an offset and rotated extension of the Paintbrush Canyon Fault penetrated by boreholes UE-25c #1 and UE-25c #2, or it is a different fault than the Paintbrush Canyon Fault. Ambiguity about the fault penetrated by borehole UE-25c #3 is based on its altitude, orientation, and character with respect to the fault penetrated by boreholes UE-25c #1 and UE-25c #2. If a plane were drawn connecting the fault penetrated by borehole UE-25c #3 with the fault penetrated by the other two C-holes, the dip of the fault would be only about 7°, and its orientation would not correspond with any other faults known to be in the area. In other words, the fault penetrated by borehole UE-25c #3 occurs too high in the borehole to be a continuous extension of the fault penetrated by the other two C-holes. Secondly, fractures associated with the fault penetrated by borehole UE-25c #3 are oriented differently than those associated with the fault penetrated by boreholes UE-25c #1 and UE-25c #2. Fractures detected on the acoustic-televiewer log of borehole UE-25c #3 within and adjacent to the fault penetrated by the borehole all strike between S. 37° W. and S. 55° W. and dip between 55° and 68° NW. In contrast, fault-related fractures detected on acoustic-televiewer logs of boreholes UE-25c #1 and UE-25c #2 strike between S. 7° E. and S. 21° W. and dip between 48° and 69° mostly to the northwest. Based on the average orientation of fault-related fractures on acoustic-televiewer logs, one might conclude that the fault penetrated by borehole UE-25c #3 is oriented approximately S. 49° W., 63° NW., whereas the fault penetrating boreholes UE-25c #1 and UE-25c #2 is oriented approximately S. 9° W., 59° NW. Finally, the fault penetrated by borehole UE-25c #3 has a completely different character than the fault penetrated by boreholes UE-25c #1 and UE-25c #2. Whereas the faulted interval penetrated by borehole UE-25c #3 is about 6 m thick and contains bands of brecciated rock, the faulted interval observed in each of the other two C-holes is less than 1 m thick and lacks bands of breccia (Richard Spengler, U.S. Geological Survey, written commun., 1989).

The orientation of the fault penetrating borehole UE-25c #3, as interpreted from fracture data, is consistent with the fault being a conjugate fault of the Walker Lane Belt. The lack of offset of beds in borehole UE-25c #3 with respect to the other two C-holes implies that the fault penetrating borehole UE-25c #3 is a strike-slip fault, which also is consistent with the fault being part of the Walker Lane Belt. Alternatively, the fault that offsets and thickens the bedded zone of the Bullfrog Member in borehole UE-25c #2 could extend between boreholes UE-25c #1 and UE-25c #2 on the east and borehole UE-25c #3 on the west down below the level of the Paintbrush Canyon Fault. The Paintbrush Canyon Fault could be displaced upward and rotated westward west of the unnamed, subsurface fault detected in borehole UE-25c #2. The latter interpretation accounts for both the unexpectedly "high" position and southwest strike of the fault penetrated by borehole UE-25c #3 and explains why no fracture zone was detected in borehole UE-25c #3 at a depth of about 885 m, where the Paintbrush Canyon Fault, projected along its dip from boreholes UE-25c #1 and UE-25c #2, should have intersected borehole UE-25c #3.

Fracturing in the C-holes

Several lines of evidence from previous borehole investigations indicate that ground-water flow at Yucca Mountain may be influenced strongly by the presence of fractures. (See, for example, Whitfield and others, 1990). Consequently, fracture geometry at the C-hole complex is discussed in some detail in this report. The fracture characteristics that are most important hydrogeologically are orientation, linear frequency, density, length, aperture, and interconnectivity. These characteristics can be determined most accurately by mapping. Barton and Larsen (1985), for example, mapped fractures in the Paintbrush Tuff at Yucca Mountain after first clearing soil and vegetation from outcrops. The information obtained from these "pavements", however, may not pertain to the saturated zone at the C-hole complex because the geologic units below the water table, in particular the tuffs and lavas of Calico Hills and the Crater Flat Tuff, may not have responded in the same way as the Paintbrush Tuff to the mechanisms that fractured the rock, and because fractures tend to close at depth as the pressure increases. Another problem in interpreting the C-hole fracture data is that the boreholes are not oriented optimally to ascertain fracture frequency and density. Because most of the fractures at Yucca Mountain are steeply dipping to vertical, it is possible that in the vertical C-holes, specific fracture sets and, consequently, fracture spacing in general could be underrepresented. Comparisons with fracture data obtained by pavement mapping (Barton and Larsen, 1985; Barton and others, 1989), transects (U.S. Geological Survey, 1984), angled and horizontal coring (Spengler and Rosenbaum, 1980; Norris and others, 1986), and vertical coring (Scott and Castellanos, 1984) were made to substantiate analyses of fracture data from the C-holes or indicate the margin of error in these analyses.

As noted previously, fracture information for the C-holes was obtained exclusively from acoustic televiewer logs and videotapes. The two methods are not directly comparable. Strikes recorded by the acoustic televiewer can differ slightly to substantially from those recorded for the same fractures by the television camera, and the acoustic televiewer can indicate dip angles, which the television camera only can do qualitatively. Also, the acoustic televiewer can indicate the presence of fractures that are not visible on the videotapes. Because the television camera provides a direct image of the borehole, whereas the acoustic televiewer indirectly detects fractures, fractures detectable by the acoustic televiewer that are not detectable on the videotapes are enigmatic. One possible explanation of these "invisible" fractures (Michael Chornack, U.S. Geological Survey, oral commun., 1991) is that they were caused by hydrofracturing between the time when the television camera was operated (during and shortly after drilling) and the time when the acoustic televiewer was operated (after demobilization of the drill rig). Alternatively, the acoustic televiewer might be able to detect fractures that are covered with mud and, hence, not visible on videotapes (Alfred Hess, U.S. Geological Survey, oral commun., 1992). Only fractures detectable by the acoustic televiewer that also could be seen on videotapes were used in analyses of the fracture data.

The videotape data, like the acoustic-televiewer data, must be used with caution. Although the videotapes of borehole UE-25c #1 generally are good to excellent in quality, intervals exist where fractures may be obscured by casing, by foam in the borehole, by rough-textured borehole walls (for example, in lithophysal or nonwelded tuff zones), or by poor picture clarity. Only the

intervals in borehole UE-25c #1 where the picture quality was good to excellent were used in fracture analyses. For borehole UE-25c #2, the videotapes generally were poor to fair in quality, often making it impossible to detect thin ("hairline") or mineral-filled fractures. Consequently fewer fractures are visible in borehole UE-25c #2 than in borehole UE-25c #1, making the videotape record of borehole UE-25c #2 unreliable for determining fracture frequency. Although videotapes of borehole UE-25c #3 were obtained in 1990, they had not been analyzed at the time of this writing and could not be used in the preparation of this report. Interpretations of fracture orientation, frequency, and density in this report, therefore, are based largely on videotapes of selected intervals of borehole UE-25c #1 and might not apply much beyond this borehole.

As indicated in figure 23, videotapes of the Crater Flat Tuff, the tuffs and lavas of Calico Hills, and the Paintbrush Tuff penetrated in borehole UE-25c #1 indicate that fractures at the C-hole complex strike preferentially between 160° and 200° (S. 20° E. to S. 40° W.) and secondarily between 120° and 160° (S. 60° E. to S. 20° E.). In general, the predominant fractures are oriented approximately perpendicular to the principal directions of Miocene extension (Rehrig, 1986) and to the least principal horizontal stress at Yucca Mountain (Stock and Healy, 1988). The fewest fractures in borehole UE-25c #1 occur between 20° and 60° (N. 20° E. to N. 60° E.) and between 240° and 300° (S. 60° W. to N. 60° W.), approximately parallel to the direction of the least principal horizontal stress (Stock and Healy, 1988). Although corroborative measurements have not been made, fractures oriented perpendicular to the least principal horizontal stress generally would be expected to be the most open, whereas those oriented orthogonally generally would be expected to be the least open. Adjacent to faults and in other zones of ground-water movement, fractures commonly are filled with minerals without regard for their orientation. The apertures of these fractures, hence, are independent of the stress regime.

In the Crater Flat Tuff alone, 30 percent of the fractures for which strikes could be determined in borehole UE-25c #1 strike between 160° and 200° (S. 20° E. to S. 20° W.). These south-southeasterly to south-southwesterly striking fractures predominate in all three members (fig. 24). Of secondary importance in the Tram Member are fractures striking between 300° and 340° (N. 60° W. and N. 20° W.), whereas fractures striking between 120° and 160° (S. 60° E. and S. 20° E.) are the secondmost abundant fractures in the Bullfrog and Prow Pass Members. Most of the fractures in all three members are steeply dipping. For 59 fractures recorded by both the acoustic televiewer and television camera in borehole UE-25c #1, dips ranged from 16° to 82°, with medians of 64° in the Tram Member, 76° in the Bullfrog Member, and 70° in the Prow Pass Member. Shallowly dipping fractures are most abundant in nonwelded to partially welded tuff, bedded tuff, and tuff breccia zones. Fractures partly or completely filled with minerals are common in the tuff breccia zone of the Tram Member and predominate in the central, moderately to densely welded zone of the Bullfrog Member.

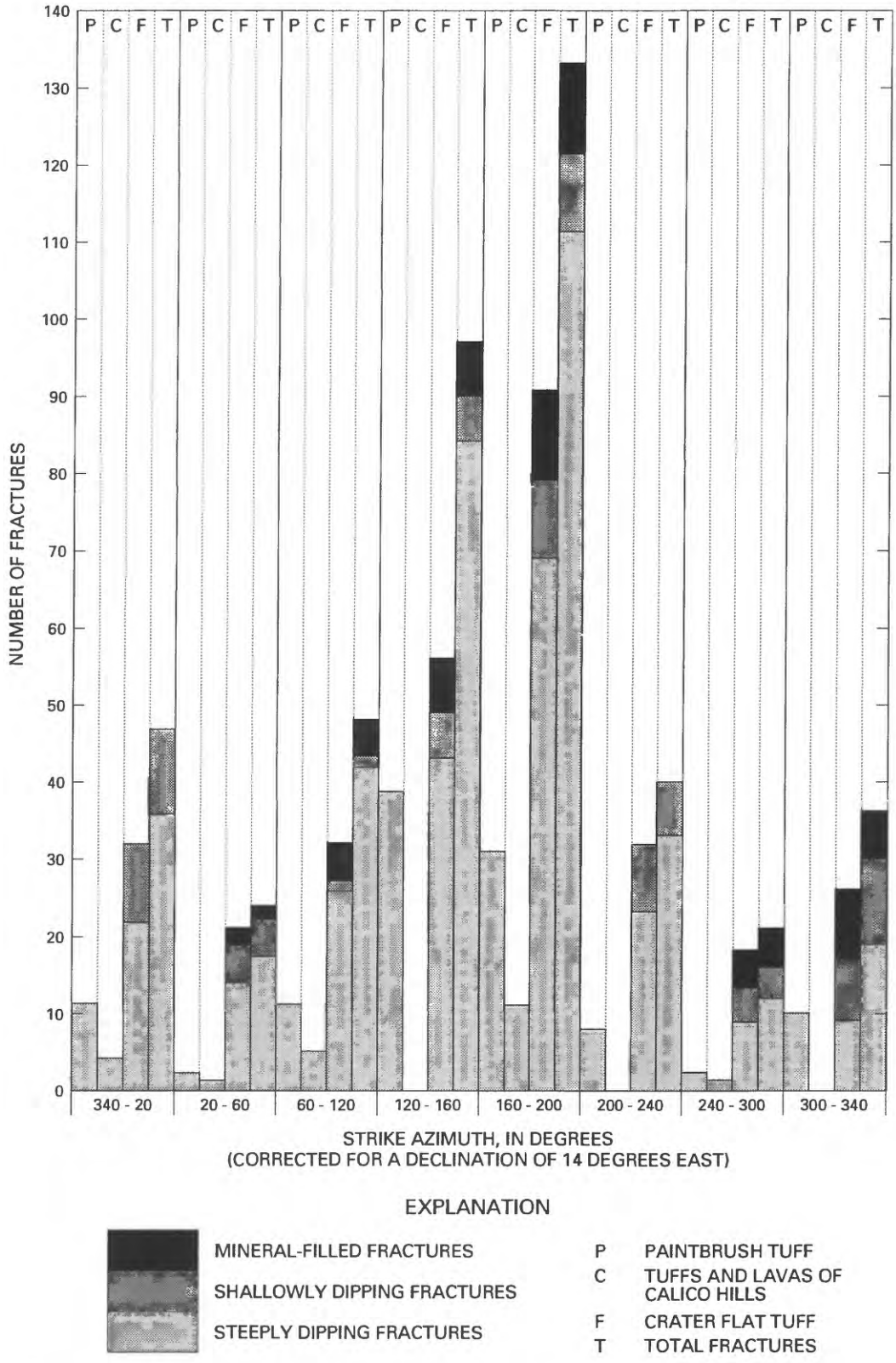

Figure 23.--Frequency distribution of fractures detectable on videotapes of borehole UE-25c #1 (at least 58 additional fractures with indeterminate strikes were detected in analyzed intervals of these geologic units).

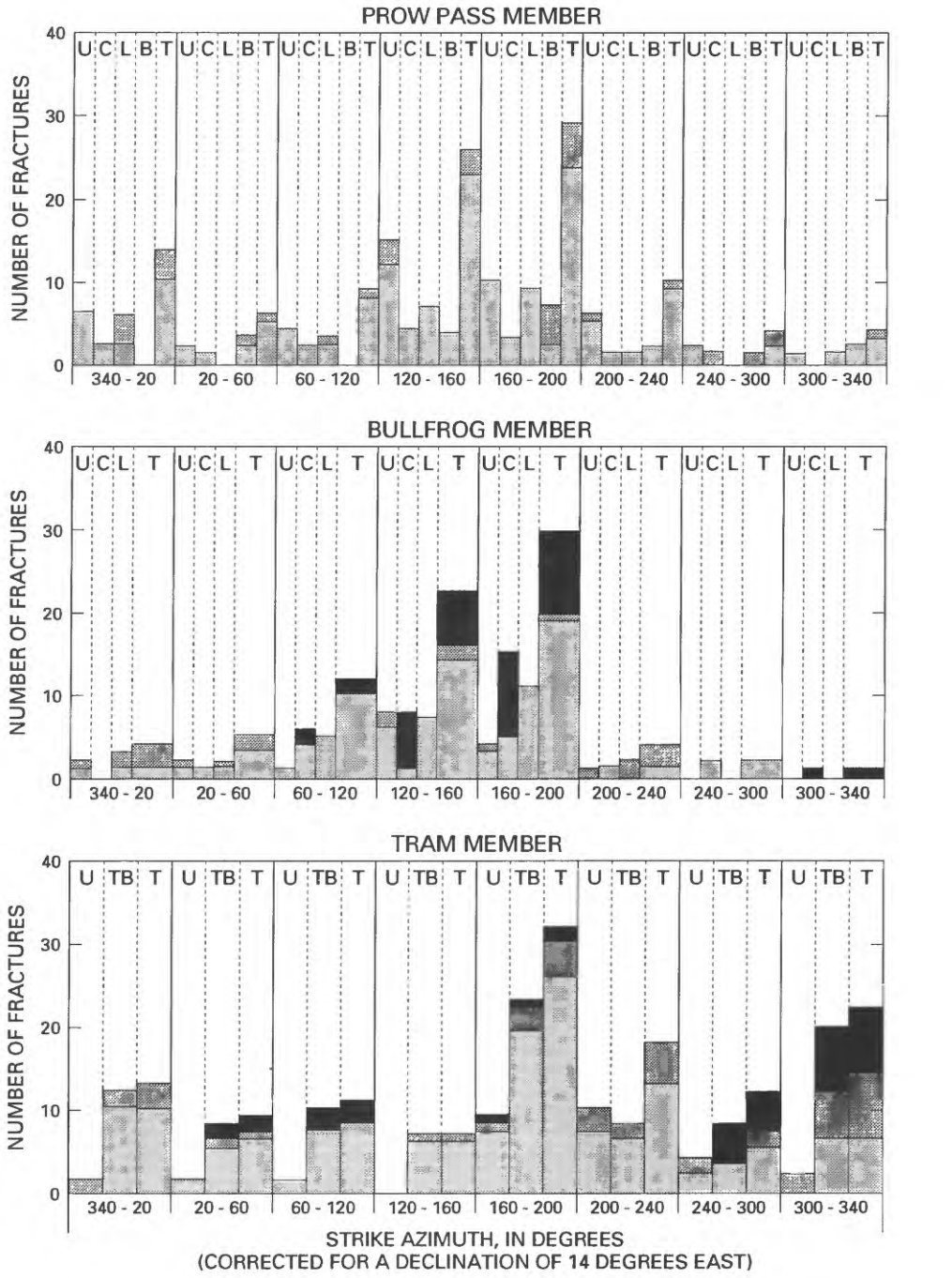

Figure 24.--Frequency distribution of fractures in the Crater Flat Tuff detectable on videotapes of borehole UE-25c #1 (at least 25 additional fractures with indeterminate strikes were detected in the Crater Flat Tuff).

The most consistently fractured interval in the Crater Flat Tuff at the C-hole complex is the tuff breccia zone of the Tram Member (table 6). The fracturing in this zone and possibly in the nonwelded to partially welded tuff at the top of the Tram Member probably is related to the faults that transect the Tram Member at the C-hole complex. The tuff breccia zone contains about 33 percent of the fractures identified on videotapes of the Crater Flat Tuff in borehole UE-25c #1, and the observed frequency of these fractures is 1.93 per meter. The bedded zone at the base of the Prow Pass Member contains about 5 percent of the known fractures in borehole UE-25c #1, a frequency of 1.59 fractures per meter, but because the bedded zone at the base of the Bullfrog Member could not be seen clearly, it cannot be determined if the fracture frequency in the bedded zone of the Prow Pass Member is representative of all bedded zones in the Crater Flat Tuff at the C-hole complex. Contrary to what might be expected, nonwelded to partially welded zones of the Crater Flat Tuff in borehole UE-25c #1 are more fractured than moderately to densely welded zones. Nonwelded to partially welded zones contain about 47 percent of the observed fractures, an average frequency of 0.98 fracture per meter, whereas moderately to densely welded zones contain about 15 percent of the observed fractures, an average frequency of only 0.68 fracture per meter. If representative of the entire C-hole complex, the fracture data for borehole UE-25c #1 indicate that fracture frequency in the Crater Flat Tuff is unrelated or inversely related to the degree of welding.

Like the Crater Flat Tuff, fractures in the tuffs and lavas of Calico Hills in borehole UE-25c #1 strike preferentially between 160° and 200°

Table 6.--*Fracture frequency in the Crater Flat Tuff, determined from videotapes of borehole UE-25c #1*

Lithology	Number of fractures	Percent of total	Interval thickness (meters)	Frequency (fractures per meter)
Prow Pass Member				
Upper (nonwelded to partially welded) zone	50	15.0	44.5	1.13
Central (moderately welded) zone	14	4.2	6.7	2.09
Lower (nonwelded to partially welded) zone	29	8.7	37.2	.78
Bedded zone	17	5.1	10.7	1.59
Bullfrog Member				
Upper (nonwelded to partially welded) zone	18	5.4	32.6	.55
Central (moderately to densely welded) zone	36	10.8	67.1	.54
Lower (nonwelded to partially welded) zone	32	9.6	29.9	1.07
Tram Member				
Upper (nonwelded to partially welded) zone	28	8.4	18.0	1.56
Tuff breccia zone	110	32.8	57.0	1.93
	334	100.0	303.7	

(fig. 25). Of the fractures visible on sections of videotapes that were sufficiently clear for reliable estimates of frequency, 73 percent were in nonwelded ash-flow tuff, and 27 percent were in bedded tuff. Nearly all observed fractures were steeply dipping, although some shallowly dipping fractures were detected in the bedded zone. Three fractures detected by both the television camera and acoustic televiewer in boreholes UE-25c #1 and UE-25c #2 had a median dip of 75°. The observed fracture frequency in borehole UE-25c #1 was 0.80 fracture per meter in the nonwelded zone and 0.23 fracture per meter in the bedded zone (table 7).

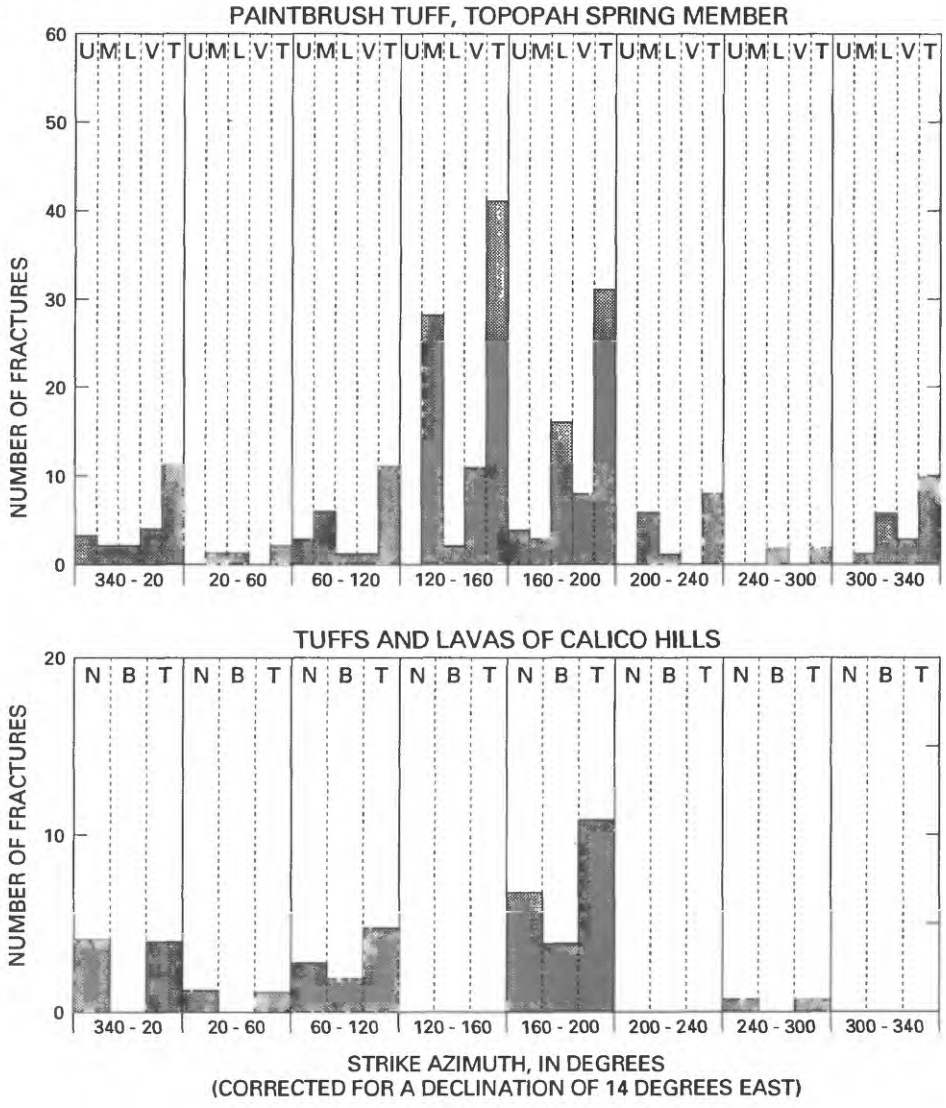

EXPLANATION

U	UPPER WELDED ZONE	N	NONWELDED ZONE
M	MIDDLE WELDED ZONE	B	BEDDED ZONE
L	LOWER WELDED ZONE	T	TOTAL FRACTURES
V	LOWER VITROPHYRE		

Figure 25.--Frequency distribution of fractures in the tuffs and lavas of Calico Hills and the Topopah Spring Member of the Paintbrush Tuff detectable on videotapes of borehole UE-25c #1 (at least 33 additional fractures with indeterminate strikes were detected in these geologic units).

Table 7.--*Fracture frequency in the tuffs and lavas of Calico Hills and the Topopah Spring Member of the Paintbrush Tuff, determined from videotapes of borehole UE-25c #1*

Geologic unit	Number of fractures	Percent of total	Interval thickness (meters)	Frequency (fractures per meter)
Paintbrush Tuff				
Topopah Spring Member				
Upper (moderately) welded zone	14	9.9	19.8	0.71
Middle (densely) welded zone	61	43.3	43.0	1.42
Lower (densely) welded zone	33	23.4	45.4	.73
Lower vitrophyre zone	33	23.4	16.4	2.01
Total	141	100.0	124.6	
Tuffs and Lavas of Calico Hills				
Nonwelded zone	19	73.1	23.8	.80
Bedded zone	7	26.9	30.2	.23
Total	26	100.0	64.0	

Fracture orientation in the Paintbrush Tuff, on the basis of data from four zones in the Topopah Spring Member penetrated in borehole UE-25c #1 (fig. 25), appears to be somewhat different than in previously discussed geologic units. Although the predominant strike of fractures in the lower welded zone of the Topopah Spring Member, as in underlying geologic units, is 160° to 200°, the strike of most fractures in the middle welded and lower vitrophyre zones and the Topopah Spring Member in general is more to the southeast, between 120° and 160° (S. 60° E. to S. 20° E.). If corroborated by data from the Tiva Canyon Member and other zones in the Topopah Spring Member penetrated in borehole UE-25c #1 and by data from boreholes UE-25c #2 and UE-25c #3, the apparent predominance of southeasterly striking fractures in the Paintbrush Tuff could indicate that the regional tectonic stress regime shifted during the time elapsed between deposition of the tuffs and lavas of Calico Hills and the Paintbrush Tuff (Michael Chornack, U.S. Geological Survey, oral commun., 1991).

Although quantitative data are lacking, all of the observed fractures in the Paintbrush Tuff in borehole UE-25c #1 appear to be steeply dipping. In borehole UE-25h #1, a horizontal borehole drilled at Fran Ridge, 3.2 km southeast of the C-hole complex (fig. 1), the average dip of fractures (excluding bedding planes) in core from the Paintbrush Tuff was 49° (Norris and others, 1986). Few observed fractures in the Paintbrush Tuff in borehole UE-25c #1 contained minerals, and one fracture, during drilling, had a stream of water jetting from it.

Fracture frequency in the Paintbrush Tuff is difficult to estimate, except for zones of nonlithophysal welded tuff (which comprise most of the geologic unit) and vitrophyre. For three zones of nonlithophysal welded tuff in borehole UE-25c #1, the observed fracture frequency ranged from 0.71 to 1.42 fractures per meter (table 7) and averaged 1.00 fracture per meter.

Fracture frequency in the lower vitrophyre zone is at least twice that of the welded tuff. Excluding five intervals of intensely fractured rock totaling 5.2 m, the observed fracture frequency in the lower vitrophyre zone was 2.01 fractures per meter (table 7).

More important than fracture frequency in assessing the ability of the tuffaceous rocks at the C-hole complex to transmit water is the fracture density, the number of fractures per unit volume. Determination of fracture density in a volume of rock based on fracture frequency in boreholes where the axes of most fractures are subparallel to the borehole axis requires a correction factor to account for the angle between the borehole and the dip of the fractures (Scott and Castellanos, 1984, p. 63). An equation for calculating fracture density given by Scott and Castellanos (1984, p. 63) that takes into account the requisite correction factor in a unit sphere of rock can be rewritten as:

$$D = \frac{1.24}{b} \sum_{\theta=1°}^{\theta=90°} \frac{f}{\cos\theta} \qquad (1)$$

where D = fracture density, in fractures per cubic meter;
b = thickness of geologic unit, in meters;
θ = dip angle of fractures, in degrees; and
f = the number of fractures for each angle θ.

Because for most of the fractures detected at the C-hole complex, the dip angle was unknown, equation 1 was modified to:

$$D = \frac{1.24 \times f/b}{\cos\bar{\theta}} \qquad (2)$$

where $\bar{\theta}$ = the average dip angle of fractures in a geologic unit, and all other variables are the same as in equation 1.

Fracture-density values for geologic units penetrated in borehole UE-25c #1 that were calculated from fracture-frequency values using equation 2 are listed in table 8. For comparison, fracture-density values in the Crater Flat Tuff, the tuffs and lavas of Calico Hills, and the Paintbrush Tuff determined from transect mapping, from core obtained from boreholes USW GU-3/G-3 at Yucca Mountain, and from core obtained at Fran Ridge, also are listed in table 8. In comparing fracture densities determined for the C-hole complex with those determined elsewhere, it readily is apparent that determinations of fracture density based on direct observation--core logging and transect mapping--nearly always are larger than estimates based on videotapes. In intervals of the Paintbrush Tuff, fracture-density values estimated for the C-hole complex from videotapes may be as much as an order of magnitude less than actual values. Estimated fracture-density values in the lower part of the Bullfrog Member and in the upper part of the Tram Member may be about two-tenths to one-half of actual values. Estimated fracture-density values in the tuffs and lavas of Calico Hills, the Prow Pass Member, and the upper nonwelded to partially welded zone of the Bullfrog Member, seem to be about the correct order of magnitude.

Table 8.--*Fracture density in geologic units penetrated in borehole UE-25c #1, corrected for the angle between the borehole and the dip of the fracture*

[--, No information]

Geologic unit	Fracture density (fractures per cubic meter)				Ratio of fracture density[4]
	Yucca Mountain			Fran Ridge	
	C-holes	Transects[1]	Boreholes [2]USW GU-3/G-3	Borehole [3]UE-25h #1	
Paintbrush Tuff					
Topopah Spring Member	2.1	--	--	--	--
Upper (moderately) welded zone	1.3	--	--	--	--
Middle (densely) welded zone	2.7	--	42	26	13-21
Lower (densely) welded zone	1.4	--			
Lower vitrophyre zone	3.8	--	10	--	2.6
Tuffs and lavas of Calico Hills	1.9	1.2	3	--	1.6-2.5
Nonwelded zone	3.8	--		--	
Bedded zone	1.1	--		--	
Crater Flat Tuff	3.5	--		--	
Prow Pass Member	4.0	--		--	
Upper (nonwelded to partially welded) zone	4.1	--		--	
Central (moderately welded) zone	7.6	--		--	
Lower (nonwelded to partially welded) zone	2.8	--		--	
Bedded zone	5.8	--		--	
Bullfrog Member	3.4	--		--	
Upper (nonwelded to partially welded) zone	2.8	--		--	
Central (moderately to densely welded) zone	2.8	--	18	--	6.4
Lower (nonwelded to partially welded) zone	5.5	--	12		2.4
Tram Member	5.2	--			
Upper (nonwelded to partially welded) zone	4.4	--			
Tuff breccia zone	5.5	--	--	--	--

[1]U.S. Geological Survey (1984) and figure 18.

[2]Scott and Castellanos (1984).

[3]Calculated from Norris and others (1986), eliminating assumed bedding planes.

[4]Ratio of fracture density estimated from cores or transects to fracture density estimated for C-holes.

Winograd and Thordarson (1975) divided the Paleozoic, Tertiary, and Quaternary formations present in the vicinity of the NTS into 11 hydrogeologic units. The 10 hydrogeologic units and the geologic units comprising them at and near Yucca Mountain are listed in table 9. This table is somewhat generalized, in that the upper clastic aquitard is not present throughout the Yucca Mountain area. Where it is absent, the upper and lower carbonate aquifers form a single aquifer, which Mifflin (1968) first called the carbonate aquifer and, more recently, the carbonate-rock province (Mifflin, 1988). The approximate extent of the carbonate-rock province is shown in figure 26, but the

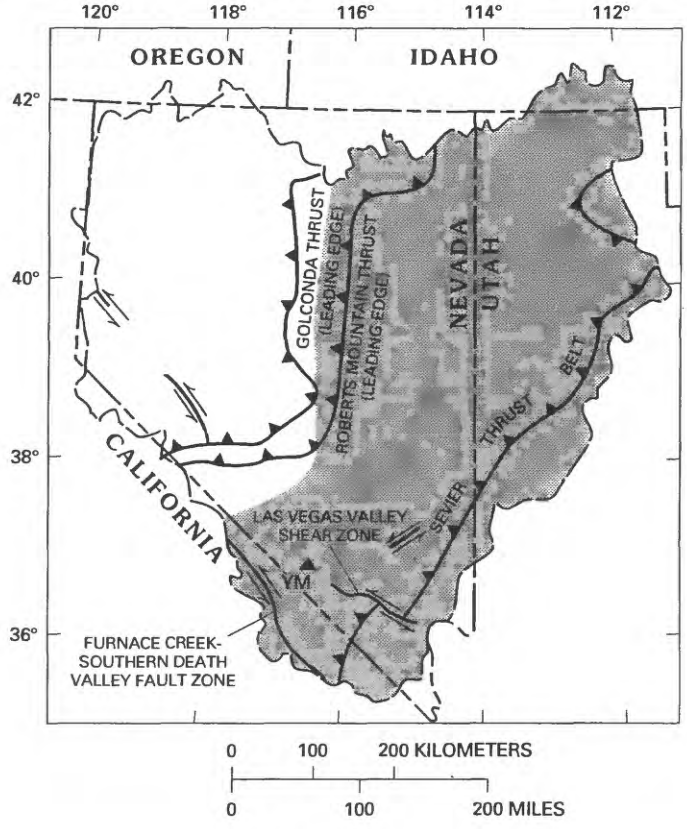

EXPLANATION

CARBONATE ROCK PROVINCE—Shows approximate extent of Middle Cambrian to Lower Triassic carbonate rocks and associated clastic rocks. Western boundary corresponds to easternmost extent of Paleozoic transitional-assemblage sedimentary rocks.

STRIKE-SLIP FAULT—Arrows indicate relative direction of movement.

THRUST FAULT—Barbs on upper plate.

STUDY AREA BOUNDARY

YM YUCCA MOUNTAIN

Figure 26.--Extent of the carbonate-rock province in the Great Basin (modified from Plume and Carlton, 1988).

Table 9.--*Hydrogeologic units at and near Yucca Mountain*

[Modified from Winograd and Thordarson, 1975)]

System	Geologic unit		Hydrogeologic unit
Quaternary and Tertiary	Channel and fan alluvium, talus, slopewash, and lakebeds		Valley-fill aquifer
Tertiary	Basalts of Kiwi Mesa and Skull Mountain; rhyolites of Shoshone Mountain and Fortymile Canyon		Lava-flow aquifer
	Timber Mountain Tuff		Welded tuff aquifer
	Paintbrush Tuff		
	Bedded tuffs		Bedded tuff aquifer
	//////////////	Wahmonie Formation	Lava flow aquitard
	Tuffs and lavas of Calico Hills	Salyer Formation	Tuff aquitard
	Crater Flat Tuff		
	Dacite lava		
	Lithic Ridge Tuff	Rocks of Pavits Spring	
	Quartz latite and rhyolite		
	Older tuffs and conglomerate		
	Tuff of Yucca Flat		
	Horse Spring Formation		
Pennsylvanian and Permian	Tippipah Limestone		Upper carbonate aquifer
Mississippian and Devonian	Eleana Formation		Upper clastic aquitard
	Mississippian carbonate rocks		Lower carbonate aquifer
	Devils Gate Limestone		
	Devonian carbonate rocks		
Silurian and Ordovician	Unnamed carbonate rocks		
Ordovician	Ely Springs Dolomite		
	Eureka Quartzite		
	Pogonip Group		
Cambrian	Nopah Formation		
	Bonanza King Formation		
	Carrara Formation		
	Zabriskie Quartzite		Lower clastic aquitard
	Wood Canyon Formation		
Proterozoic	Stirling Quartzite		
	Johnnie Formation		

carbonate rocks have been deeply buried or replaced by volcanic rocks in caldera centers, such as the Timber Mountain caldera (Byers and others, 1976) or a probable caldera complex centered beneath Crater Flat (Carr, 1988). In some areas, such as at Yucca Mountain, the upper carbonate aquifer has been removed by erosion (Winograd and Thordarson, 1975). Also, information compiled since Winograd and Thordarson's (1975) report indicates that the subdivisions of the Tertiary sequence are somewhat arbitrary. The occurrence of water in the Tertiary volcanic and tuffaceous rocks seems to be controlled by factors other than the lithology and, hence, ground water may not be strata-bound. This is demonstrated by the fact that the major production zones in boreholes drilled into the Tertiary rocks at Yucca Mountain can occur in almost every formation below the water table (fig. 27), and most production zones are associated with faults or fracture zones (table 10). However, some of the water in these boreholes is produced from intervals that contain relatively few fractures, and many fractured intervals do not produce water.

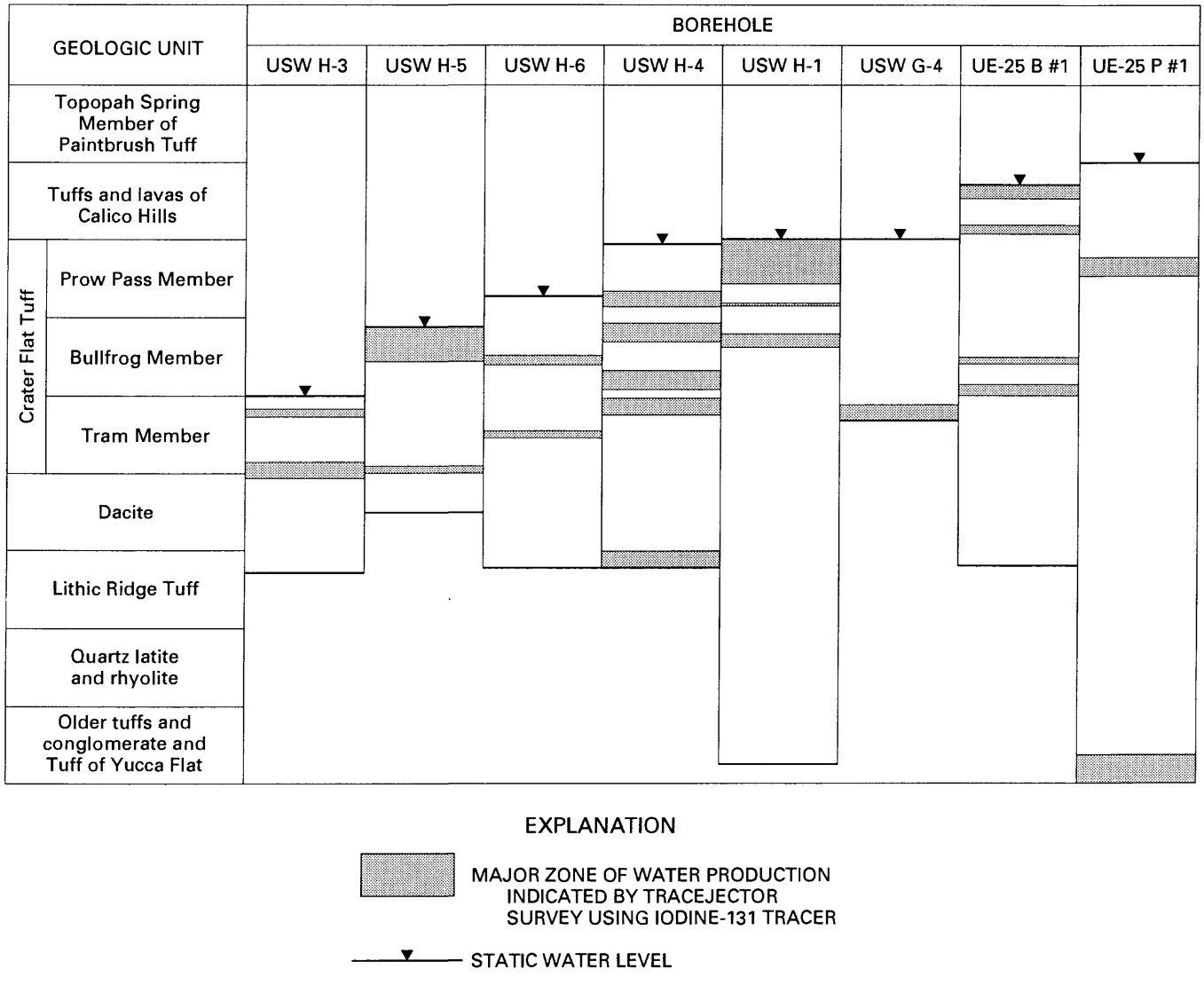

Figure 27.--Major water-production zones in Tertiary rocks and static water levels in boreholes drilled at Yucca Mountain.

Table 10.--*Origin of water-production zones in boreholes at Yucca Mountain*

[m = meters]

Borehole	Production zone (depth below land surface, in meters)	Percent of production	Geologic unit	Origin of water	Source of information
USW H-6	572 to 604	8	Bullfrog Member of Crater Flat Tuff	Fracture zone at 592 to 640 m	Craig and others (1983); Craig and Reed (1991)
	616 to 631	60	Bullfrog Member of Crater Flat Tuff	Fracture zone at 592 to 640 m	
	777 to 788	32	Tram Member of Crater Flat Tuff	Fracture zone at 768 to 800 m	
USW H-5	704 to 771	90	Bullfrog Member of Crater Flat Tuff	Hole enlargements on caliper log indicate possible fracture zones at 721 to 726 and 752 to 758 m	Robison and Craig (1991)
	1,033 to 1,043	8	Tram Member of Crater Flat Tuff	Water may be trapped in permeable, bedded tuff by underlying lava flow	
USW H-4	561 to 584	6	Prow Pass Member of Crater Flat Tuff	Hole enlargement on caliper log log indicates possible fracture zone at 567 to 604 m	Whitfield and others (1985): Erickson and Waddell (1985)
	623 to 669	13	Prow Pass Member of Crater Flat Tuff	Fracture zone at 610 to 640 m	
	707 to 733	28	Bullfrog Member of Crater Flat Tuff	Fracture zone at 724 to 744 m	
	779 to 805	9	Bullfrog Member of Crater Flat Tuff	Fracture zone at 777 to 808 m	
	820 to 876	14	Tram Member of Crater Flat Tuff	Fracture zone at 847 to 869 m	
	892 to 922	16	Tram Member of Crater Flat Tuff	Fracture zone at 878 to 896 m	
	1,181 to 1,219	12	Lithic Ridge Tuff	Hole enlargement indicates possible fracture zones at 1,186 to 1,189, 1,202 to 1,207, and 1,214 to 1,215 m	
USW H-3	809 to 841	70	Tram Member of Crater Flat Tuff	Interval contains seven steeply dipping fractures	Thordarson and others (1984)

Table 10.--*Origin of water-production zones in boreholes at Yucca Mountain*--Continued

Borehole	Production zone (depth below land surface, in meters)	Percent of production	Geologic unit	Origin of water	Source of information
USW H-3--Continued					
	1,060 to 1,120	30	Tram Member and Lithic Ridge Tuff	Interval contains five steeply dipping fractures	
USW H-1	572 to 597	17	Prow Pass Member of Crater Flat Tuff	Water seep (from fracture ?) at 570 m; fracture at 580 m	Rush and others (1983, 1984)
	597 to 653	18	Prow Pass Member of Crater Flat Tuff	Fracture at 608 m	
	687 to 690	9	Prow Pass Member of Crater Flat Tuff	Fracture at 688 m	
	736 to 758	56	Bullfrog Member of Crater Flat Tuff	Hole enlargement indicates possible fracture zone at 707 to 762 m	
USW G-4	879 to 915	98	Tram Member of Crater Flat Tuff	Shear fractures from 885 to 914 m indicate a fault zone	Lobmeyer (1986)
UE-25b #1	471 to 502	12	Tuffs and lavas of Calico Hills	Possible faults or fractures	Lobmeyer and others (1983)
	546 to 564	20	Tuffs and lavas of Calico Hills	Possibly faults or fractures	
	579 to 626	19	Prow Pass Member of Crater Flat Tuff	Four shear zones indicative of faulting from 579 to 626 m	
	811 to 818	19	Bullfrog Member of Crater Flat Tuff	Shear (fault) zone present	
	866 to 872	30	Bullfrog Member of Crater Flat Tuff	Shear (fault) zone from 866 to 879 m	
UE-25p #1	469 to 501	58	Prow Pass Member of Crater Flat Tuff	Possibly from fractures related to inferred fault at top of unit	Craig and Robison (1984); Carr and others (1986a)
	1,000 to 1,119	8	Lithic Ridge and older tuffs	Shear (fault) zone present at 1,012 m	
	1,197 to 1,244	28	Older tuffs and Tuff of Yucca Flat	Production probably from fault zones at 1,197 and 1,244 m	

Presumably, lithophysal zones of the Paintbrush Tuff, nonwelded to partially welded zones of the Paintbrush Tuff, tuffs and lavas of Calico Hills, Crater Flat Tuff, and Lithic Ridge Tuff, and the ash-fall tuff, reworked tuff, and tuffaceous sandstone at the base of most members of the Lithic Ridge, Crater Flat, Paintbrush, and Timber Mountain Tuffs are sufficiently permeable to transmit water in the absence of fractures. Values of porosity and permeability for the Paleozoic and Tertiary rocks at and near Yucca Mountain that were determined from laboratory analyses of core sampled prior to drilling the C-holes are summarized in table 11.

Local-scale hydrologic properties (determined by onsite aquifer tests) have been difficult to assess for the Yucca Mountain area because of the effects of fractures on ground-water flow. Water levels during pumping and injection tests at Yucca Mountain generally have not responded as expected for an infinite, homogeneous, isotropic, confined, porous medium. Nevertheless, some investigators have used methods, such as those of Theis (1935), Cooper and Jacob (1946), or Papadopulos and others (1973), that are based on the above assumptions to calculate values of hydraulic conductivity and transmissivity (see, for example, Rush and others, 1984). Other investigators, including Thordarson (1983), Craig and Robison (1984), and Craig and Reed (1991), recognized that the Tertiary and Paleozoic aquifers at Yucca Mountain are anisotropic and heterogeneous and have used more elaborate analytical solutions, such as those of Stallman (1965), Neuman (1975), Cinco-Ley and Samaniego (1981), or Moench (1984). The result of using these various approaches, regardless of their appropriateness, has been an accumulated record of reported hydraulic conductivity and transmissivity values that are not directly comparable and, thus, cannot be used together in regional syntheses of hydrologic investigations, as was done by Waddell and others (1984) to show distributions of hydraulic conductivity and transmissivity in the Tertiary rocks at Yucca Mountain. It is beyond the scope of this report to resolve discrepancies in reported values of hydrologic properties, but the subject of aquifer tests will be addressed in more detail later in this report in developing a conceptual model of ground-water occurrence in the Tertiary rocks at the C-hole complex.

On a regional scale, anisotropy and heterogeneity tend to affect ground-water movement less significantly than on a local scale; average hydrologic properties, thus, can be estimated with some confidence using regional-scale numerical models based on the assumption of an equivalent isotropic, homogeneous, porous medium (John Czarnecki, U.S. Geological Survey, written commun., 1990). Using a two-dimensional, finite-element model of the Yucca Mountain area, Czarnecki and Waddell (1984) estimated that the transmissivity of the lower carbonate aquifer near Yucca Mountain is 12,000 m^2/d, whereas the transmissivity of the Tertiary volcanic and tuffaceous rocks near Yucca Mountain ranges from 4 to 3,000 m^2/d.

Hydrologic properties, stratigraphic and structural information, and hydraulic-head data for the NTS and vicinity (Winograd and Thordarson, 1975, pl. 1; Robison and others, 1988) indicate that the Tertiary and Paleozoic rocks in the Yucca Mountain area comprise two separate and distinct ground-water flow systems. As envisioned by Mifflin (1968), ground water in the Basin and Range province flows locally from mountainous areas to intermontane basins through the Tertiary rocks and Quaternary-Tertiary valley fill and regionally, from basin to basin, primarily through Paleozoic carbonate rocks.

Table 11.--*Laboratory-determined porosity and permeability of the Tertiary rocks at Yucca Mountain and Paleozoic rocks at the Nevada Test Site*

[Data for the Tertiary rocks from boreholes USW H-1, USW G-3, USW G-4, UE-25a #1, and UE-25b #1, as reported by Spengler and others (1979), Lobmeyer and others (1983), Rush and others (1983), and Anderson (1984); data for the Paleozoic rocks from Winograd and Thordarson (1975); -- = no information]

Geologic unit and rock type	Effective porosity (percent)			Number of samples	Pore-scale (matrix) permeability to water (millidarcies)						Number of samples
					Horizontal			Vertical			
	Minimum	Maximum	Median		Minimum	Maximum	Median	Minimum	Maximum	Median	
Paintbrush Tuff					4.0×10^{-4}	5.4	3.4×10^{-3}	--	--	--	8
Vitrophyre	1.4	3.7	3.1	3							
Densely welded tuff	5.5	20.3	16	17							
Moderately to densely welded tuff	5.1	13.8	9.4	23							
Moderately welded tuff	11.0	27.9	16.4	12							
Nonwelded tuff	28.7	51.9	38.8	5							
Tuffs and lavas of Calico Hills					0.23	0.23	0.23	0.050	0.050	0.050	1
Nonwelded tuff	25	43	34.3	14							
Crater Flat Tuff					1.1×10^{-3}	1.3	0.094	2.3×10^{-3}	0.67	0.067	33
Moderately to densely welded tuff	5.8	8.5	7.8	6							
Moderately welded tuff	10.1	23.7	19.5	12							
Partially welded tuff	10.0	39.7	26.0	40							
Partially welded to nonwelded tuff	15.2	35.0	26.7	12							
Nonwelded tuff	28.6	43.6	32.2	4							
Bedded tuff	10.9	30.2	23.4	4							
Lithic tuff and tuff breccia	1.8	24.4	17.2	27							
Lithic Ridge Tuff											
Moderately welded tuff	11.6	19.5	16.4	8							
Partially to moderately welded tuff	9.2	16.1	13.9	6							
Partially welded to nonwelded tuff	16.9	23.5	20.3	7							
Older tuffs					0.081	0.40	0.24	0.027	0.54	0.28	2
Moderately to densely welded tuff	8.8	17	13.8	5							
Dacite lava and flow breccia	7.3	7.3	7.3	1	1.1×10^{-3}	1.1×10^{-3}	1.1×10^{-3}	1.1×10^{-3}	1.1×10^{-3}	1.1×10^{-3}	1
Upper clastic aquitard	0.6	15.1	3.4	22							
Lower carbonate aquifer	0.0	9.0	1.1	25	1.1×10^{-3}	5.5	4.5×10^{-3}	--	--	--	13
Lower clastic aquitard					3.9×10^{-5}	5.6×10^{-4}	1.1×10^{-4}	--	--	--	18
Quartzite	0.6	5.0	1.4	10							
Argillite and siltstone	0.7	3.6	2.0	10							

As modeled by Czarnecki and Waddell (1984) and by Peter Sinton and Joseph Downey (U.S. Geological Survey, written commun., 1989), ground water from Yucca Mountain flows southward toward the Amargosa Desert, ultimately discharging to Alkali Flat (Franklin Lake playa) and Death Valley, south and east of the Funeral Mountains (location of Funeral Mountains shown in fig. 1). The local flow system is recharged by precipitation in the Pahute Mesa area and by subsurface inflows from the Ash Meadows and Oasis Valley ground-water basins (Czarnecki and Waddell, 1984). As indicated by Peter Sinton and Joseph Downey (U.S. Geological Survey, written commun., 1989), a downward flux between the local and regional flow systems occurs northeast of Yucca Mountain (in the Yucca Flat area), whereas an upward flux (recorded in the C-holes and boreholes USW H-1 and UE-25p #1) occurs at Yucca Mountain. Faults, such as the Solitario Canyon and Paintbrush Canyon Faults, could be functioning as conduits for the exchange of water between the local and regional flow systems.

Water Levels in the C-holes

Most of the water levels measured in the C-holes from 1983 to 1986 are summarized in table 12. In general, depths to water in the C-holes ranged from 400 to 402 m below land surface during the measuring period, and the composite water level in each of the three boreholes fluctuated without any apparent trend between 730.0 and 730.5 m above the NGVD of 1929. Measurements made above and below the packers in boreholes UE-25c #1 and UE-25c #3 uniformly indicate that a positive hydraulic-head difference of 0.33 to 0.35 m exists between the bottom and top of the C-holes. Therefore, according to Darcy's law, upward ground-water movement should take place at the C-hole complex. However, considering the small vertical hydraulic-head gradient, unanticipated factors, such as impermeable rock, could limit upward ground-water flow.

The water-level data for the C-holes are consistent with measurements in other boreholes completed in the Tertiary rocks east of the crest of Yucca Mountain, south of Drill Hole Wash, and west of Fortymile Wash (Robison, 1984; Robison and others, 1988). The average hydraulic gradient through this area is 1.3 m/km. Throughout the central part of this area, including the C-hole complex, there is no detectable gradient. Northwest and west of the crest of Yucca Mountain, the average hydraulic gradient abruptly steepens to as much as 430 m/km, and hydraulic heads of 1,029 to 1,034 m have been recorded in boreholes USW G-2 and UE-25 WT #6. The reason for the abrupt steepening of the gradient is unknown. Possible explanations are that the Solitario Canyon Fault functions as a barrier boundary, or that the central (repository) block (fig. 1) is much less fractured and, therefore, less permeable than adjacent blocks to the north and west. The flatness of the hydraulic gradient east of the crest of Yucca Mountain is inexplicable at present.

Matrix Hydrologic Properties of Rocks at the C-hole Complex

The matrix hydrologic properties discussed in this section are porosity, pore-scale permeability, and storativity. Values of these properties all were determined either by laboratory or geophysical methods and, thus, are considered to be representative of only a small volume of rock surrounding each of the C-holes. Extrapolation of these values throughout the C-hole complex and beyond to Yucca Mountain would not be justified without further study.

Table 12.--*Water-level measurements in boreholes UE-25c #1, UE-25c #2, and UE-25c #3*

[Data from Robison and others, 1988; U.S. Geological Survey, unpublished; -- = not applicable]

Date	Borehole	Interval (meters below top of casing)	Measuring device	Land-surface datum (meters)	Measured depth to water (meters)	Corrections				Altitude of water surface (meters)
						Borehole deviation (meter)	Thermal expansion (meter)	Mechanical stretch (meter)	Cable[1]	
10-25-83	UE-25c #1	418 - 914	Cable	1,130.6	400.36	-0.06	--	--	0.99961	730.46
11-29-83	UE-25c #1	418 - 914	Cable	1,130.6	400.39	-.06	--	--	.99956	730.45
12-19-83	UE-25c #1	418 - 914	Cable	1,130.6	400.44	-.06	--	--	.99952	730.41
01-23-84	UE-25c #1	418 - 914	Cable	1,130.6	400.49	-.06	--	--	.99947	730.38
02-13-84	UE-25c #1	418 - 914	Cable	1,130.6	400.41	-.06	--	--	.99942	730.48
03-02-84	UE-25c #1	418 - 914	Cable	1,130.6	400.55	-.06	--	--	.99937	730.36
	UE-25c #2	418 - 914	Cable	1,132.2	402.20	-.055	--	--	.99937	730.31
04-06-84	UE-25c #2	418 - 914	Cable	1,130.6	402.09	-.055	--	--	.99932	730.44
04-11-84	UE-25c #1	418 - 914	Cable	1,130.6	400.66	-.06	--	--	.99932	730.27
05-02-84	UE-25c #2	416 - 914	Cable	1,132.2	402.20	-.055	--	--	.99928	730.34
	UE-25c #3	417 - 914	Cable	1,132.3	402.16	-.095	--	--	.99928	730.42
10-23-84	UE-25c #2	416 - 914	Cable	1,132.2	402.36	-.055	--	--	.99903	730.28
	UE-25c #3	417 - 914	Cable	1,132.3	402.32	-.095	--	--	.99903	730.46
10-24-85	UE-25c #1	418 - 796	Tape	1,130.6	400.31	-.06	0.021	-0.044	--	730.21
		799 - 914	Tape	1,130.6	399.98	-.06	.021	-.044	--	730.54
12-03-85	UE-25c #1	418 - 796	Tape	1,130.6	400.61	-.06	.021	-.044	--	729.91
		799 - 914	Tape	1,130.6	400.27	-.06	.021	-.044	--	730.25
12-03-85	UE-25c #3	417 - 751	Tape	1,132.3	402.27	-.095	.021	-.044	--	730.15
		754 - 914	Tape	1,132.3	401.92	-.095	.021	-.044	--	730.50
04-24-86	UE-25c #1	799 - 914	Tape	1,130.6	400.23	-.06	.021	-.052	--	730.28
05-22-86	UE-25c #1	799 - 914	Tape	1,130.6	400.30	-.06	.021	-.052	--	730.21

[1]The cable correction factor is applied in the following manner: Altitude of water surface = land-surface datum - [(measured depth to water × cable correction factor) - borehole deviation correction].

Porosity

Porosity was determined in the C-holes by laboratory and geophysical methods. For boreholes UE-25c #2 and UE-25c #3, there generally was good agreement between the porosity determined from the epithermal neutron and gamma-gamma logs; for borehole UE-25c #1, however, the porosity determined from the gamma-gamma log consistently was smaller than that determined from the epithermal-neutron log by 4 to 15 percent. When laboratory-determined values of porosity for core samples from borehole UE-25c #1 were compared with the geophysically determined values of porosity for this borehole, good agreement occurred between porosity determined for the core by helium injection and porosity determined from the gamma-gamma log (fig. 28). On the basis of these comparisons, the most reliable values of porosity were judged to be those determined by helium injection and gamma-gamma logging. Porosity values determined for geologic units at the C-hole complex from the gamma-gamma log of borehole UE-25c #1, as listed in table 13, range from 12 to 43 percent,

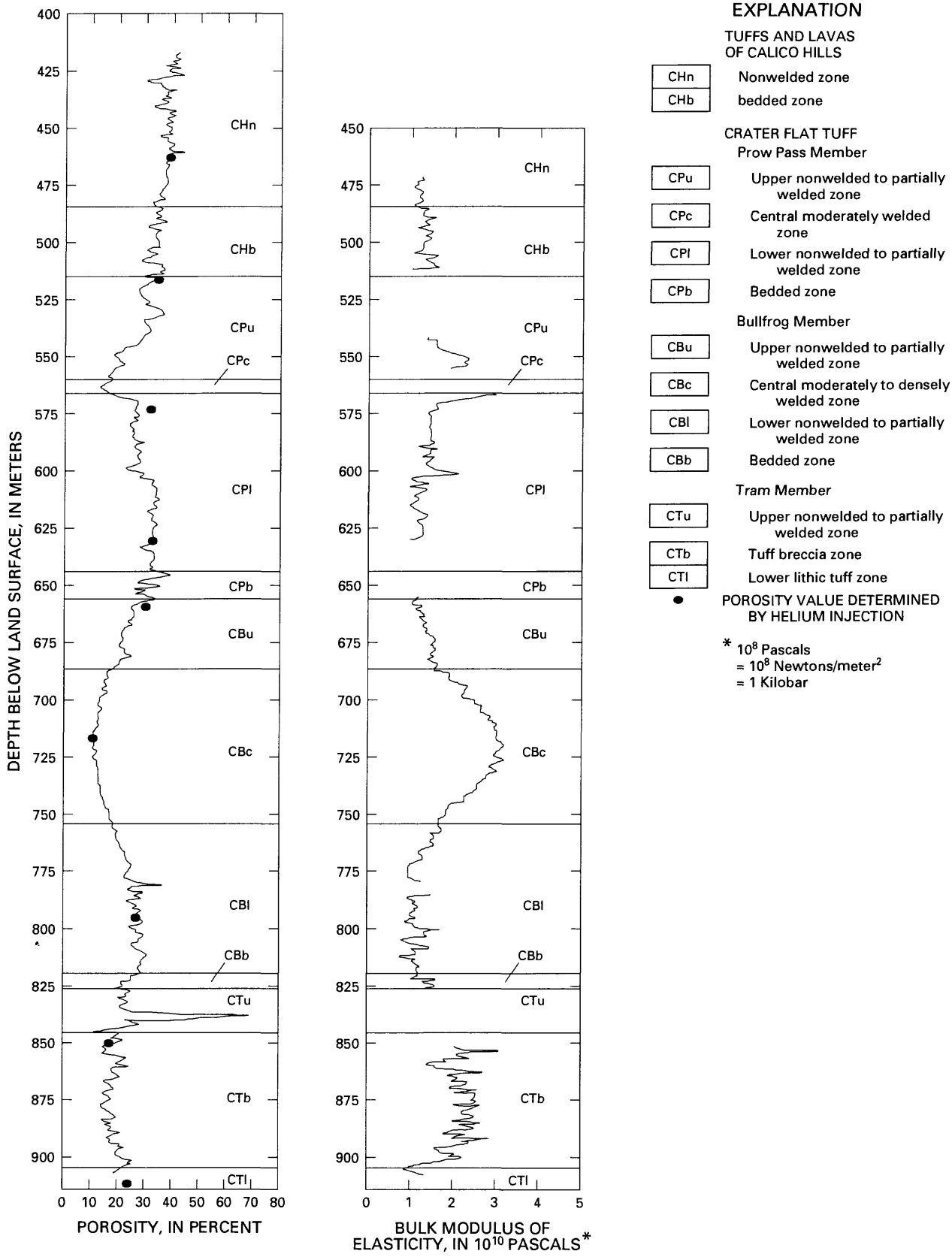

Figure 28.--Porosity determined by helium injection and gamma-gamma logging and the calculated bulk modulus of elasticity of rocks penetrated in borehole UE-25c #1.

Table 13.--*Porosity statistics for geologic units at the C-hole complex, based on gamma-gamma logging of borehole UE-25c #1*

Geologic unit	Porosity (percent)		
	Minimum	Maximum	Mean
Tuffs and lavas of Calico Hills			
Nonwelded zone	28	43	37
Bedded zone	26	36	32
Crater Flat Tuff			
Prow Pass Member			
Upper nonwelded to partially welded zone	14	35	26
Central moderately welded zone	12	16	14
Lower nonwelded to partially welded zone	15	33	28
Bedded zone	26	40	31
Bullfrog Member			
Upper nonwelded to partially welded zone	16	32	22
Central moderately to densely welded zone	11	18	14
Lower nonwelded to partially welded zone	17	37	26
Bedded zone	19	29	24
Tram Member			
Upper nonwelded to partially welded zone[1]	12	26	22
Tuff breccia zone	13	25	18

[1]An interval within this geologic unit, between depths of 806 and 809 meters below land surface, has a porosity of 69 percent. This value is excluded from the statistics, however, because it is considered to be indicative of one or more enlarged fractures.

except for an anomalous 3-m-thick interval in the Tram Member of the Crater Flat Tuff, the "porosity" of which is believed to be the result of one or more enlarged fractures. Nonwelded to partially welded and bedded tuff zones of the Crater Flat Tuff are more porous than moderately to densely welded tuff zones. On the average, the tuffs and lavas of Calico Hills are more porous than the tuffaceous rocks within the Crater Flat Tuff. The porosity data from borehole UE-25c #1 compare favorably with porosity values for the Crater Flat Tuff and the tuffs and lavas of Calico Hills in other boreholes at Yucca Mountain that are listed in table 11.

Pore-Scale Permeability

Permeameter measurements using water as the fluid indicate that pore-scale horizontal and vertical permeability, both, generally range from about 6×10^{-3} to about 2 mD; the horizontal permeability can be slightly larger, and the vertical permeability can be slightly smaller (table 14). There is no consistent relation between pore-scale horizontal and vertical permeability; ratios of horizontal to vertical permeability generally range from 0.7 to 2. The pore-scale permeability of moderately to densely welded tuff in the Crater Flat Tuff seems to be smaller than that of partially welded to nonwelded tuff. The pore-scale permeability data for the C-holes are consistent with data from other boreholes at Yucca Mountain (fig. 29).

Table 14.--*Pore-scale permeability values determined by analyses of core from borehole UE-25c #1*

Depth (meters)	Geologic unit	Lithology	Pore-scale permeability (millidarcies)			
			Air injection		Water injection	
			Horizontal	Vertical	Horizontal	Vertical
462.5	Tuffs and lavas of Calico Hills	Nonwelded tuff	0.31/0.15	0.38/0.22	0.033	0.042
517.3	Crater Flat Tuff, Prow Pass Member	Partially welded to nonwelded tuff	1.8	1.5	.91	1.2
572.5	Crater Flat Tuff, Prow Pass Member	Partially welded to nonwelded tuff	.69	.79	.56	.77
630.1	Crater Flat Tuff, Prow Pass Member	Partially welded to nonwelded tuff	5.0/5.6	2.2/3.1	2.9	.69
658.6	Crater Flat Tuff, Bullfrog Member	Partially welded to nonwelded tuff	1.8	1.6	1.6	1.5
716.0	Crater Flat Tuff, Bullfrog Member	Moderately to densely welded tuff	9.8×10^{-3}	4.1×10^{-3}	5.7×10^{-3}	3.7×10^{-3}
794.7	Crater Flat Tuff, Bullfrog Member	Partially welded to nonwelded tuff	.39	.39/.23	.065	.035
850.3	Crater Flat Tuff, Tram Member	Tuff breccia	.011	.016	8.2×10^{-3}	5.7×10^{-3}
914.2	Crater Flat Tuff, Tram Member	Partially welded lithic tuff	.13	.49/.30	.030	.034

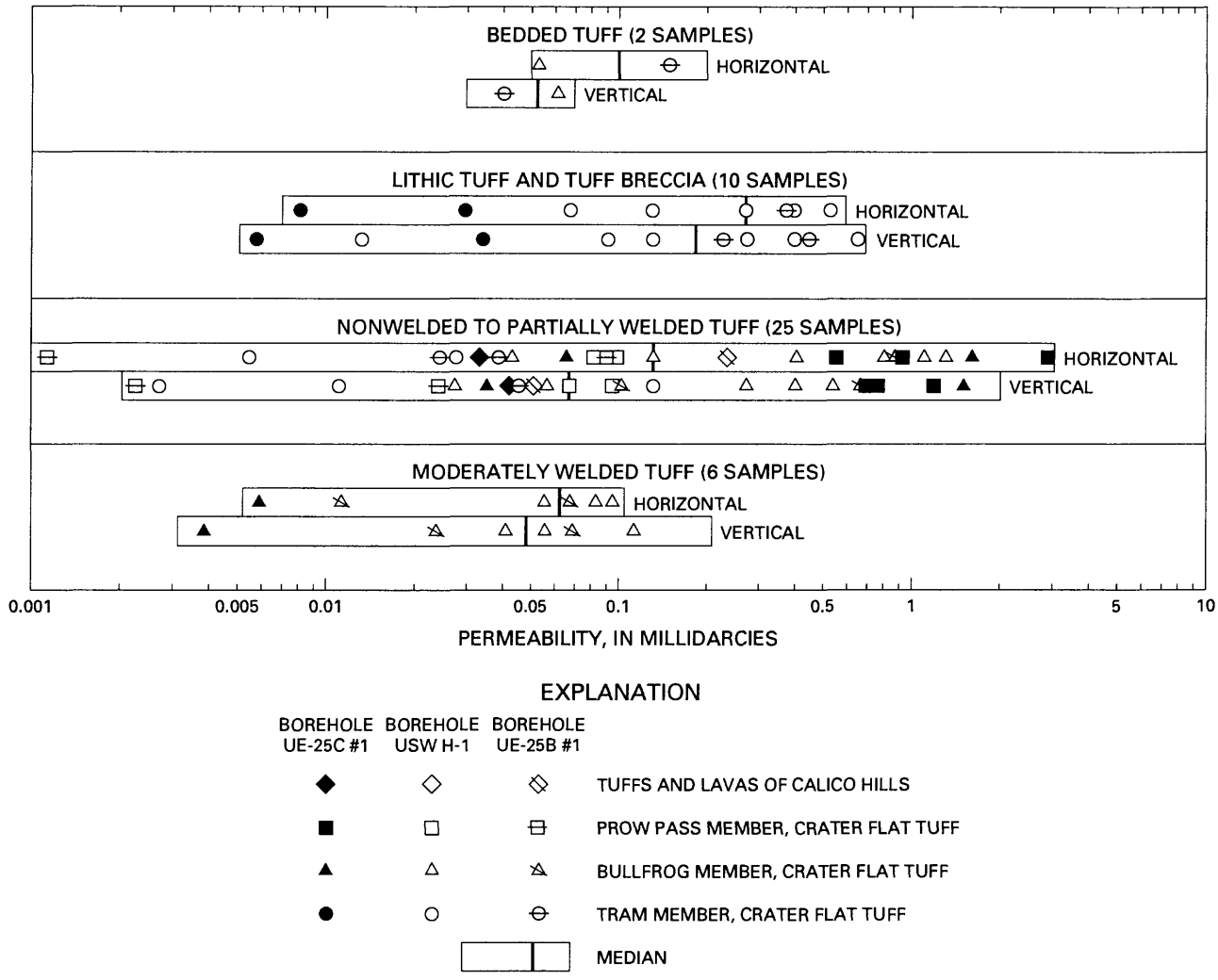

Figure 29.--Pore-scale permeability in the Crater Flat Tuff and the tuffs and lavas of Calico Hills determined by analyses of core from boreholes at Yucca Mountain.

Storativity

Storativity is a measure of the water released from storage in a confined aquifer (during pumping, for example) by contraction of the aquifer skeleton and expansion of the water. The storativity divided by the aquifer thickness is the specific storage. According to Lohman (1979, p. 9), specific storage can be calculated by the following equation:

$$S_s = \gamma(\beta\theta + 1/E) \qquad (3)$$

where S_s = specific storage, in reciprocal meters;

γ = specific weight of water=9.8×10^{3} newtons per cubic meter;

β = compressibility of water=4.4×10^{-10} meters squared per newton;

θ = porosity of the rock, dimensionless; and

E = bulk modulus of elasticity of the rock, in newtons per square meter.

Values of the bulk modulus of elasticity and porosity for zones within the Crater Flat Tuff and the tuffs and lavas of Calico Hills generally are inversely related, as shown in figure 28. Using equation 3 and average values of porosity and elasticity for geologic units penetrated in borehole UE-25c #1, the specific storage of bedded tuff, nonwelded tuff, and nonwelded to partially welded tuff zones in this borehole was determined to be 2×10^{-6} m^{-1}, twice the specific storage of moderately to densely welded tuff and tuff breccia zones (table 15). Using the information from tables 5 and 15, average values of the storativity for zones within the Crater Flat Tuff and the tuffs and lavas of Calico Hills at the C-hole complex were estimated to range from 1×10^{-5} to 2×10^{-4} (fig. 30).

Table 15.--*Specific storage in the tuffs and lavas of Calico Hills and the Crater Flat Tuff in borehole UE-25c #1*

[Only intervals that have sufficient elasticity data for calculating specific storage are listed]

Geologic unit	Thickness (meters)[1]	Porosity (dimensionless)	Bulk modulus of elasticity (newtons per square meter)	Specific storage (per meter)
Tuffs and lavas of Calico Hills				
Nonwelded zone	14.9	0.35	9.62×10^{9}	2×10^{-6}
Bedded zone	26.0	.32	1.16×10^{10}	2×10^{-6}
Crater Flat Tuff				
Prow Pass Member				
Lower nonwelded to partially welded zone	63.4	.27	1.28×10^{10}	2×10^{-6}
Bullfrog Member				
Upper nonwelded to partially welded zone	32.6	.22	1.38×10^{10}	2×10^{-6}
Central moderately to densely welded zone	67.1	.14	2.53×10^{10}	1×10^{-6}
Lower nonwelded to partially welded zone	59.2	.26	1.28×10^{10}	2×10^{-6}
Bedded zone	6.4	.24	1.45×10^{10}	2×10^{-6}
Tram Member				
Tuff breccia zone	55.2	.18	2.23×10^{10}	1×10^{-6}

[1]Listed thickness is that for which elasticity data are available.

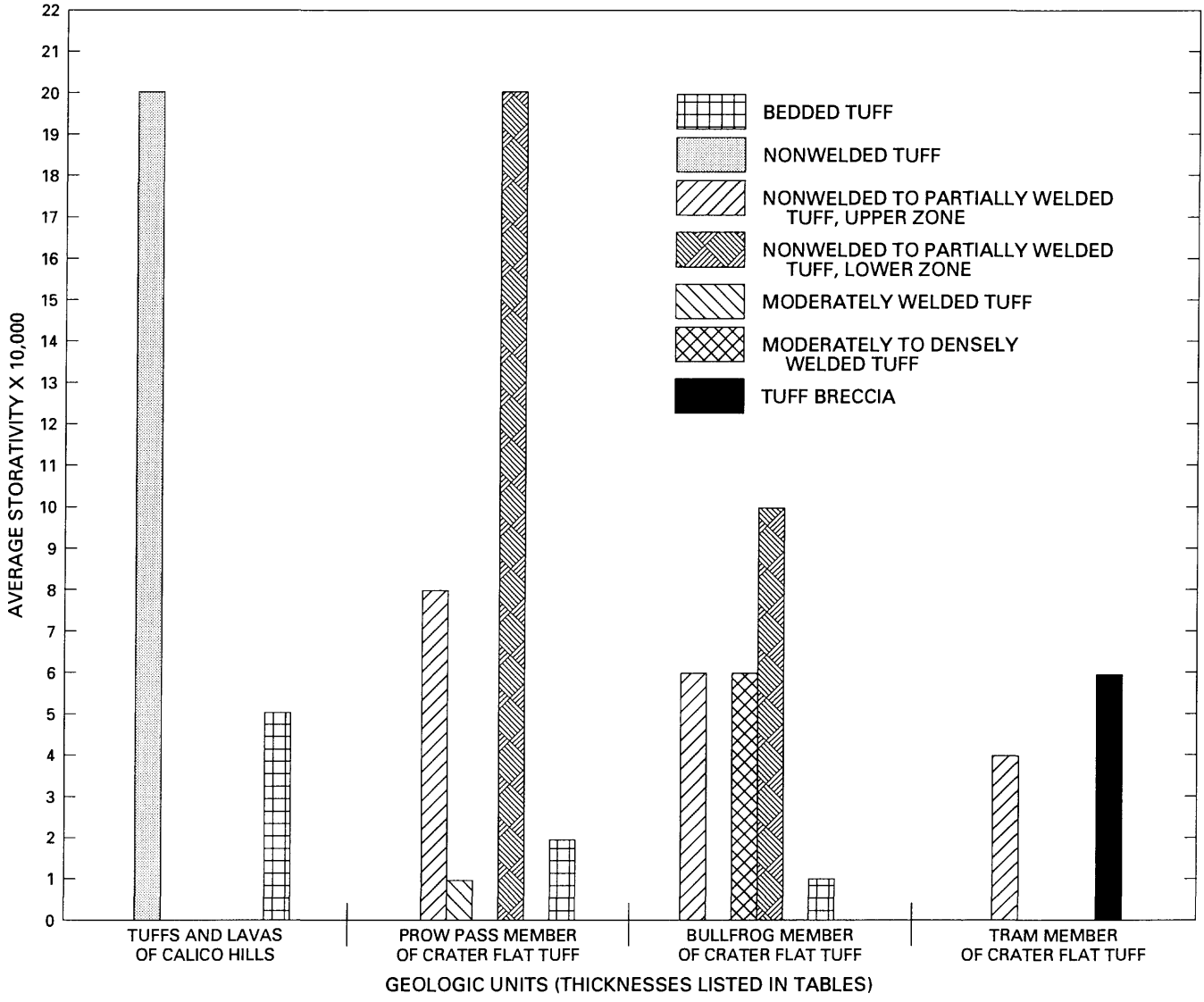

Figure 30.--Average storativity of geologic units at the C-hole complex.

Ground-Water Occurrence and Movement in the C-holes

Zones of ground-water inflow to the C-holes under dynamic (pumping) conditions were determined from temperature logs and tracejector surveys. On the temperature logs, points of ground-water inflow were indicated where convex deflections from a vertical or near-vertical (isothermal) line occurred. The tracejector surveys, which produce plots of flow as a function of depth, similarly indicated zones of ground-water inflow where departures from the vertical occurred. In general, the temperature logs of the C-holes indicated all of the zones of ground-water inflow indicated by the tracejector surveys, plus additional zones of ground-water inflow.

Ground-water inflows under dynamic conditions are a function of hydraulic-head gradients created while a well is pumped and do not necessarily indicate ground-water flow directions under natural (undisturbed) hydraulic-head gradients. In fact, static heat-pulse flow-meter surveys conducted in the C-holes in 1991 (Alfred E. Hess, U.S. Geological Survey, written commun., 1992) indicate that nearly all zones of water production in the C-holes detected during pumping tests from 1983 to 1984 are zones of ground-water outflow under static conditions.

The data in figures 31, 32, and 33 indicate that ground-water inflow from geologic units is distributed differently among the C-holes. In borehole UE-25c #1, 64 percent of the production during a pumping test came from the lower nonwelded to partially welded zone of the Bullfrog Member; the remaining production during this test came from the Tram Member. Ground-water inflow points during the pumping test were identified by inflections in the thermal gradient at depths of 560.8 and 579.1 m, in the nonwelded to partially welded zones of the Prow Pass Member; at depths of 756.8, 757.7, 764.4, and 780.3 m, in the lower nonwelded to partially welded zone of the Bullfrog Member; and at depths of 845.8, 859.8, 882.7, and 911.4 m, in the tuff breccia and lower (lithic tuff) zones of the Tram Member. In borehole UE-25c #2, 93 percent of the production during a pumping test came from the central moderately to densely welded zone of the Bullfrog Member; the remaining production during this test came from the upper nonwelded to partially welded zone of the Bullfrog Member. Ground-water inflow points during the pumping test were identified by inflections in the thermal gradient at a depth of 503.0 m, in the bedded tuff zone of the tuffs and lavas of Calico Hills; at depths of 729.0, 738.5, and 747.4 m, in the central moderately to densely welded zone of the Bullfrog Member; and at a depth of 880.5 m, in the tuff breccia zone of the Tram Member. In borehole UE-25c #3, 44 percent of the production during a pumping test came from the central moderately to densely welded zone of the Bullfrog Member, 31 percent of the production during this test came from the lower nonwelded to partially welded zone of the Bullfrog Member; and 25 percent of the production during the pumping test came from the tuff breccia zone of the Tram Member. Ground-water inflow points in borehole UE-25c #3 during the pumping test were identified by inflections in the thermal gradient at a depth of 461.6 m, in the nonwelded zone of the tuffs and lavas of Calico Hills; at a depth of 493.5 m, in the upper nonwelded to partially welded zone of the Prow Pass Member; at depths of 700.4 and 728.4 m, in the central moderately to densely welded zone of the Bullfrog Member; at depths of 742.7, 746.2, 750.0, and 771.8 m, in the lower nonwelded to partially welded zone of the Bullfrog Member; and at a depth of 868.7 m, in the tuff breccia zone of the Tram Member. The production of water during pumping tests in different proportions from different geologic units in boreholes only 30 to 77 m apart indicates that ground water at the C-hole complex probably is not stratabound.

Television logs of borehole UE-25c #1 were examined to determine if specific fractures or fracture zones could be affecting ground-water movement. The following criteria were considered indicative of possible flow from or into fractures: (1) open fractures within a water-production zone; (2) numerous intersecting fractures within a water-production zone; (3) faults intersecting a water-production zone; (4) fractures coincident with inflection (inflow) points on temperature logs; and (5) substantially increased water clarity above a fracture.

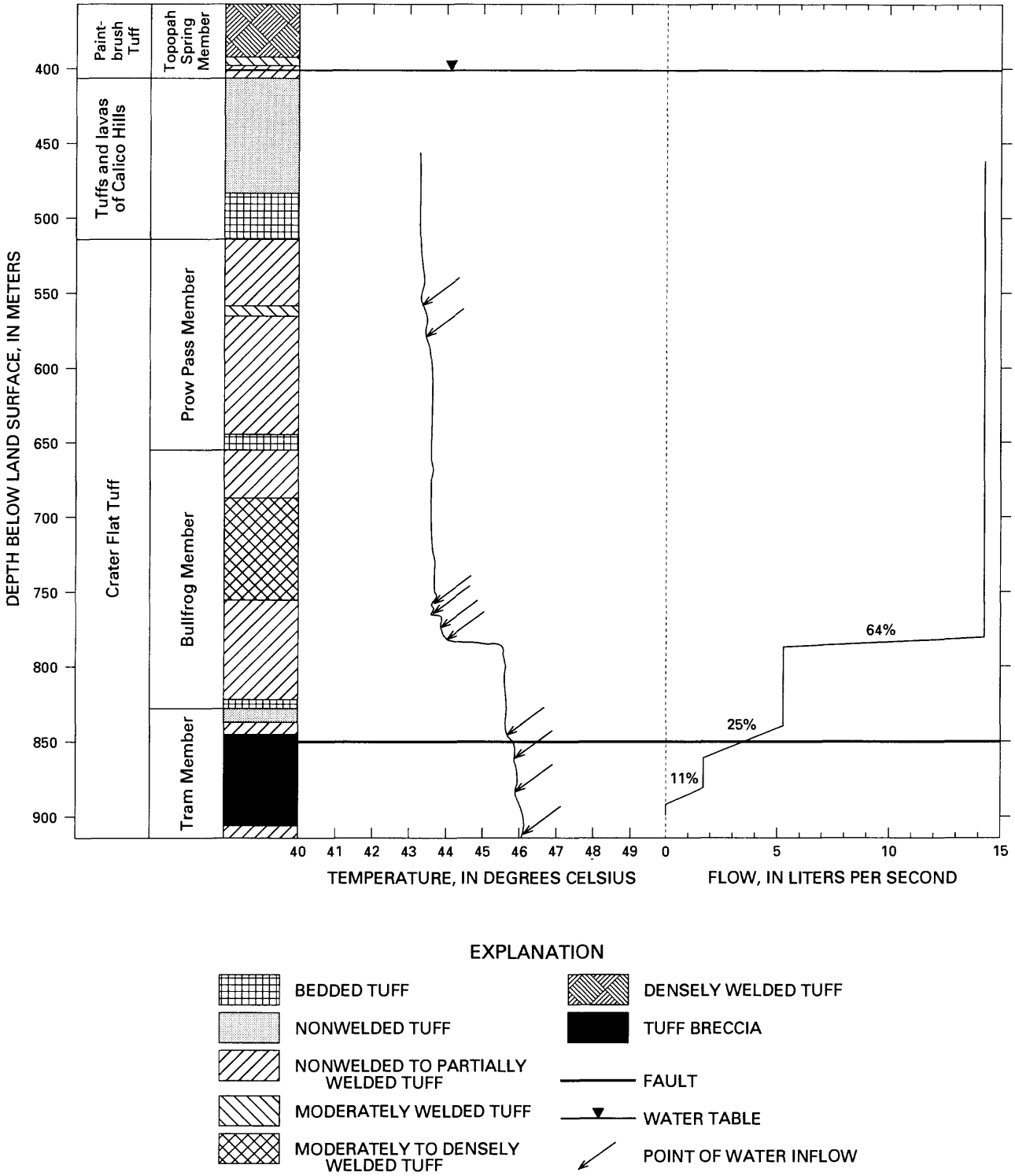

Figure 31.--Zones of ground-water production and points of inflow during pumping in borehole UE-25c #1, as indicated by temperature and tracejector data.

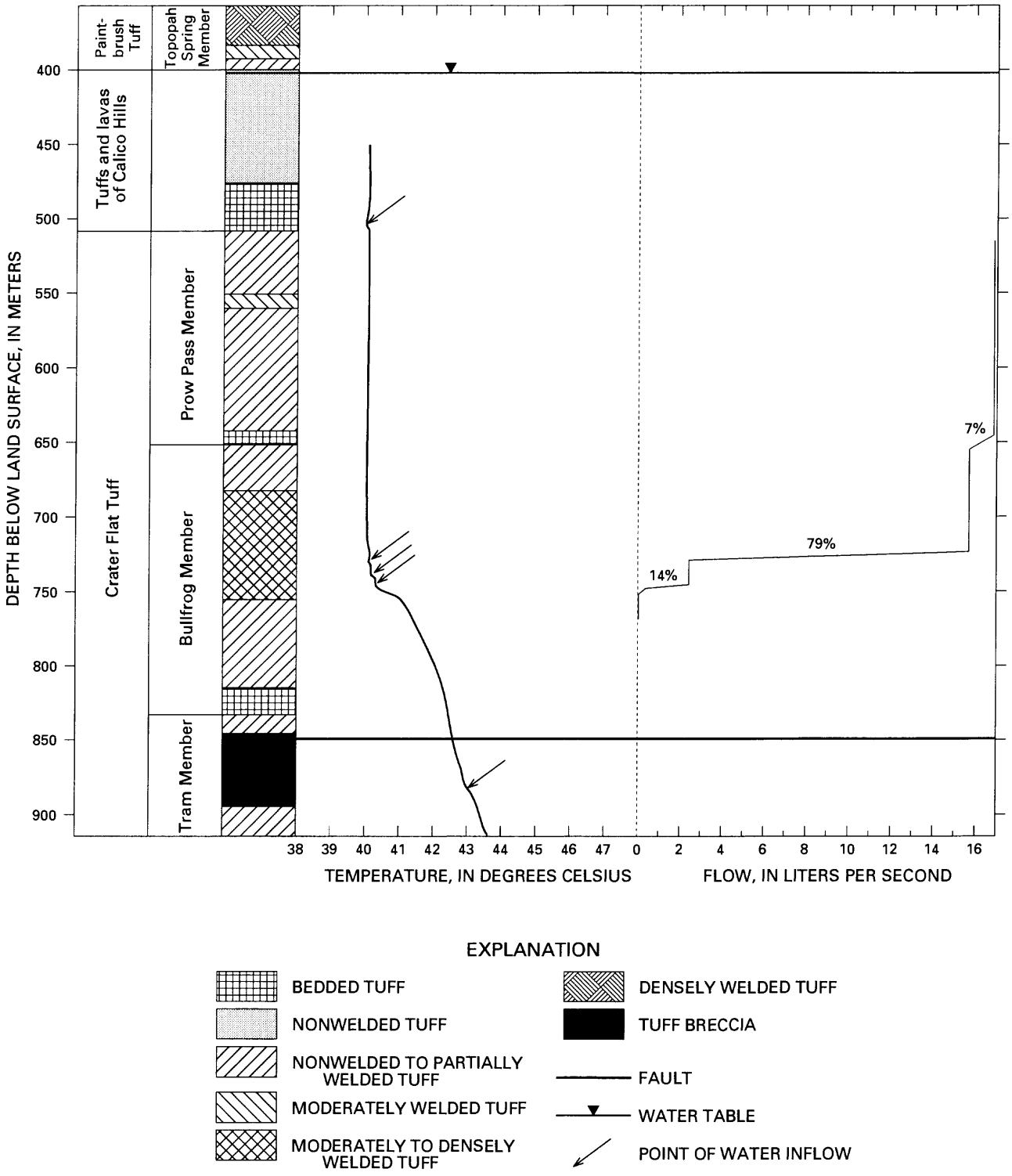

Figure 32.--Zones of ground-water production and points of inflow during pumping in borehole UE-25c #2, as indicated by temperature and tracejector data.

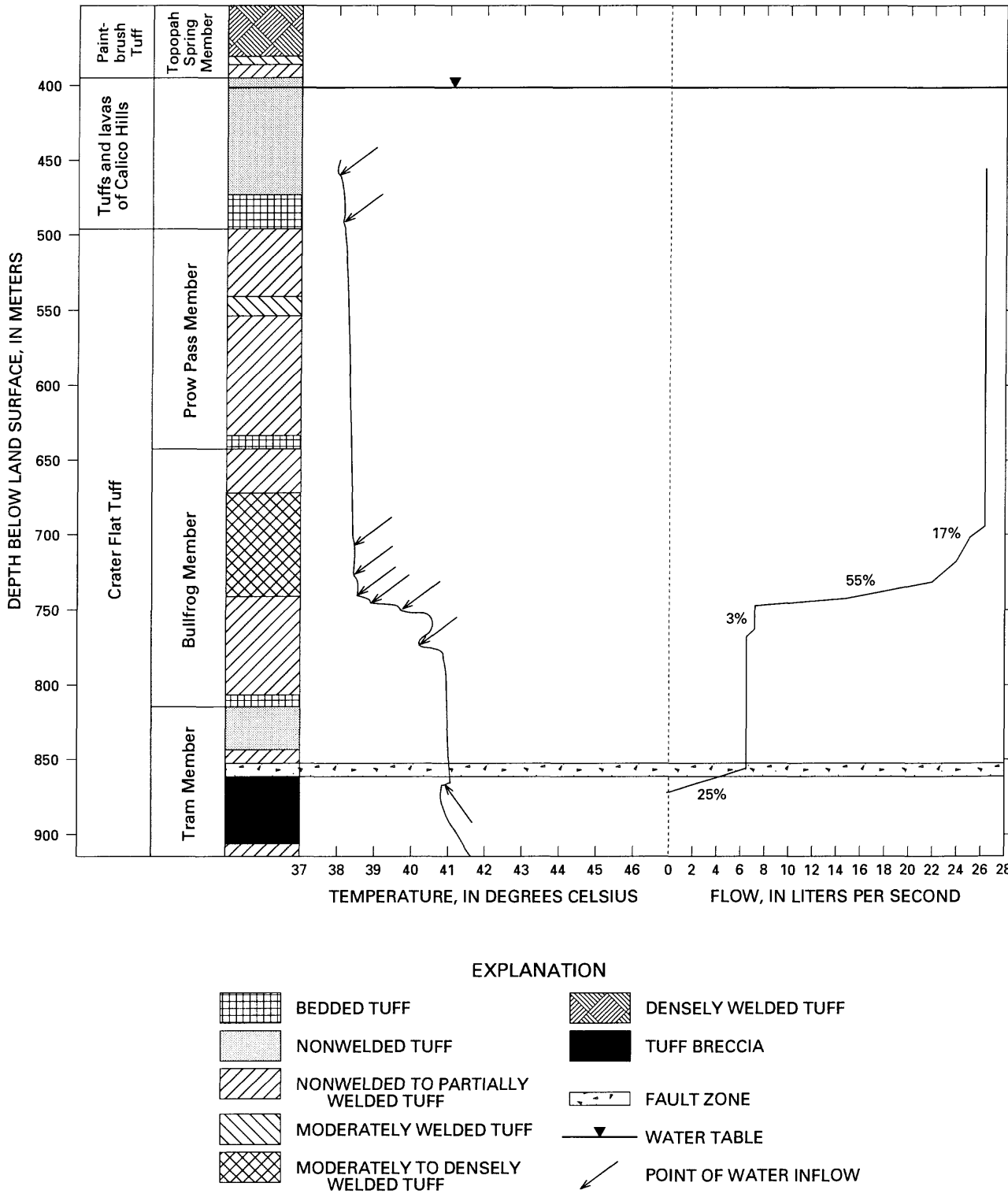

Figure 33.--Zones of ground-water production and points of inflow during pumping in borehole UE-25c #3, as indicated by temperature and tracejector data.

In borehole UE-25c #1, all three water-production zones during pumping contain fractures that could be sources of water. In the uppermost production zone, between depths of 779 and 785 m, the following fractures inferred to be possible sources of water were identified: (1) an open, southerly striking, steeply dipping fracture between depths of 779 and 780 m; (2) a zone of intersecting, variably striking, shallowly and steeply dipping fractures at a depth of 784 m; and (3) three open, variably striking, shallowly dipping fractures between depths of 784 and 786 m. In the middle production zone, between depths of 838 and 858 m, the following fractures inferred to be sources of water were identified: (1) a cavernous, south-southwesterly striking, steeply dipping fracture between depths of 836 and 839 m; (2) intersecting south-southeasterly and south-southwesterly striking, steeply dipping fractures between depths of 846 and 847 m; and (3) the south-southwesterly striking Paintbrush Canyon Fault between depths of 849 and 850 m. In the lowest production zone, between depths of 879 and 891 m, the only possible source of water identified was an open, northwesterly striking, steeply dipping fracture at a depth of 884 m.

Of the 10 water-inflow zones in borehole UE-25c #1 identified during pumping by inflections in the temperature gradient, 8 of these zones coincide with fractures identified on videotape. Three of these zones are associated with south-southeasterly to south-southwesterly striking, steeply dipping fractures. Three zones are related to intersecting south-southeasterly to south-southwesterly and either northeasterly, southeasterly, or southwesterly striking, steeply dipping fractures. One zone is related to a northeasterly striking, steeply dipping fracture, and another is related to a northwesterly striking, steeply dipping fracture.

On the basis of data from borehole UE-25c #1, it appears that water-producing zones in the C-holes generally are related to fractures, although no particular set of fractures controls ground-water production. Furthermore, although some water-producing zones are intensely fractured, others contain few fractures, and some intensely fractured zones produce no water when the C-holes are pumped. There is no apparent relation between fracture density and the tendency of the tuffaceous rocks at the C-hole complex to yield water.

Pumping tests conducted in the C-holes support the conceptual model of fracture-dominated ground-water flow. However, the typical three-segmented curve produced by these and other aquifer tests in the vicinity of Yucca Mountain (figs. 12 and 34) also could indicate that boundaries were reached during the tests (Lohman, 1979).

In general, plots of drawdown as a function of the log of time consist of two relatively steep straight lines separated by a relatively flat segment. According to Gringarten (1982), the first segment represents water released from fractures; the second segment represents water released from the matrix blocks into the fractures, and the third segment represents water released from fractures and matrix blocks functioning together as an equivalent porous medium. Thus, the transmissivity of the aquifer can be obtained by conventional (porous-medium) analysis of the third segment. According to Craig and Reed (1991), if the pumping test ends before the third segment is obtained, as commonly happens, the transmissivity can be obtained from the second segment if a factor of 0.5 is introduced into the numerator of the analytical equation of Cooper and Jacob (1946), and the equation is modified to:

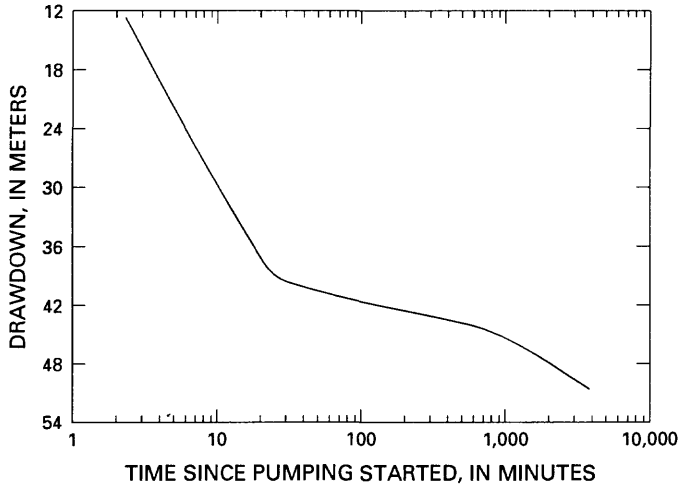

Figure 34.--Typical curve of drawdown as a function of time during pumping tests of Tertiary volcanic and tuffaceous rocks and Paleozoic carbonate rocks at the Nevada Test Site (modified from Winograd and Thordarson, 1975).

$$T = \frac{15.8\ Q}{\Delta s} \qquad (4)$$

where T = transmissivity, in meters squared per day;
Q = discharge, in liters per second; and
Δs = change in drawdown over one log cycle of time, in meters.

Alternatively, fracture-dominated flow systems can be analyzed by methods described by Streltsova-Adams (1978) and Gringarten (1982).

In addition to supporting a conceptual model of a fracture-dominated ground-water flow system, the pumping tests in the C-holes to date (1992) have indicated two other important considerations. First, as generally exemplified by the late-time drawdown in monitored intervals during the pumping tests in boreholes UE-25c #2 and UE-25c #3 (figs. 12-14), oscillations in water levels caused by earth tides and barometric effects can and do occur at Yucca Mountain (Devin L. Galloway, U.S. Geological Survey, written commun., 1989). Secondly, all three pumping tests in the C-holes during 1983 and 1984 indicated that borehole storage can delay drawdown during the early parts of pumping tests in boreholes drilled at Yucca Mountain. According to Gringarten (1982), borehole storage is indicated by a slope of 1:1 on a log-log plot of drawdown as a function of time, and, as shown in figure 35, such slopes were observed for several monitored intervals in the C-holes during the first 1 to 15 minutes of pumping tests in 1983 and 1984.

The conceptual model of ground-water occurrence and movement at the C-hole complex presented in this report has far-reaching implications for understanding the factors affecting ground-water occurrence and movement at Yucca Mountain. First, aquifer tests at Yucca Mountain need to be analyzed using methods that assume fracture flow. For tests involving observation wells, packers need to be placed carefully in the observation wells to monitor zones connected from well to well by fractures and not by formations, members,

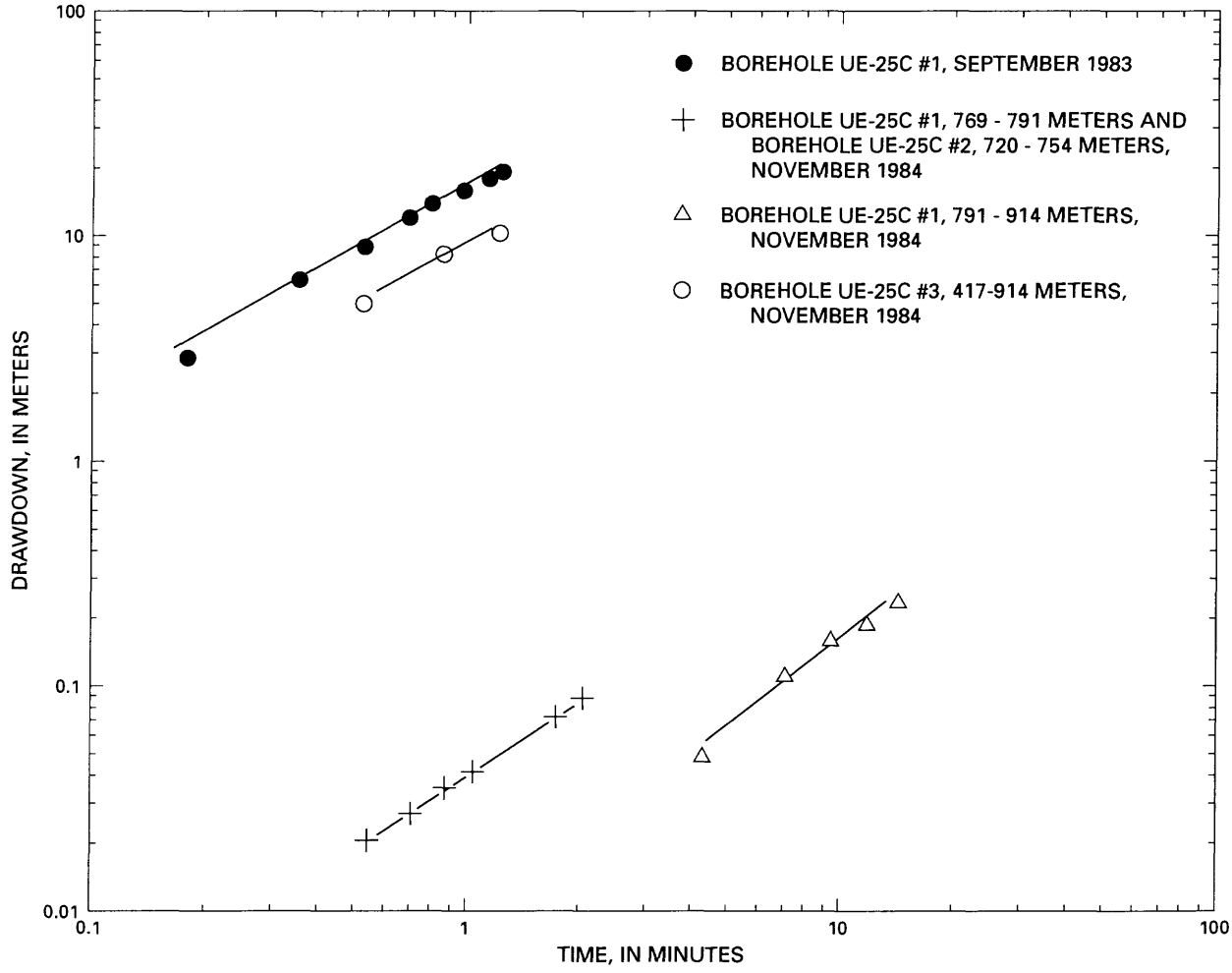

Figure 35.--Plots of drawdown as a function of time indicative of borehole storage during pumping tests in the C-holes in 1983 and 1984.

or lithologic zones. Ironically, given the randomness by which water probably travels from fracture to fracture, it may not be possible to predict where water-producing zones will occur in the Yucca Mountain area at any point far removed from a borehole. At the scale of Yucca Mountain, it may be possible to estimate aquifer properties and simulate ground-water flow by using numerical models that are based on the assumption that the aquifer is an equivalent porous medium.

Ground-Water Chemistry

As indicated by major-ion concentrations listed in table 16, the water from the C-holes is a sodium bicarbonate type. The water chemistry is consistent with that of ground water sampled elsewhere at Yucca Mountain and in nearby areas (fig. 36). Kerrisk (1987) interprets the sodium bicarbonate ground water at Yucca Mountain to be the result of cation exchange between calcium bicarbonate water and sodium-rich zeolites in the tuffaceous rocks that form the mountain.

Table 16.--*Chemical composition of water samples obtained from boreholes UE-25c #1, UE-25c #2, and UE-25c #3*

[All constituents in milligrams per liter, except where noted; μS = microsiemens per centimeter at 25°C; °C = degrees Celsius; pCi/L = picocuries per liter; % = percent modern carbon; YBP = years before present; ‰ = parts per thousand relative to standard mean ocean water]

Property or constituent	Borehole		
	UE-25c #1	UE-25c #2	UE-25c #3
Collection date	09-30-83	03-13-84	05-09-84
Specific conductance (μS)	290	295	298
pH (onsite; standard units)	7.6	7.7	7.7
Temperature (°C)	41.5	40.5	40.8
Calcium	11	12	11
Magnesium	.34	.40	.40
Sodium	56	54	55
Potassium	2.0	2.1	1.9
Bicarbonate (onsite)	151	139	137
Sulfate	23	22	22
Chloride	7.4	7.1	7.2
Fluoride	2.1	2.1	2.0
Silica	56	54	53
Dissolved solids (calculated)	229	233	229
Lithium	.12	.094	.11
Strontium	.030	.045	.044
Carbon-14 (%)	15.0	16.6	15.7
Tritium (pCi/L)	<1	<2	2
Delta deuterium (‰)	-102	-100	-103
Delta oxygen-18 (‰)	-13.5	-13.4	-13.5
Apparent carbon-14 age (YBP)	15,200	14,400	14,900

Several types of evidence indicate that ground water at the C-hole complex is not recharged locally, although numerical models by Czarnecki and Waddell (1984) and Peter Sinton and Joseph Downey (U.S. Geological Survey, written commun., 1989) indicate that a flux from Fortymile Wash to Yucca Mountain may exist when Fortymile Wash is carrying storm runoff. Ground water at the C-hole complex is about 402 m below land surface and has an average temperature at the wellhead of 40.9°C. If the water were recharged locally, one would expect the water to be much shallower and to have a temperature similar to the ambient mean annual air temperature of 17°C (Mifflin, 1968). Small concentrations of tritium in the water indicate that the water has been circulating underground (out of contact with the atmosphere) since before the onset of hydrogen bomb testing in 1952. The "lightness" of the water in deuterium and oxygen-18 with respect to modern meteoric water (fig. 37) and an apparent carbon-14 age for the water of about 15,000 years before present (table 16) also indicate that the water has been circulating underground for some time.

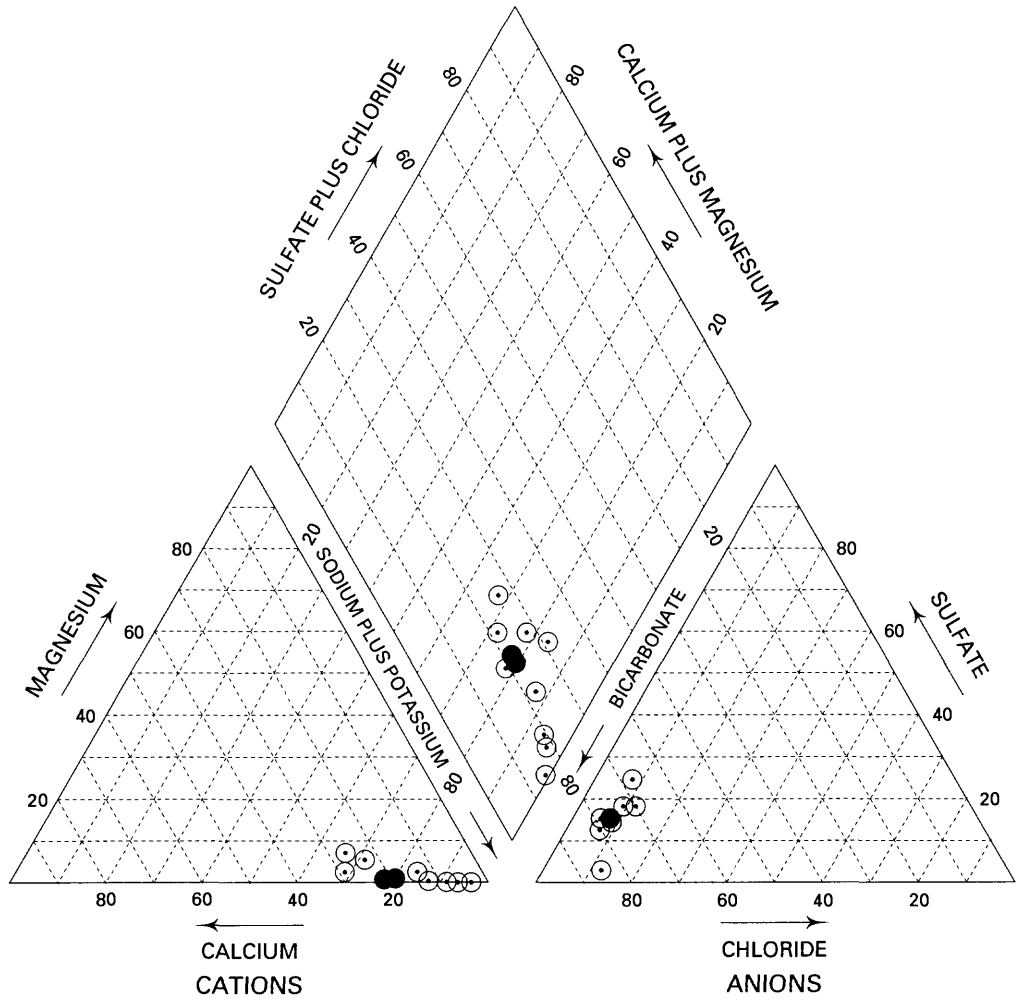

Figure 36.--Relative concentrations of major ions in ground water from Yucca Mountain, Crater Flat, and Jackass Flats (modified from Benson and McKinley, 1985).

Combined with the previously discussed upward hydraulic-head gradient at the C-hole complex, the hydrochemical data indicate that water in the Tertiary rocks probably originates in the underlying Paleozoic carbonate aquifer of the regional flow system. In borehole UE-25p #1, which is about 600 m east of the C-holes, the Paleozoic rocks are only about 1.2 km below land surface (Carr and others, 1986a). A fault penetrated at the base of the Tertiary rocks in this borehole probably transmits water from the Paleozoic rocks into the Tertiary rocks, because a 50-m-thick interval of tuffaceous and sedimentary rocks above the fault is argillized and calcified (Carr and others, 1986a).

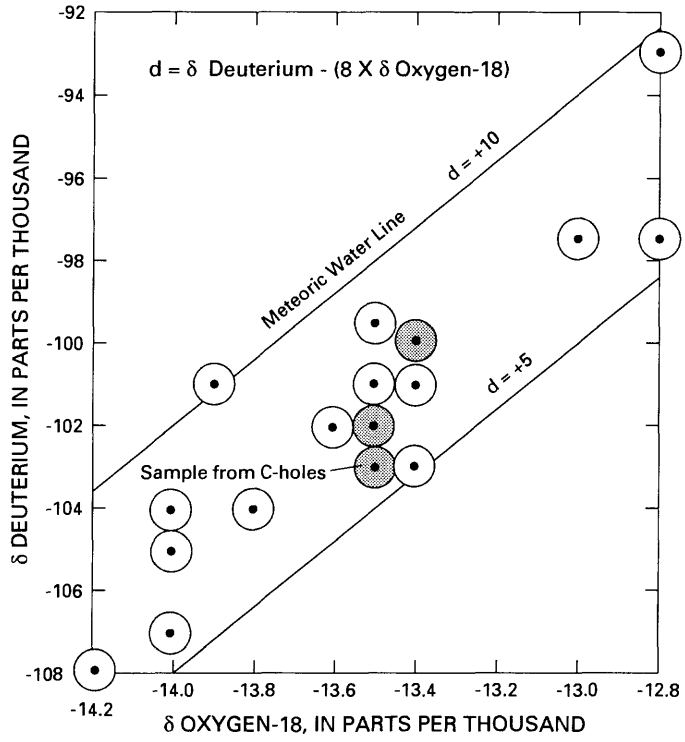

Figure 37.--Meteoric water line and relation between delta oxygen-18 and delta deuterium concentrations in water from the tuffaceous rocks at Yucca Mountain, Crater Flat, and Jackass Flats (modified from Benson and McKinley, 1985.)

If, as proposed by Scott and Whitney (1987), the fault at the base of the Tertiary rocks is a detachment fault, the low angle of this fault and possible splays (inferred but not confirmed in borehole UE-25p #1) would allow water to be transmitted not only in borehole UE-25p #1 but also down the dip of the fault to the C-hole complex.

SUMMARY AND CONCLUSIONS

Boreholes UE-25c #1, UE-25c #2, and UE-25c #3 (collectively called the C-holes) were drilled east of Yucca Mountain at the Nevada Test Site in 1983 and 1984 for the purpose of conducting aquifer and tracer tests. Yucca Mountain is located in the Basin and Range physiographic province, a region characterized by extensional tectonics. Block-faulted mountains rise above basins filled with Tertiary and Quaternary sedimentary deposits that are hundreds of meters thick. At Yucca Mountain, Paleozoic carbonate and clastic rocks are overlain by more than 1,000 m of Tertiary volcanic and tuffaceous rocks that erupted from several nearby calderas. The volcanic and tuffaceous rocks dip eastward at angles generally between 5° and 40° and are transected by normal and strike-slip faults. The normal faults mostly strike south-southeasterly to south-southwesterly and dip steeply westward. The strike-slip faults, part of the Walker Lane Belt, strike mostly southeasterly, but some strike southwesterly.

The C-holes, each, were drilled to a depth of 914.4 m. Each borehole penetrated the Tiva Canyon and Topopah Spring Members of the Paintbrush Tuff, the tuffs and lavas of Calico Hills, and the Prow Pass and Bullfrog Members of the Crater Flat Tuff and bottomed in the Tram Member of the Crater Flat Tuff. The geologic units penetrated consist of thick intervals of nonwelded to densely welded ash-flow tuff separated by thin intervals of ash-fall tuff, reworked tuff, and tuffaceous sandstone. A tuff breccia within the Tram Member near the bottom of the C-holes is interpreted to be the result of faulting. The tuffaceous rocks at the C-hole complex are devitrified to vitrophyric. Below the water table, which is at an average depth of 401.6 m, the rocks are argillic and zeolitic.

The geologic units at the C-hole complex strike about N. 2° W. and have an east-northeasterly dip that increases with depth from about 15° to about 21°. The strata are transected by the Paintbrush Canyon Fault, which is oriented S. 9° W., 52.2° NW. at the site. The Paintbrush Canyon Fault intersects borehole UE-25c #1 within the Tram Member between depths of 849.5 and 850.1 m, and borehole UE-25c #2 within the Tram Member at a depth of 851.3 m. A high-angle fault between boreholes UE-25c #1 and UE-25c #2 on the east and borehole UE-25c #3 on the west apparently offsets and rotates the Paintbrush Canyon Fault. Borehole UE-25c #3 intersects a fault in the Tram Member between depths of 855.2 and 861.4 m that has an orientation estimated to be about S. 49° W., 63° NW. If the fault intersected by borehole UE-25c #3 is not an offset and rotated segment of the Paintbrush Canyon Fault, it could be a strike-slip fault in the Walker Lane Belt.

The rocks penetrated in the C-holes are fractured extensively, with most fractures oriented between S. 20° E. and S. 20° W. The predominant fracture set is oriented approximately perpendicular to the regional direction of least principal horizontal stress (N. 60° W. to N. 65° W.). In the Crater Flat Tuff, fractures strike mainly between S. 20° E. and S. 20° W. and secondarily between S. 20° E. and S. 60° E., although fractures striking between N. 20° W. and N. 60° W. are of secondary importance in the Tram Member. Most fractures in the Crater Flat Tuff are steeply dipping and open, although shallowly dipping fractures occur in nonwelded and reworked tuff zones, and mineral-filled fractures are common to abundant in the tuff breccia zone of the Tram Member and the moderately to densely welded zone of the Bullfrog Member. As in the Crater Flat Tuff, most fractures in the tuffs and lavas of Calico Hills strike between S. 20° E. and S. 20° W., but southeasterly striking fractures predominate in the Topopah Spring Member of the Paintbrush Tuff.

The fracture density of geologic units penetrated in the C-holes, based mainly on analysis of videotapes of borehole UE-25c #1, ranges from 1.3 to 7.6 fractures per cubic meter. Because of faulting, zones within the Tram Member of the Crater Flat Tuff consistently have relatively large fracture-density values of 4.4 to 5.5 fractures per cubic meter. In the tuffs and lavas of Calico Hills and the Crater Flat Tuff, fracture density appears to be no greater in moderately to densely welded tuff than in nonwelded to partially welded tuff. In comparison to transect data and core data from other boreholes in the Yucca Mountain area, the fracture density of some geologic units at the C-hole complex, particularly zones in the Paintbrush Tuff, probably was underestimated by 0.3 to 1.3 orders of magnitude, but estimates for most zones in the Crater Flat Tuff and the tuffs and lavas of Calico Hills appear to be about the correct order of magnitude.

As indicated by helium injection tests of core samples and gamma-gamma logs, the porosity of the tuffs and lavas of Calico Hills and the Crater Flat Tuff ranges from 12 to 43 percent. Nonwelded to partially welded and bedded tuff zones of the Crater Flat Tuff at the C-hole complex have mean porosity values ranging from 22 to 31 percent, as moderately to densely welded tuff zones have mean porosity values of 14 percent. Nonwelded and bedded tuff zones of the tuffs and lavas of Calico Hills have mean porosity values of 32 to 37 percent. The porosity values at the C-hole complex are consistent with values from other boreholes at Yucca Mountain.

Eighteen permeameter measurements using water as the fluid indicate that the pore-scale horizontal permeability of the tuffs and lavas of Calico Hills and Crater Flat Tuff ranges from 5.7×10^{-3} to 2.9 mD, and the pore-scale vertical permeability of these geologic units ranges from 3.7×10^{-3} to 1.5 mD. In comparison, the pore-scale horizontal permeability of the tuffs and lavas of Calico Hills and the Crater Flat Tuff in other boreholes at Yucca Mountain ranges from 1.1×10^{-3} to 1.3 mD, and the pore-scale vertical permeability ranges from 2.3×10^{-3} to 0.67 mD. As elsewhere at Yucca Mountain, the pore-scale permeability of moderately to densely welded tuff in the Crater Flat Tuff at the C-hole complex appears to be smaller than that of nonwelded to partially welded tuff.

On the basis of average values of porosity and elasticity for geologic units penetrated in borehole UE-25c #1, the specific storage of nonwelded to partially welded ash-flow tuff, ash-fall tuff and reworked tuff in the tuffs and lavas of Calico Hills and the Crater Flat Tuff at the C-hole complex was estimated to be 2×10^{-6} m^{-1}, twice the specific storage of moderately to densely welded ash-flow tuff and tuff breccia. In the tuffs and lavas of Calico Hills and Crater Flat Tuff at the C-hole complex, the storativity of moderately to densely welded ash-flow tuff, tuff breccia, ash-fall tuff, and reworked tuff zones was estimated on the basis of specific storage and average thickness (corrected for dip) to range from 1×10^{-5} to 6×10^{-5}; the storativity of nonwelded to partially welded ash-flow tuff zones was estimated to range from 4×10^{-5} to 2×10^{-4}.

Water in the Tertiary rocks of the Yucca Mountain area probably is not stratabound but apparently occurs randomly at the intersection of water-bearing fractures and faults. As indicated by tracejector surveys during pumping tests, boreholes in the area can produce water from any geologic unit below the water table. Even within the C-hole complex, a 1,027-m^2 area, water-producing zones differ from borehole to borehole. In borehole UE-25c #1, 64 percent of the water during a pumping test came from the lower nonwelded to partially welded zone of the Bullfrog Member, and 36 percent of the water came from the tuff breccia zone of the Tram Member. In borehole UE-25c #2, 7 percent of the water during a pumping test came from the upper nonwelded to partially welded zone of the Bullfrog Member, and 93 percent of the water came from the central moderately to densely welded zone of this geologic unit. In borehole UE-25c #3, 44 percent of the water during a pumping test came from the central moderately to densely welded zone of the Bullfrog Member, 31 percent of the water came from the lower nonwelded to partially welded zone of this geologic unit, and 25 percent of the water came from the tuff breccia zone of the Tram Member.

Although water production is not associated consistently with specific geologic units or the degree of welding of ash-flow tuff, all water-producing zones identified by tracejector surveys in boreholes at Yucca Mountain, including the C-holes, and most ground-water-inflow points identified in the C-holes by inflections in the thermal gradient during pumping tests are associated with fractures. Although south-southeasterly to south-southwesterly striking fractures appear to be transmitting most of the water, this situation probably is an artifact of the predominance of these fractures in the area. In the C-holes, water apparently is transmitted by south-southeasterly to south-southwesterly, southwesterly, and northeasterly striking joints and shear zones connected to the south-southwesterly trending Paintbrush Canyon Fault and other faults. No particular set of fractures appears to have a controlling effect on water production. Plots of drawdown as a function of time during pumping tests in the C-holes, although affected by borehole storage, earth tides, and barometric pressure, support the interpretation of fracture-dominated ground-water flow.

Hydraulic-head data for the Nevada Test Site and vicinity indicate that ground water in the area flows locally from block-faulted mountains to intermontane basins through Tertiary volcanic and tuffaceous rocks and Quaternary and Tertiary valley fill, and regionally from basin to basin toward Death Valley and Alkali Flat, primarily through Paleozoic carbonate rocks. A downward flux between the local and regional flow systems occurs northeast of Yucca Mountain, in the Yucca Flat area, whereas an upward flux occurs at Yucca Mountain.

Hydrochemical evidence indicates that the water discharging from the C-holes probably is derived from the regional flow system. The water from the C-holes is a sodium bicarbonate type believed to be formed by cation exchange between calcium bicarbonate water and sodium-rich zeolites in the Tertiary tuffaceous rocks. Evidence indicative of long residence times associated with regional flow paths includes small (pre-1952) concentrations of tritium in the water, the "lightness" of the water in deuterium and oxygen-18 with respect to modern meteoric water, an apparent carbon-14 age for the water of about 15,000 years before present, and elevated water temperatures. A detachment fault at the base of the Tertiary rocks and related faults in calcified and argillized tuffs above the detachment fault may be conduits for water movement from the regional flow system to the Tertiary rocks at Yucca Mountain in the vicinity of the C-hole complex.

SELECTED REFERENCES

American Petroleum Institute, 1960, API recommended practice for core-analysis procedure, RP40: Dallas, Tex., 55 p. (NNA.910215.0242)

American Society for Testing and Materials, 1971, Annual book of ASTM Standards, volume 04.03: Philadelphia, Pa. (NNA.910215.0243)

Anderson, L.A., 1984, Rock property measurements on large-volume core samples from Yucca Mountain USW GU-3/G-3 and USW G-4 boreholes, Nevada Test Site, Nevada: U.S. Geological Survey Open-File Report 84-552, 39 p. (NNA.870323.0195)

Barton, C.C., and Larsen, Eric, 1985, Fractal geometry of two-dimensional fracture networks at Yucca Mountain, southwest Nevada, *in* Stephannsen, Ove, ed., Fundamentals of rock joints: Bjorklidden, Sweden, Proceedings of the International Symposium on Fundamentals of Rock Joints, p. 77-84. (HQS.880517.1058)

Barton, C.C., Page, W.R., and Morgan, T.L., 1989, Fractures in outcrops in the vicinity of drill hole USW G-4, Yucca Mountain Nevada: Data analysis and compilation: U.S. Geological Survey Open-File Report 89-92, 133 p. (NNA.900108.0155)

Benson, L.V., and McKinley, P.W., 1985, Chemical composition of ground water in the Yucca Mountain area, 1971-84: U.S. Geological Survey Open-File Report 85-484, 10 p. (HQS.880517.1890)

Bentley, C.B., 1984, Geohydrologic data for test well USW G-4, Yucca Mountain area, Nye County, Nevada: U.S. Geological Survey Open-File Report 84-063, 48 p. (NNA.870519.0100)

Bentley, C.B., Robison, J.H., and Spengler, R.W., 1983, Geohydrologic data for test well USW H-5, Yucca Mountain area, Nye County, Nevada: U.S. Geological Survey Open-File Report 83-853, 34 p. (NNA.870519.0098)

Blankennagel, R.K., 1967, Hydraulic testing techniques of deep drill holes at Pahute Mesa, Nevada Test Site: U.S. Geological Survey Open-file Report 67-18, 51 p. (HQS.880517.2621)

Brooks, R.H., and Corey, A.T., 1964, Hydraulic properties of porous media: Fort Collins, Colorado State University Hydrology Paper no. 3, 19 p. (HQS.880517.1737)

_____1966, Properties of porous media affecting fluid flow: American Society of Civil Engineers, Irrigation and Drainage Division Journal, IR2, p. 61-88. (NNA.870407.0356)

Byers, F.M., Jr., Carr, W.J., Orkild, P.P., Quinlivan, W.D., and Sargent, K.A., 1976, Volcanic suites and related cauldrons of Timber Mountain-Oasis Valley caldera complex, southern Nevada: U.S. Geological Survey Professional Paper 919, 70 p. (NNA.870406.0239)

Byers, F.M., Jr., and Warren, R.G., 1983, Revised volcanic stratigraphy of drill hole J-13, Fortymile Wash, Nevada, based on petrographic modes and chemistry of phenocrysts: Los Alamos, N. Mex., Los Alamos National Laboratory Report LA-9652-MS, 23 p. (NNA.870406.0422)

Caporuscio, F., Vaniman, D., Bish, D., Broxton, D., Arney, B., Heiken, G., Byers, F., Gooley, R., and Semarge, E., 1982, Petrologic studies of drill cores USW G-2 and UE-25b-1H, Yucca Mountain, Nevada: Los Alamos, N. Mex., Los Alamos National Laboratory Report LA-9255-MS, 111 p. (NNA.870519.0041)

Carr, M.D., Waddell, S.J., Vick, G.S., Stock, J.M., Monsen, S.A., Harris, A.G., Cork, B.W., and Byers, F.M., Jr., 1986a, Geology of drill hole UE-25p #1: A test hole into pre-Tertiary rocks near Yucca Mountain, southern Nevada: U.S. Geological Survey Open-File Report 86-175, 87 p. (HQS.880519.2633)

Carr, W.J., 1988, Volcano-tectonic setting of Yucca Mountain and Crater Flat, southwestern Nevada, *in* Carr, M.D., and Yount, J.C., eds., Geologic and hydrologic investigations of a potential nuclear waste disposal site at Yucca Mountain, southern Nevada: U.S. Geological Survey Bulletin 1790, p. 35-49. (NNI.881128.0011)

Carr, W.J., Byers, F.M., Jr., and Orkild, P.P., 1986b, Stratigraphic and volcano-tectonic relations of Crater Flat Tuff and some older volcanic units, Nye County, Nevada: U.S. Geological Survey Professional Paper 1323, 28 p. (HQS.880517.1115)

Carr, W.J., and Parrish, L.D., 1985, Geology of drill hole USW VH-2, and structure of Crater Flat, southwestern Nevada: U.S. Geological Survey Open-File Report 85-475, 41 p. (HQS.880517.1918)

Christensen, R.L., and Lipman, P.W., 1965, Geologic map of the Topopah Spring NW quadrangle, Nye County, Nevada: U.S. Geological Survey Geologic Quadrangle Map GQ-444, scale 1:24,000. (HQS.880517.1118)

Cinco-Ley, H., and Samaniego, F.V., 1981, Transient pressure analysis for fractured wells: Journal of Petroleum Technology, September 1981, p. 1749-1766. (NNA.891220.0164)

Cooper, H.H., Jr., and Jacob, C.E., 1946, A generalized graphical method for evaluating formation constants and summarizing well-field history: American Geophysical Union Transactions, v. 2, no. 4, p. 526-534. (NNA.891220.1660)

Cooper, H.H., Jr., Bredehoeft, J.D., and Papadopulos, I.S., 1967, Response of a finite-diameter well to an instantaneous charge of water: Water Resources Research, v. 3, no. 1, p. 263-269. (HQS.880517.2643)

Cornwall, H.R., and Kleinhampl, F.J., 1961, Geology of the Bare Mountain quadrangle, Nevada: U.S. Geological Survey Geologic Quadrangle Map GQ-157, scale 1:62,500. (HQS.880517.1129)

Craig, R.W., and Reed, R.L., 1991, Geohydrology of rocks penetrated by test well USW H-6, Yucca Mountain area, Nye County, Nevada: U.S. Geological Survey Water-Resources Investigations Report 89-4025, 40 p. (NNA.900615.0030)

Craig, R.W., Reed, R.L., and Spengler, R.W., 1983, Geohydrologic data for test well USW H-6, Yucca Mountain area, Nye County, Nevada: U.S. Geological Survey Open-File Report 83-856, 35 p. (NNA.870406.0058)

Craig, R.W., and Robison, J.H., 1984, Geohydrology of rocks penetrated by test well UE-25p #1, Yucca Mountain area, Nye County, Nevada: U.S. Geological Survey Water-Resources Investigations Report 84-4248, 57 p. (HQS.880517.1133)

Czarnecki, J.B., and Waddell, R.K., 1984, Finite-element simulation of groundwater flow in the vicinity of Yucca Mountain, Nevada-California: U.S. Geological Survey Water-Resources Investigations Report 84-4349, 38 p. (NNA.870407.0173)

Dagan, Gedeon, 1986, Statistical theory of groundwater flow and transport: Pore to laboratory, laboratory to formation, and formation to regional scale: American Geophysical Union, Water Resources Research, v. 22, no. 9, p. 1205-1345. (NNA.891107.0098)

Dockery, H.A., Byers, F.M., Jr., and Orkild, P.P., compilers, 1985, Nevada Test Site field trip guidebook: Los Alamos, N. Mex., Los Alamos National Laboratory Report LA-10428-MS, 49 p. (NNA.890330.0001)

Erickson, J.R., and Waddell, R.K., 1985, Identification and characterization of hydrologic properties of fractured tuff using hydraulic and tracer tests--Test well USW H-4, Yucca Mountain, Nye County, Nevada: U.S. Geological Survey Water-Resources Investigations Report 85-4066, 30 p. (NNA.870407.0184)

Frizzell, V.A., Jr., and Shulters, Jacqueline, 1990, Geologic map of the Nevada Test Site, Southern Nevada: U.S. Geological Survey Miscellaneous Investigations Map I-2046, scale 1:100,000. (NNA.910123.0073)

Gale, J.E., 1982, Assessing the permeability characteristics of fractured rock, *in* Narasimhan, T.N., ed., Recent trends in hydrogeology: Boulder, Colo., Geological Society of America Special Paper 189, p. 163-181. (CRX.860912.0004)

Gringarten, A.C., 1982, Flow-test evaluation of fractured reservoirs, *in* Narasimhan, T.N., ed., Recent trends in hydrogeology: Boulder, Colo., Geological Society of American Special Paper 189, p. 237-263. (NNA.870729.0096)

International Mathematical and Statistical Libraries, Inc. (IMSL), 1982, IMSL Library, Edition 9, Reference manual: Houston, Tex., variable paging. (NNA.910215.0246)

Kerrisk, J.F., 1987, Groundwater chemistry at Yucca Mountain, Nevada, and vicinity: Los Alamos, N. Mex., Los Alamos National Laboratory Report LA-10929-MS, 118 p. (NNA.870507.0017)

Keys, W.S., 1988, Borehole geophysics applied to ground-water investigations: U.S. Geological Survey Open-File Report 87-539, 305 p. (NNA.910215.0248)

Lahoud, R.G., Lobmeyer, D.H., and Whitfield, M.S., Jr., 1984, Geohydrology of volcanic tuff penetrated by test well UE-25b #1, Yucca Mountain, Nye County, Nevada: U.S. Geological Survey Water-Resources Investigations Report 84-4253, 44 p. (NNA.890511.0117)

Lipman, P.W., Christiansen, R.L., and O'Connor, J.T., 1966, A compositionally zoned ash-flow sheet in southern Nevada: U.S. Geological Survey Professional Paper 524-F, 47 p. (NNA.870519.0035)

Lipman, P.W., and McKay, E.J., 1965, Geologic map of the Topopah Spring SW quadrangle, Nye County, Nevada: U.S. Geological Survey Geologic Quadrangle Map GQ-439, scale 1:24,000. (HQS.880517.1314)

Lobmeyer, D.H., 1986, Geohydrology of rocks penetrated by test well USW G-4, Yucca Mountain, Nye County, Nevada: U.S. Geological Survey Water-Resources Investigations Report 86-4015, 38 p. (NNA.890922.0287)

Lobmeyer, D.H., Whitfield, M.S., Lahoud, R.R., and Bruckheimer, Laura, 1983, Geohydrologic data for test well UE-25b #1, Nevada Test Site, Nye County, Nevada: U.S. Geological Survey Open-File Report 83-855, 48 p. (NNA.870406.0060)

Lohman, S.W., 1979, Ground-water hydraulics: U.S. Geological Survey Professional Paper 708, 70 p. (NNA.891220.0169)

Maldonado, Florian, 1985, Geologic map of the Jackass Flats area, Nye County, Nevada: U.S. Geological Survey Miscellaneous Investigations Map I-1519, scale 1:48,000. (HQS.880517.1925)

McKay, E.J., and Sargent, K.A., 1970, Geologic map of the Lathrop Wells quadrangle, Nye County, Nevada: U.S. Geological Survey Geologic Quadrangle Map GQ-883, scale 1:24,000. (NNA.910215.0250)

McKay, E.J., and Williams, W.P., 1964, Geology of the Jackass Flats quadrangle, Nye County, Nevada: U.S. Geological Survey Geologic Quadrangle Map GQ-368, scale 1:24,000. (HQS.880517.1339)

Mifflin, M.D., 1968, Delineation of ground-water flow systems in Nevada: University of Nevada, Desert Research Institute Publication 42004, 111 p. (HQS.880517.1796)

_____1988, Region 5, Great Basin, *in* Back, W., Rosenshein, J.S., and Seaber, P.R., eds., Hydrogeology: Boulder, Colo., Geological Society of America, The geology of North America, v. 0-2. (NNA.910215.0251)

Moench, A.E., 1984, Double porosity models for a fissured ground-water reservoir with fracture skin: American Geophysical Union, Water Resources Research, v. 20, no. 7, p. 831-846. (HQS.880517.2762)

Mualem, Y., 1976, A new model for predicting the hydraulic conductivity of unsaturated porous media: Water Resources Research, v. 12, no. 3, p. 513-522. (HQS.880517.1803)

Muller, D.C., and Kibler, J.E., 1983, Commercial geophysical well logs from the USW G-1 drill hole, Nevada Test Site, Nevada: U.S. Geological Survey Open-File Report 83-321, 7 p. (HQS.880517.1352)

_____1984, Preliminary analysis of geophysical logs from drill hole UE-25p #1, Yucca Mountain, Nye County, Nevada: U.S. Geological Survey Open-File Report 84-649, 14 p. (HQS.880517.1353)

Neuman, S.P., 1975, Analysis of pumping test data from anisotropic unconfined aquifers considering delayed gravity response: Water Resources Research, v. 11, no. 2, p. 329-342. (NNA.891220.0170)

Norris, A.E., Byers, F.M., Jr., and Merson, T.J., 1986, Fran Ridge horizontal coring summary report hole UE-25h #1, Yucca Mountain area, Nye County, Nevada: Los Alamos, N. Mex., Los Alamos National Laboratory Report LA-10859-MS, 78 p. (HQS.880517.1359)

Orkild, P.P., and O'Connor, J.T., 1970, Geologic map of the Topopah Spring quadrangle, Nye County, Nevada: U.S. Geological Survey Geologic Quadrangle Map GQ-849, scale 1:24,000. (HQS.880517.1368)

Papadopulos, S.S., Bredehoeft, J.D., and Cooper, H.H., Jr., 1973, On the analysis of "slug test" data: Water Resources Research, v. 9, no. 4, p. 1087-1089. (NNA.891220.0171)

Plume, R.W., and Carlton, S.M., 1988, Hydrogeology of the Great Basin region of Nevada, Utah, and adjacent States: U.S. Geological Survey Hydrologic Investigations Atlas, HA-694-A, scale 1:1,000,000. (NNA.910215.0252.0255)

Rehrig, W.A., 1986, Processes of regional Tertiary extension in the western Cordillera--Insights from the metamorphic core complexes, *in* Mayer, Larry, ed., Extensional tectonics of the Southwestern United States--A perspective on processes and kinematics: Boulder, Colo., Geological Society of America Special Paper 208, p. 97-122. (NNA.910215.0256)

Robison, J.H., 1984, Ground-water level data and preliminary potentiometric-surface maps, Yucca Mountain and vicinity, Nye County, Nevada: U.S. Geological Survey Water-Resources Investigations Report 84-4197, 8 p. (NNA.870519.0096)

Robison, J.H., and Craig, R.W., 1991, Geohydrology of rocks penetrated by test well USW H-5, Yucca Mountain, Nye County, Nevada: U.S. Geological Survey Water-Resources Investigations Report 88-4168, 44 p. (NNA.900110.0400)

Robison, J.H., Stephens, D.M., Luckey, R.R., and Baldwin, D.A., 1988, Water levels in periodically measured wells in the Yucca Mountain area, Nevada, 1981-87: U.S. Geological Survey Open-File Report 88-468, 132 p. (NNA.890306.0113)

Rush, F.E., Thordarson, William, and Bruckheimer, Laura, 1983, Geohydrologic and drill-hole data for test well USW H-1, adjacent to Nevada Test Site, Nye County, Nevada: U.S. Geological Survey Open-File Report 83-141, 38 p. (NNA.870519.0103)

Rush, F.E., Thordarson, William, and Pyles, D.G., 1984, Geohydrology of test well USW H-1, Yucca Mountain, Nye County, Nevada: U.S. Geological Survey Water-Resources Investigations Report 83-4032, 56 p. (NNA.870518.0067)

Sargent, K.A., McKay, E.J., and Burchfiel, B.C., 1970, Geologic map of the Striped Hills quadrangle, Nye County, Nevada: U.S. Geological Survey Geologic Quadrangle Map GQ-882, scale 1:24,000. (NNA.891114.0344)

Scott, R.B., and Bonk, Jerry, 1984, Preliminary geologic map of Yucca Mountain, Nye County, Nevada, with geologic sections: U.S. Geological Survey Open-File Report 84-494, scale 1:12,000. (HQS.880517.1821)

Scott, R.B., and Castellanos, Mayra, 1984, Stratigraphic and structural relations of volcanic rocks in drill holes USW GU-3 and USW G-3, Yucca Mountain, Nye County, Nevada: U.S. Geological Survey Open-File Report 84-491, 121 p. (NNA.890804.0017)

Scott, R.B., Spengler, R., Diehl, S., Lappin, H.R., and Chornack, M.P., 1983, Geologic character of tuffs in the unsaturated zone at Yucca Mountain, southern Nevada, *in* Mercer, J.M., Rao, P.S.C., and Marine, I.W., eds., Role of the unsaturated zone in radioactive and hazardous waste disposal: Ann Arbor, Ann Arbor Science, p. 289-335. (NNA.870406.0034)

Scott, R.B., and Whitney, J.W., 1987, The upper crustal detachment system at Yucca Mountain: Geological Society of America, Rocky Mountain Section, 40th Annual Meeting, Abstracts with Programs, v. 19, no. 5, p. 332. (HQS.880517.2863)

Skougstad, M.W., Fishman, M.J., Friedman, L.C., Erdmann, D.E., and Duncan, S.S., eds., 1979, Methods for determination of inorganic substances in water and fluvial sediments: U.S. Geological Survey Techniques of Water-Resources Investigations, bk. 5, chap. A1, 626 p. (HQZ.870131.6953)

Snyder, D.B., and Carr, W.J., 1984, Interpretation of gravity data in a complex volcano-tectonic setting, southwestern Nevada: Journal of Geophysical Research, v. 89, no. B12, p. 10193-10206.

Spengler, R.W., Byers, F.M., Jr., and Warren, J.B., 1981, Stratigraphy and structure of volcanic rocks in drill hole USW G-1, Yucca Mountain, Nye County, Nevada: U.S. Geological Survey Open-File Report 81-1349, 50 p. (HQS.880517.1492)

Spengler, R.W., and Chornack, M.P., 1984, Stratigraphic and structural characteristics of volcanic rocks in core hole USW G-4, Yucca Mountain, Nye County, Nevada, *with a section on* geophysical logs by D.C. Muller and J.E. Kibler: U.S. Geological Survey Open-File Report 84-789, 77 p. (NNA.870519.0105)

Spengler, R.W., Muller, D.C., and Livermore, R.B., 1979, Preliminary report on the geology and geophysics of drill hole UE 25a-1, Yucca Mountain, Nevada Test Site: U.S. Geological Survey Open-File Report 79-1244, 43 p. (NNA.870406.0349)

Spengler, R.W., and Rosenbaum, J.G., 1980, Preliminary interpretations of geologic results obtained from boreholes UE-25a-4, -5, -6, and -7, Yucca Mountain, Nevada Test Site: U.S. Geological Survey Open-File Report 80-929, 35 p. (NNA.890823.0106)

Stallman, R.W., 1965, Effects of water-table conditions on water-level changes near pumping wells: Water Resources Research, v. 1, no. 2, p. 295-312. (NNA.910215.0257)

Stock, J.M., and Healy, J.H., 1988, Stress field at Yucca Mountain, *in* Carr, M.D., and Yount, J.C., eds., Geologic and hydrologic investigations of a potential nuclear waste disposal site at Yucca Mountain, southern Nevada: U.S. Geological Survey Bulletin 1790, p. 87-93. (NNI.881128.0011)

Streltsova-Adams, T.D., 1978, Well testing in heterogeneous aquifer formations, *in* Chow, V.T., ed., Advances in hydroscience: New York, Academic Press, v. 11, p. 357-423.

Theis, C.V., 1935, The relation between the lowering of the piezometric surface and the rate and duration of discharge of a well using ground-water storage: American Geophysical Union Transactions, v. 16, p. 519-524. (HQS.880517.2888)

Thordarson, William, 1983, Geohydrologic data and test results from well J-13, Nevada Test Site, Nye County, Nevada: U.S. Geological Survey Water-Resources Investigations Report 83-4171, 57 p. (NNA.870518.0071)

Thordarson, William, and Howells, Lewis, 1987, Hydraulic tests and chemical quality of water at well USW VH-1, Crater Flat, Nye County, Nevada: U.S. Geological Survey Water-Resources Investigations Report 86-4359, 20 p. (NNA.890922.0289)

Thordarson, William, Rush, F.E., Spengler, R.W., and Waddell, S.J., 1984, Geohydrologic and drill-hole data for test well USW H-3, Yucca Mountain, Nye County, Nevada: U.S. Geological Survey Open-File Report 84-149, 28 p. (NNA.870406.0056)

Thordarson, William, Rush, F.E., and Waddell, J.J., 1985, Geohydrology of test well USW H-3, Yucca Mountain, Nye County, Nevada: U.S. Geological Survey Water-Resources Investigations Report 84-4272, 38 p. HQS.880517.1852)

U.S. Geological Survey, 1984, a summary of geologic studies through January 1, 1983, of a potential high-level radioactive waste repository site at Yucca Mountain, southern Nye County, Nevada: Open-File Report 84-792, 103 p. (NNA.891009.0304)

Waddell, R.K., 1982, Two-dimensional, steady-state model of ground-water flow, Nevada Test Site and vicinity, Nevada-California: U.S. Geological Survey Water-Resources Investigations Report 82-4085, 72 p. (NNA.870518.0055)

Waddell, R.K., Robison, J.H., and Blankennagel, R.K., 1984, Hydrology of Yucca Mountain and vicinity, Nevada-California--Investigative results through mid-1983: U.S. Geological Survey Water-Resources Investigations Report 84-4267, 72 p. (NNA.870406.0343)

Weeks, E.P., and Wilson, W.E., 1984, Preliminary evaluation of hydrologic properties of cores of unsaturated tuff, test well USW H-1, Yucca Mountain, Nevada: U.S. Geological Survey Water-Resources Investigations Report 84-4193, 30 p. (NNA.870407.0037)

Wernicke, Brian, and Burchfiel, B.C., 1982, Modes of extensional tectonics: Journal of Structural Geology, v. 4, no. 2, p. 105-115. (HQS.880517.1565)

Whitfield, M.S., Jr., Thordarson, William, and Eshom, E.P., 1984, Geohydrologic and drill-hole data for test well USW H-4, Yucca Mountain, Nye County, Nevada: U.S. Geologic Survey Open-File Report 84-449, 39 p. (NNA.870407.0317)

Whitfield, M.S., Jr., Thordarson, William, Hammermeister, D.P., and Warner, J.B., 1990, drilling and geohydrologic data for test hole USW UZ-1, Yucca Mountain, Nye County, Nevada: U.S. Geological Survey Open-File Report 90-354, 40 p. (HQS.880517.2908)

Whitfield, M.S., Jr., Eshom, E.P., Thordarson, William, and Schaefer, D.H., 1985, Geohydrology of rocks penetrated by test well USW H-4, Yucca Mountain, Nye County, Nevada: U.S. Geological Survey Water-Resources Investigations Report 85-4030, 33 p.

Winograd, I.J., and Thordarson, William, 1975, Hydrogeologic and hydrochemical framework, south-central Great Basin, Nevada-California, with special reference to the Nevada Test Site: U.S. Geological Survey Professional Paper 712-C, 126 p.

Note: Parenthesized numbers following each cited reference are for U.S. Department of Energy OCRWM Records Management purposes only and should not be used when ordering the publication.

☆ U.S. GOVERNMENT PRINTING OFFICE: 1993—573-191 / 80011 REGION NO. 8